NASA Technical Memorandum 85975

Numerical Analysis of the First Static Calibration of the RSRA Helicopter Active-Isolator Rotor Balance System

C. W. Acree, Jr.

FEBRUARY 1985

NASA

NASA Technical Memorandum 85975

Numerical Analysis of the First Static Calibration of the RSRA Helicopter Active-Isolator Rotor Balance System

C. W. Acree, Jr.
Ames Research Center
Moffett Field, California

National Aeronautics
and Space Administration

Scientific and Technical Information Branch

1985

SUMMARY

The helicopter version of the Rotor Systems Research Aircraft (RSRA) is designed to make simultaneous measurements of all rotor forces and moments in flight in a manner analogous to a wind-tunnel balance Loads are measured by a combination of load cells, strain gages, and hydropneumatic active isolators with built-in pressure gages Complete evaluation of system performance requires calibration of the rotor force- and moment-measurement system when installed in the aircraft Derivations of calibration corrections for various combinations of calibration data are discussed

INTRODUCTION

A major goal of the Rotor Systems Research Aircraft is measurement of the forces and moments generated by a helicopter rotor in flight There are two RSRA, each with a unique system for measuring rotor loads, as described by Burks (ref 1) The first static-loads calibration of the compound version of the RSRA is described in reference 2, and the first calibration of the helicopter version of the RSRA is summarized in reference 3 The present paper covers a numerical analysis of the data from the calibration of the helicopter version Appendix A discusses revisions to the data sets used in the analysis Appendix B summarizes a few preliminary analytical approaches Because the two aircraft have entirely different load-measurement systems, the calibrations and analytical results are consequently completely independent The distinction between the two aircraft should be kept in mind when the information presented in this paper is interpreted

THE ACTIVE-ISOLATOR SYSTEM

The rationale for the original active-isolator system requirement is presented by Walton, Hedgepeth, and Bartlett (ref 4) Kuczynski and Madden (ref 5) describe the details of the isolator design, a summary is given here Figure 1 shows the basic concept of RSRA rotor-loads measurement, whereby rotor loads are transmitted from the base of the transmission to the airframe through a collection of force transducers The system used on the RSRA helicopter is shown in more detail in figure 2 The main rotor transmission is mounted to a baseplate, which is in turn connected to the airframe by the load-measurement system Four vertical load cells in a focused configuration take up vertical loads, and four hydropneumatic isolators react in-plane loads The load cells are canted 15° inward at the bottom toward the extended main rotor shaft centerline There is also a torque linkage (partly hidden in the figure) which allows free in-plane translation of the transmission, but resists in-plane rotation The aft isolator is a safety backup unit, and is normally deactivated and unloaded in flight There are also optional displacement transducers for each isolator The entire system functions analogously to a wind-tunnel balance for rotor loads measurement Vibrations in the horizontal plane are isolated from the airframe, but vertical loads are not isolated

Figure 3 schematically illustrates an active-isolator unit Loads are carried by a piston moving in a cylinder filled with hydraulic fluid Each end of the cylinder is connected to an accumulator, where a flexible diaphragm separates the fluid from an air chamber The air chambers constitute pneumatic springs that absorb vibratory loads, and a servo valve keeps the piston centered under large steady loads Hydraulic power is supplied by conventional aircraft hydraulic pumps A differential pressure transducer provides load data In the

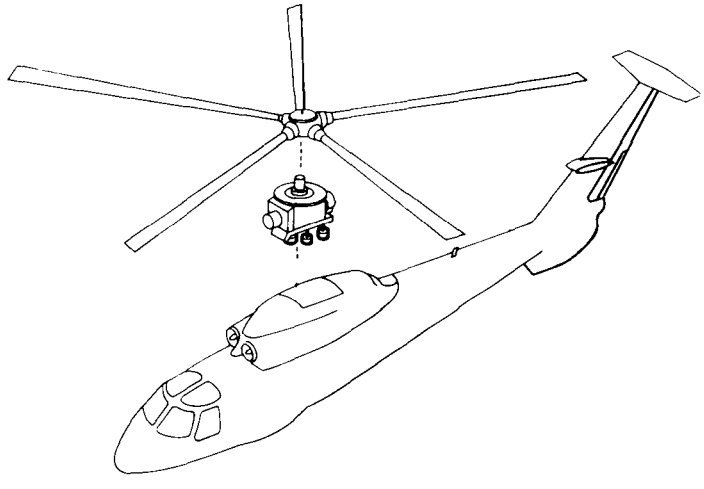

Figure 1 – RSRA helicopter rotor-loads measurement system

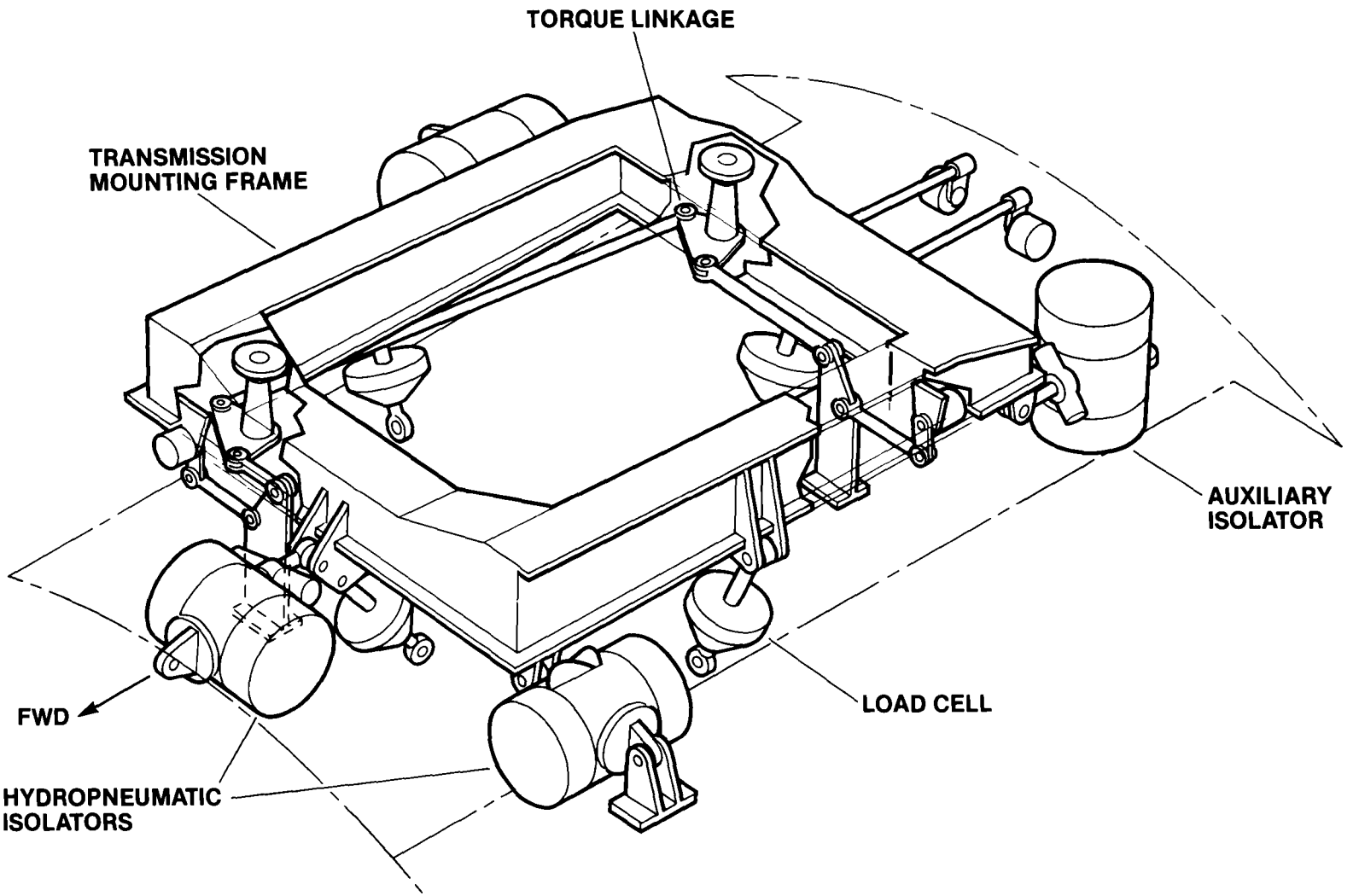

Figure 2 – Active-isolator configuration of the RSRA rotor-load measurement system

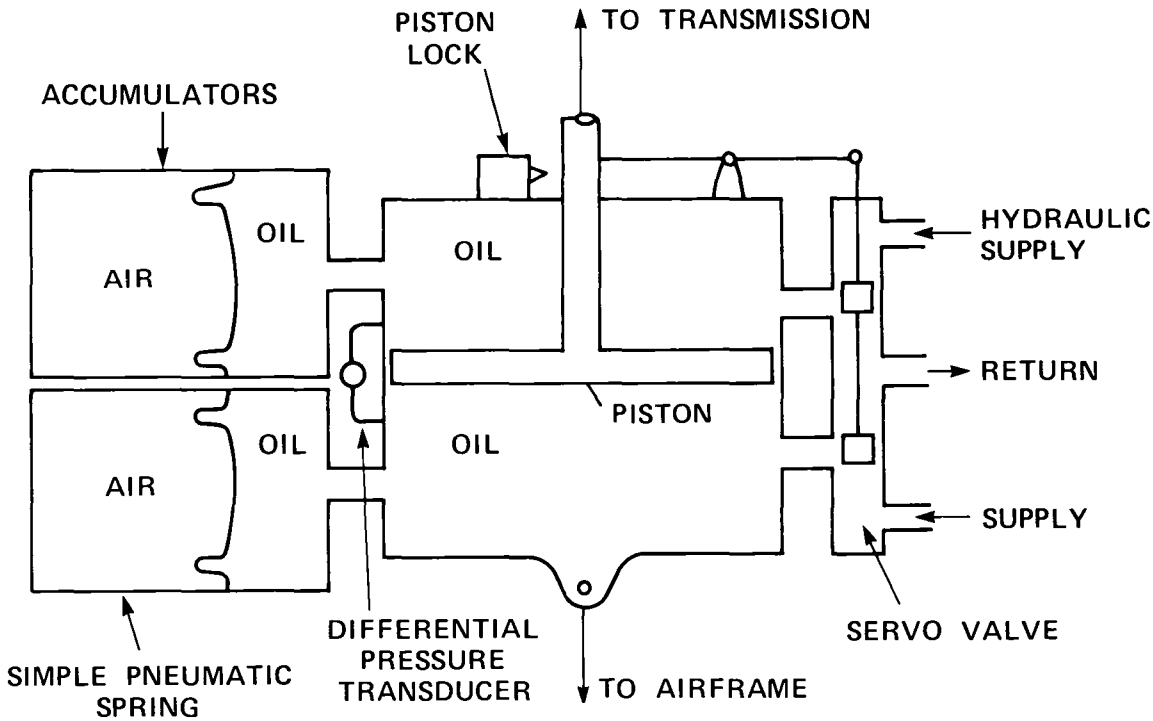

Figure 3 – Schematic of RSRA hydropneumatic active isolator

event of isolator or hydraulic system failure, a piston lock creates a separate load path for safety The servo-valve feedback gains and accumulator precharge pressures may be altered as needed to match different rotors or different testing requirements

The torque linkage provides structural redundancy for safety, so that the large, steady torque loads are properly reacted if an isolator unit should fail Three load tubes and two bellcranks compose the torque linkage, the airframe itself and the transmission baseplate make up the last two elements of a seven-bar linkage with two degrees of freedom The transmission is restrained from rotation, but is otherwise free to translate in the horizontal plane so that in-plane loads are taken up by the load cells and isolators The linkage is preloaded so that at normal rotor torques the two lateral isolators are loaded near the middle of their operating range, with the torque linkage sharing part of the torque loads One of the load tubes has conventional strain gages so that torque-linkage loads can be monitored

In order to isolate rotor vibrations from the airframe, the active isolators must allow the transmission to move slightly with respect to the rest of the aircraft This motion – up to ±0 24 in – would apply undesired control inputs to the rotor through motion relative to the flight controls, which are normally grounded to the airframe To eliminate this effect a mechanical motion-compensation system adds corrective motions to the flight-control system (ref 6) The system is designed so that applied, corrective, and reaction control forces all cancel at the transmission, preventing any net unmeasured control forces from being applied to the rotor or transmission There are some residual linkage moments, but these are negligible compared to aerodynamic rotor loads There is also some linkage-bearing friction, which is small compared to full-scale flight loads (The friction does affect the data analysis, as discussed at the beginning of appendix B)

CALIBRATION REQUIREMENTS

It is desired that rotor forces and moments be measured with accuracies traceable to the National Bureau of Standards Individual component calibrations are insufficient, and the entire load-measurement system must be calibrated as a unit when installed on the aircraft

Figure 4 illustrates the static calibration method, which was essentially the same as that used on the compound version of the RSRA (ref 2) The static calibration method is described in detail by Acree et al (ref 7) A special calibration fixture replaced the rotor head, and the airframe was restrained by the landing-gear mounting lugs Hydraulic cylinders applied static loads through cables and pulleys, except for lift, where a solid rod and walking beam were used High-accuracy calibration-reference load cells connected the cables and rod directly to the rotor head fixture The fixture was designed for great stiffness, and for optimum placement of the reference load cells to obtain maximum accuracy

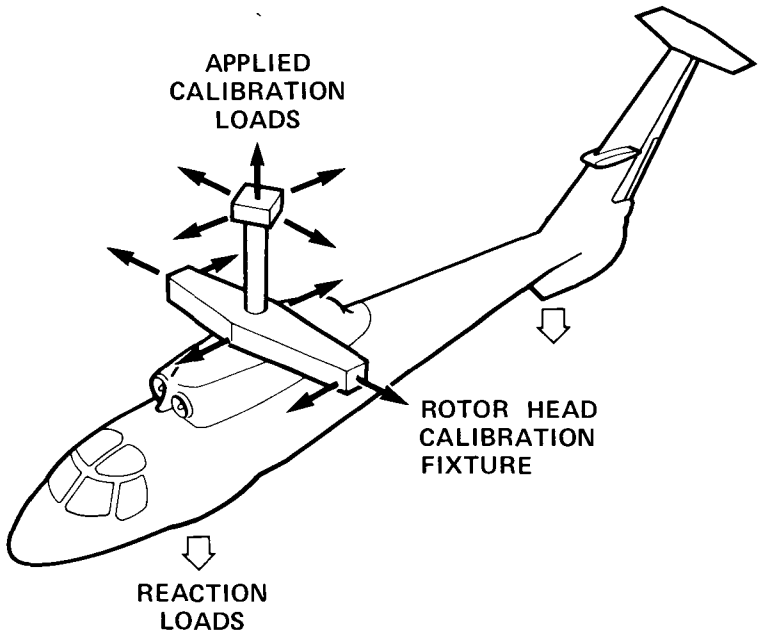

Figure 4 – Method of applying static rotor calibration loads

Figure 5 shows the reference axis system used for all calibration loads Table 1 gives the values of the calibration loads The single loads represent the performance limits of the RSRA's S-61 rotor, whereas loads in combination are reduced because of structural limitations of the airframe when it is installed in the calibration facility The most important combined loads are those with lift (Z) and torque (N), because these two loads are significant for virtually all reasonable flight conditions

The reference load cells were individually calibrated with equipment traceable to the National Bureau of Standards The calibrations of the reference load cells were used to determine the facility accuracies given in table 1 The listed values are the standard deviations of the errors in measuring each applied load, and have been rounded up to be conservative (Table 1 reflects updated component calibrations not available for inclusion in table 1 of ref 3)

Figure 6 is a simple schematic of the calibration data system (ref 7) A desk-top computer controlled a high-accuracy digital voltmeter connected to a high-speed scanner, with various accessories such as a small printer The aircraft load cells, isolator pressure transducers, and calibration reference load cells were sequentially sampled to take calibration data The scanning rate was fast enough that load drift during any data scan was less than the reference calibration accuracies (table 1) This allowed the calibration data to be treated as if each scan were perfectly simultaneous The computer converted raw voltage readings to engineering units, displayed selected parameters in real time, and stored all data on command A small local disk drive provided temporary data storage, all data were eventually transferred to a large mainframe computer for editing, plotting, and analyzing

ANALYTICAL PROCEDURES

If the active isolators performed perfectly and if the airframe were completely rigid, measurement accuracy would be limited only by pressure-transducer and load-cell accuracies Equivalent measurement root-mean-square (rms) errors based on this assumption are given in table 2 in the column labeled "transducer errors " These values are derived from individual component calibrations performed shortly before the full system calibration, with the results converted to equivalent rotor loads They do not include torque-linkage or aft-isolator errors, because the torque linkage was not highly loaded at maximum applied torque load, and the aft isolator was always deactivated during the system calibration For comparison, table 2 also includes predictions of full-system performance, including all analytically expected sources of error, listed under "all errors" (Madden, J , RSRA AIB's Development Requirements Unpublished memo, June 1979)

Structural flexibility of the aircraft changes the load distribution among the load cells, active isolators, and torque linkage, causing interactions (cross talk) and errors in total sensitivity Accumulated manufacturing and installation errors cause additional measurement errors As was shown in an earlier publication (ref 3), these nonrandom errors are significant Moreover, the isolator pistons must move slightly to absorb vibration, and any motion under static loads will further change the load distribution Proper analysis of a full-system calibration can eliminate nonrandom linear errors, and can reduce the effects of other errors by adjusting the calibration coefficients in the data-reduction equations

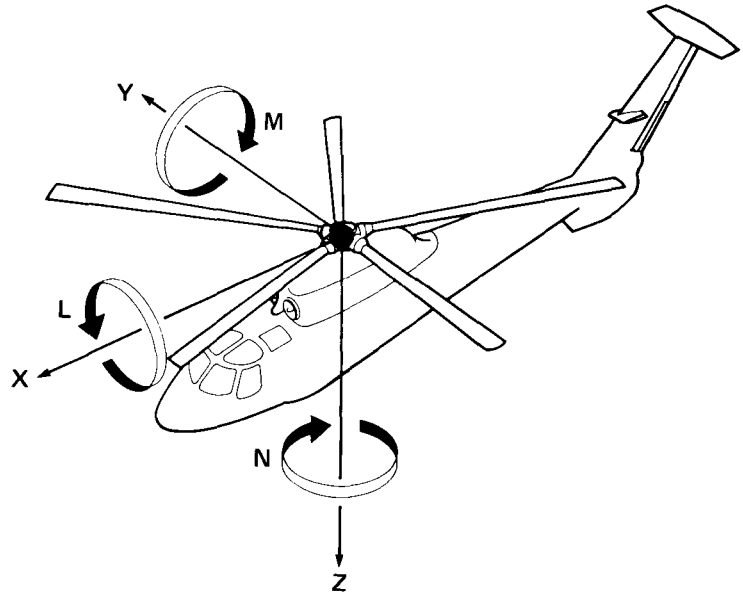

Figure 5 – RSRA rotor calibration axis system

TABLE 1 – CALIBRATION FACILITY STATIC LOAD APPLICATION CAPABILITIES (1983)

Axis	Positive direction	Single load limit (100%)	Combination load limit	Applied Load accuracy
X = Longitudinal	Forward	±8,620 lb	±4,000 lb	13 lb, 0 2% fs[a]
Y = Lateral	Right	±5,420 lb	±2,500 lb	11 lb, 0 2% fs
Z = Vertical	Down	-48,800 lb	-24,400 lb	47 lb, 0 1% fs
L = Roll	Right down	±16,667 ft-lb	±8,333 ft-lb	42 ft-lb, 0 3% fs
M = Pitch	Nose up	+25,000 ft-lb (-16,667)	±12,500 ft-lb	50 ft-lb, 0 2% fs
N = Torque	Left forward	+58,167 ft-lb	+50,000 ft-lb	25 ft-lb, 0 05% fs

[a] fs = full scale

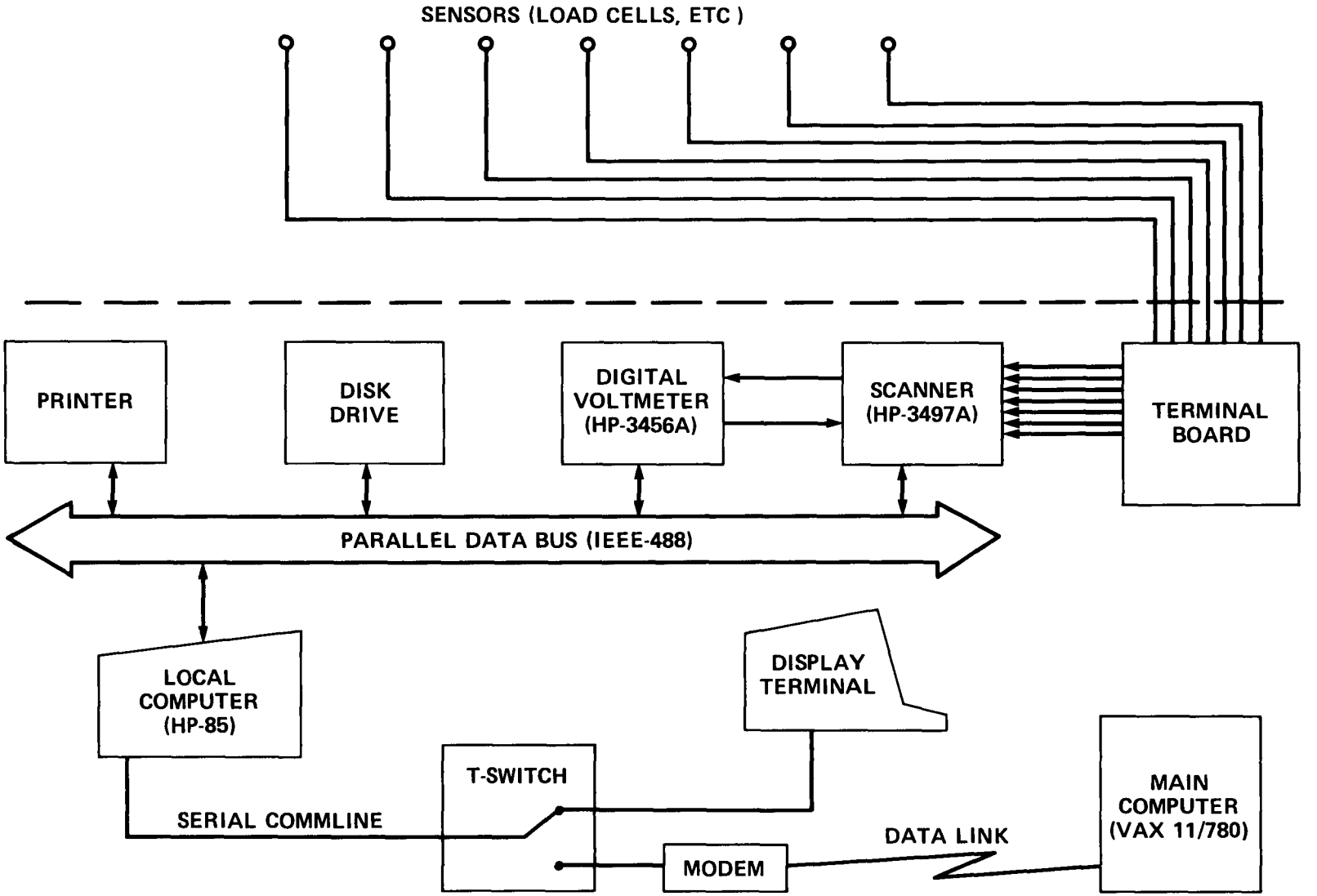

Figure 6 – Simplified block diagram of the data acquisition system

TABLE 2 – PREDICTED ERRORS FOR ACTIVE-ISOLATOR BALANCE SYSTEM

Axis	Maximum load	Transducer errors[a]	All errors[b]
X, lb	±8,620	74	177
Y, lb	±5,420	121	171
Z, lb	-48,800	31	47
L, ft-lb	±16,667	578	893
M, ft-lb	+25,000 -16,667	328	687
N, ft-lb	+58,167	180	302

[a]Not including torque linkage or aft isolator
[b]Representative of 120-knot level flight (Madden)

Analytical procedures are similar to those earlier described by Acree (ref 2), except that a conventional direct multiple linear regression was used almost exclusively for reasons discussed in appendix B The calibration-correction equation may be written

$$\vec{F} = C\vec{L} + \vec{B}$$

where

$\vec{F}$ = applied rotor-load vector

C = calibration matrix

$\vec{L}$ = load-cell and transducer data vector

$\vec{B}$ = regression intercept vector

For calibration, $\vec{F}$ is the vector of dependent variables, taken one axis at a time, and $\vec{L}$ is the vector of independent variables The elements of each row of C are the regression coefficients for the corresponding axis of $\vec{F}$ Each element of B is derived simultaneously with a row of C Note that although the applied load vector $\vec{F}$ is under the experimenter's control during the physical calibration, it must be treated as a vector of dependent variables by the regression This is because the results of the regression are used to predict applied loads from transducer data

For reduction of flight data, terms must be added to account for inertial effects that result from accelerations of the aircraft Derivation of inertial-effects corrections is not covered by this paper, see reference 2 for the relevant equations Also required for flight-data reduction is a vector of load tares to account for the difference in masses between the calibration fixtures attached to the aircraft and actual flight hardware Calculation of the tare vector was not necessary for the analysis covered here

A forward-stepwise multiple-linear-regression technique (ref 8) was used to derive the calibration matrix and intercepts Figure 7 is a flowchart of the analytical process Note that calibration errors are not simply the regression standard errors The procedures used here were generalized to allow different calibration matrices to be tested on the same reference data set to check suboptimal performance. Also, errors in a given axis may be determined for applied loads in different axes In particular, the error of most interest for a given axis is the root-mean-square (rms) error resulting from loads applied in the same axis Unless otherwise noted, such errors are always given in this paper

The calibration data organization used is shown in table 3, organized by case It is essentially the same as table A2 in reference 3, but the table has been updated to reflect additional available data The revisions are discussed in appendix A It is sufficient here to note that the 50% Z plus 85% N data correspond to maximum-weight hover, and the 25% Z plus 40% N data correspond to an idealized lightweight hover

In table 3, each case includes a different series of constant loads in the lift (Z) and torque (N) axes, with varied loads in other axes A constant load of zero means only that there was no load held at a fixed nonzero value, varied loads in that axis were still allowed Constant loads were applied only in the Z and N axes because these are the two axes that in straight-and-level flight or hover would experience large, constant-load components in addition to relatively small trim and vibratory loads The different analytical cases were accordingly based on different levels and combinations of constant loads in these two axes

The usual calibration procedure was to hold Z and N constant while loads in other axes were varied one at a time over their maximum allowable ranges (table 1) Since a load cannot be simultaneously varied and held constant, calibration data for the Z and N axes had to be separated into individual cases in which either Z or N was held constant while the other was varied To achieve complete and consistent data distributions within each case, some data sets were repeated Data for the maximum constant loads (50% Z and 85% N) were included in cases 2, 3, and 6, as shown in table 3

ERROR ANALYSIS

Before discussing the results of numerical analysis, a few general characteristics of the raw data should be mentioned The zero-crossing errors and data skew seen during the first calibration of the compound version of the RSRA (ref 2) are almost entirely absent from the present calibration data (see the figures in appendix A, see also the figures in the appendix

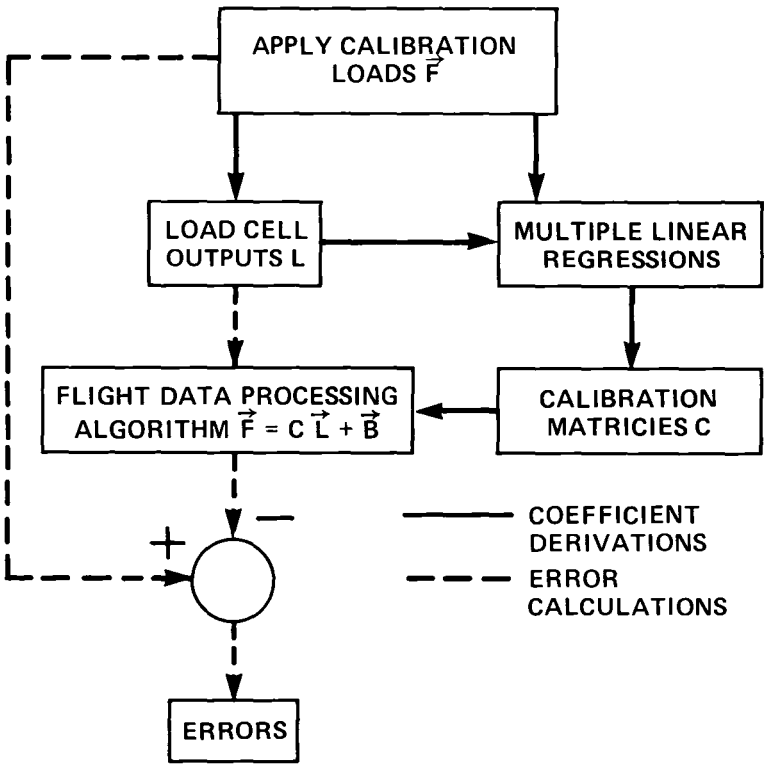

Figure 7 – RSRA calibration analysis flowchart

TABLE 3 – LOAD COMBINATIONS

Case	Constant loads		Run numbers of varied loads					
	Z, %	N, %	X	Y	Z	L	M[a]	N
1	0	0	55-58	61-64	52-53	72-75	81-83, 85	67-68
2	0	85	120-121	99-100	(34)	118-119	101-102	N/A
	25	85	47-48	93-94	N/A	107-108	103-104	N/A
	50	85	41-42	39-40	N/A	35-36	37-37	N/A
3	50	0	79-80	97-98	N/A	116-117	115	(33)
	50	40	49-50	95-96	N/A	109-110	113	N/A
	50	85	41-42	39-40	N/A	35-36	37-38	N/A
4	0	0	---	---	---	---	---	68
	25	0	---	---	---	---	---	43
	50	0	---	---	---	---	---	33
5	0	0	---	---	53	---	---	---
	0	40	---	---	44	---	---	---
	0	85	---	---	34	---	---	---
6	25	40	45-46	91-92	N/A	87-88	89-90	N/A
	50	85	41-42	39-40	N/A	35-36	37-38	N/A

[a]Unreliable pitching-moment data not included

of ref 3) As the isolator system of the RSRA helicopter is inherently more susceptible to hysteresis errors than the all-load-cell system of the RSRA compound, the reduction of error is almost certainly due to improved calibration procedures and equipment Conventional, pure hysteresis errors are still present

There is no immediate requirement to apply the calibration results to flight data Accordingly, no effort was made to eliminate pure hysteresis errors as was done in the analysis of the RSRA compound's calibration data (ref 2) The numerical results are consequently conservative in their estimates of in-flight measurement errors

The first step in the regression error analysis was to calculate the errors resulting from the use of a calibration matrix derived directly from design geometry This is the same idealized matrix used to calculate the predicted errors of table 2 Three reference data sets were used single loads, "light hover" (25% Z plus 40% N), and "heavy hover" (50% Z plus 85% N) (See appendix A for details) Table 4 gives the resulting applied-load errors calculated for loads applied solely in the same axis as that in which errors are measured For reference, table 4 also gives the overall errors for each axis, calculated by averaging (rms) the errors over all applied loads

Table 5 shows similar errors, but calculated for regression matrices derived directly from each data set – single loads, light hover, and heavy hover The applied-load errors are nearly always lower for the regression matrices (table 5) than for the geometric matrix (table 4) The exceptions are all in roll (L) and pitch (M), and are not severe. Also, the regression matrices always give better results for overall errors Note that torque errors are improved by an order of magnitude in table 5

These results were expected the matrices derived by regression analysis should give better results than the geometric matrix The overall errors are usually lower than the applied-load errors Again this was expected, because most of the errors that were averaged together resulted from conditions in which no loads were applied to the measurement axis itself Only severe cross-talk errors could force the overall errors to be consistently larger than the applied-load errors The applied-load errors are consequently conservative estimates of measurement-system accuracy

After the need for regression analysis to derive useful calibration corrections was verified, the requirement for multiple-load analysis was investigated. Table 6 gives the errors obtained when the single-loads regression matrix was applied to the three reference data sets The errors obtained for the two hover data sets are worse than those for the single-loads data set, and are worse than those shown in table 5 for calibration matrices matched to each reference

TABLE 4 – ERRORS FOR THE GEOMETRIC MATRIX[a]

Applied-load axis	Data sets		
	Single loads	Light hover	Heavy hover
Applied-load errors			
X, lb	465	357	503
Y, lb	314	192	235
Z, lb	252	139	204
L, ft-lb	832	764	597
M, ft-lb	346	618	703
N, ft-lb	8712	3302	5874
Overall errors			
X, lb	314	196	287
Y, lb	232	164	174
Z, lb	110	55	64
L, ft-lb	979	728	674
M, ft-lb	1064	580	794
N, ft-lb	3237	1405	2469

[a]RMS errors for the geometric matrix applied to three reference data sets Intercepts have been adjusted to give zero mean total errors for each axis in each data set

TABLE 5 – ERRORS FOR THREE REFERENCE DATA SETS[a]

Applied-load axis	Data sets		
	Single loads	Light hover	Heavy hover
Applied-load errors			
X, lb	249	213	273
Y, lb	268	175	170
Z, lb	107	84	104
L, ft-lb	737	807	641
M, ft-lb	393	521	564
N, ft-lb	359	320	265
Overall errors			
X, lb	196	129	179
Y, lb	188	148	148
Z, lb	63	33	35
L, ft-lb	806	679	588
M, ft-lb	604	413	490
N, ft-lb	341	209	267

[a]Using separate regression matrices derived directly from each data set

TABLE 6 – APPLIED-LOAD ERRORS FOR THE SINGLE-LOADS MATRIX APPLIED TO THREE REFERENCE DATA SETS

Applied-load axis	Data sets		
	Single loads	Light hover	Heavy hover
X, lb	249	321	410
Y, lb	268	217	314
Z, lb	107	159	118
L, ft-lb	737	1315	774
M, ft-lb	393	645	776
N, ft-lb	359	629	471

data set This shows that a single-loads calibration is inadequate to get good results for normal flight conditions

Table 7 gives applied-load errors for regression matrices derived from progressively larger data sets Again, the reference data sets were the light-hover and heavy-hover data sets The "combined hover" matrix is a compromise derived by combining both the light- and heavy-hover data sets (case 6 in table 3) The "all triple" matrix is derived from a combination of all multiple loads (everything but case 1 in table 3)

TABLE 7 – APPLIED-LOAD RMS ERRORS FOR HOVER DATA SETS

(a) Light-hover data set

Applied-load axis	Regression matrix		
	Light hover	Combined hover	All triple
X, lb	213	211	205
Y, lb	175	164	161
Z, lb	84	88	86
L, ft-lb	807	869	987
M, ft-lb	521	512	741
N, ft-lb	320	350	364

(b) Heavy-hover data set

Applied-load axis	Regression matrix		
	Heavy hover	Combined hover	All triple
X, lb	273	311	322
Y, lb	170	188	197
Z, lb	104	120	114
L, ft-lb	641	613	659
M, ft-lb	564	586	768
N, ft-lb	265	437	411

The results shown here have a wider range of applicability than may be immediately apparent The heavy-hover data set in also appropriate for many straight-and-level flight conditions of the RSRA pure helicopter, and the light-hover data are appropriate for similar flight conditions at lower speeds and weights The light-hover data also apply to some partially wing-borne flight conditions of the RSRA compound

In the absence of any immediate flight test requirements for the active-isolator system, and given the better-than-expected results presented above, the analysis was terminated at the level shown in table 7 The analysis can be readily expanded to include different reference data sets to match a variety of possible RSRA compound flight conditions If a more detailed analysis is required, the effects of different constant loads can be checked by comparing data sets with either Z or N held at a fixed value while the other is varied The data organization shown in table 3 was chosen in part to readily allow such an analysis for 50% Z and 85% N The data could be regrouped to allow an analysis for 25% Z and 40% N, as well However, such an analysis would probably not be useful as long as hysteresis remains the dominant error mechanism

IMPROVEMENTS AND FUTURE OPTIONS

It is known that a major error mechanism is hysteresis (Madden, J , RSRA AIB's Development Requirements Unpublished memo, June 1979) Furthermore, test flights with the other aircraft have shown that hysteresis resulting from rod-end bearing friction is largely dithered out by airframe vibration (ref 2) Consequently, the loads-measurement system has measurement accuracy potential beyond that demonstrated here

It is strongly desired that the active isolators not be rebuilt internally to improve performance, because this would violate the original requirement that the isolation system be sufficiently flexible in design to accommodate virtually any conventional rotor system without major modification Moreover, it would be expensive and would require complete system requalification However, there are a few simple changes that can be easily made

It was envisioned that servo-valve gains and accumulator working pressures would occasionally be changed to accommodate new testing requirements Also, the pressure transducers are significantly less accurate than the vertical load cells, direct substitution of improved transducers could easily be accomplished Finally, hysteresis of the assembled system could be reduced by replacing the existing rod-end bearings with elastomeric units

Priorities for improvements cannot be properly set until the exact sources of system hysteresis and other errors are better known It is recommended that laboratory calibrations

of the individual active isolators be carried out This procedure would determine how much error is contributed by the isolators themselves, which is distinct from errors resulting from total system behavior Only the latter errors are addressed by the analysis discussed in this report

CONCLUSIONS

Whether the RSRA active-isolator rotor-load-measurement system could accurately measure static rotor loads was a major unanswered question of the research aircraft's development The first static calibration of the system showed that it is capable of meeting and even exceeding most performance predictions It further appears that system measurement accuracy can be improved by straightforward, low-risk component upgrades The RSRA active-isolator system can accurately measure six-component rotor loads on a routine research basis

Ames Research Center
National Aeronautics and Space Administration
Moffett Field, California, June 27, 1984

APPENDIX A

REGRESSION DATA SETS

The data used for regression analysis are largely based on that given in a previous paper by Acree (ref. 3, see table A2 in the appendix of that paper) Some revisions and extensions have been made to the data sets for purposes of regression analysis These changes are discussed in this appendix

REVISIONS TO PITCHING-MOMENT DATA

As was mentioned in reference 3, nonrepeatability of pitching-moment (M) data was suspected to result from malfunctioning calibration facility equipment Investigation revealed that it was possible for one of the facility hydraulic cylinders to bind on its support as load-cable slack was taken up The resulting force imbalance would cause exactly the sort of one-sided slope error in pitching-moment response as was noted Unfortunately, it was not possible to determine the exact magnitudes of the errors, so the suspect data could not be corrected Therefore, all questionable data had to be deleted to get a valid calibration Not all data runs were affected, so there was only a slight loss in comprehensiveness and a definite gain in reliability of the data

Single-load M data are shown in the figures for case 1 at the end of this appendix For reasons given above, run 84 was deleted entirely To help fill in for the missing positive-side data, some of the run 81 data were added Since run 81 was the first single-load M run, the load-measurement system did not start out on the same part of its hysteresis curve as for other M runs Once full-scale load was reached, the system had been fully "exercised," and the data followed their usual hysteresis curve Although the transition to the proper hysteresis curve was not perfect, as is especially evident in the figure of the forward-isolator output, the discrepancies were no worse than occasionally seen elsewhere Negative-going data from run 81 were consequently included

The hydraulic-cylinder binding noted above affected only positive-pitch data Therefore, negative-pitch data – runs 113 and 115 – were reinstated to the M data of case 3 Plots of the data are included at the end of this appendix

LIGHT-HOVER DATA

A special combination of constant-load data, not included in the earlier paper (ref 3), was added to allow an expanded regression analysis The new data set comprises constant loads of 25% Z (lift) and 40% N (torque), or approximately half of the maximum allowable constant loads These load values roughly correspond to a lightweight hover condition This data set was combined with the data for maximum constant loads to form a new case (case 6), plots are given at the end of this appendix These figures allow direct comparison of half-constant-load data and maximum-constant-load data, or lightweight hover and heavyweight hover conditions The equivalent data for varied Z and N loads are included in cases 4 and 5, for plots of these data see reference 3

LIST OF APPENDIX A FIGURES

[a]See table 3 for a list of all cases and loads Data plots not included here are available in reference 3

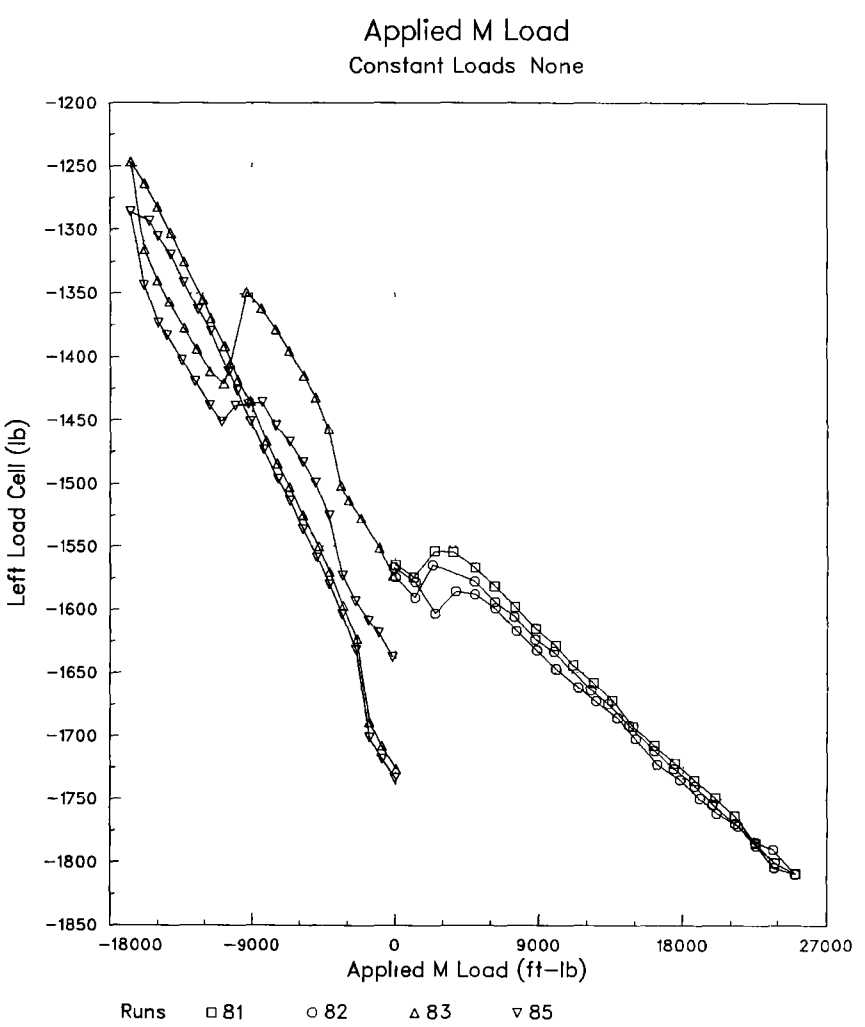

RSRA 741 1983 ROTOR CALIBRATION

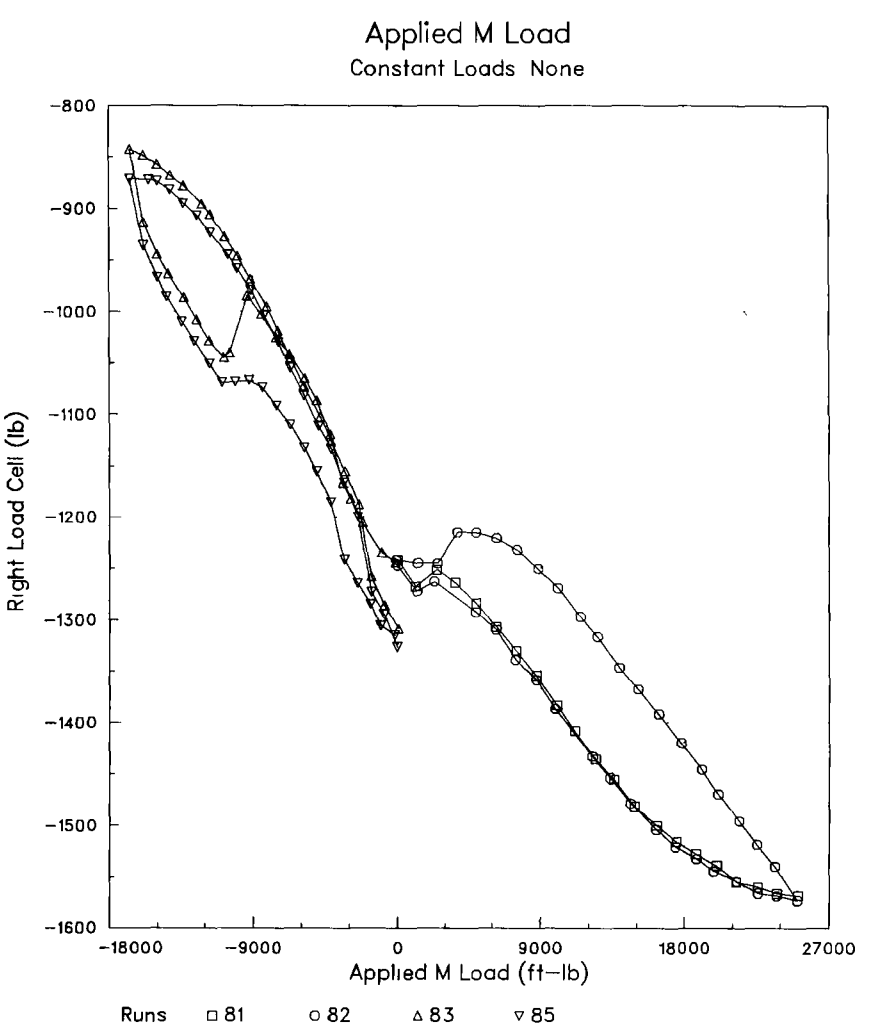

RSRA 741 1983 ROTOR CALIBRATION

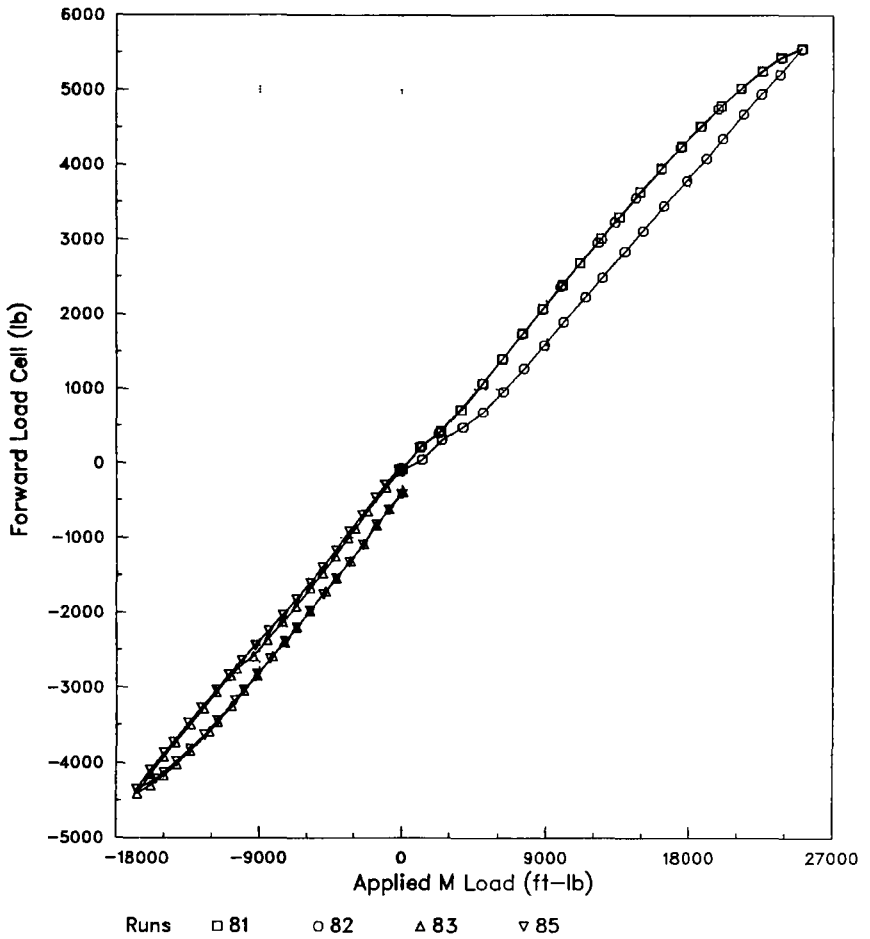

RSRA 741 1983 ROTOR CALIBRATION

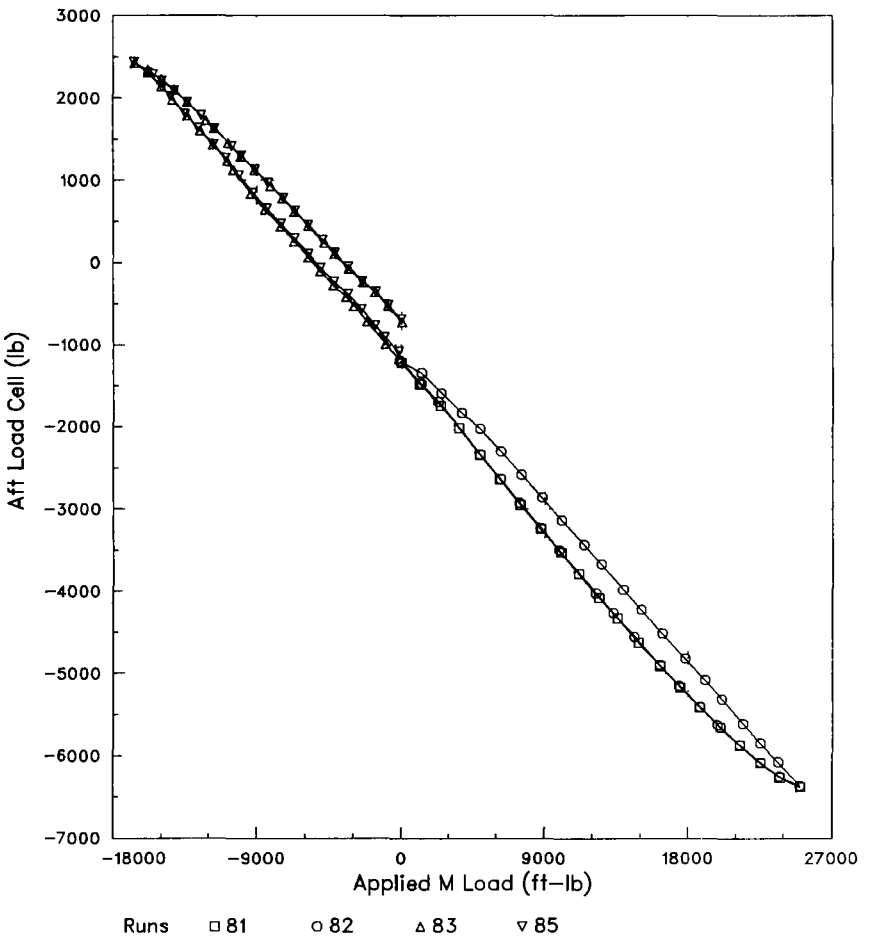

RSRA 741 1983 ROTOR CALIBRATION

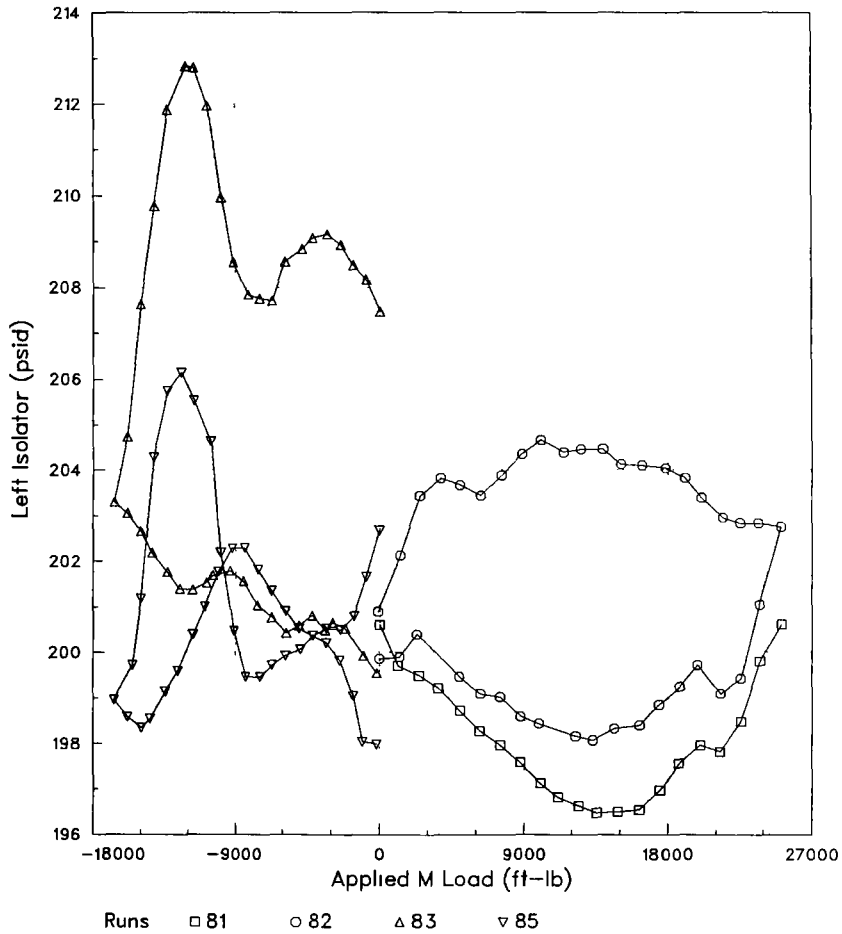

RSRA 741 1983 ROTOR CALIBRATION

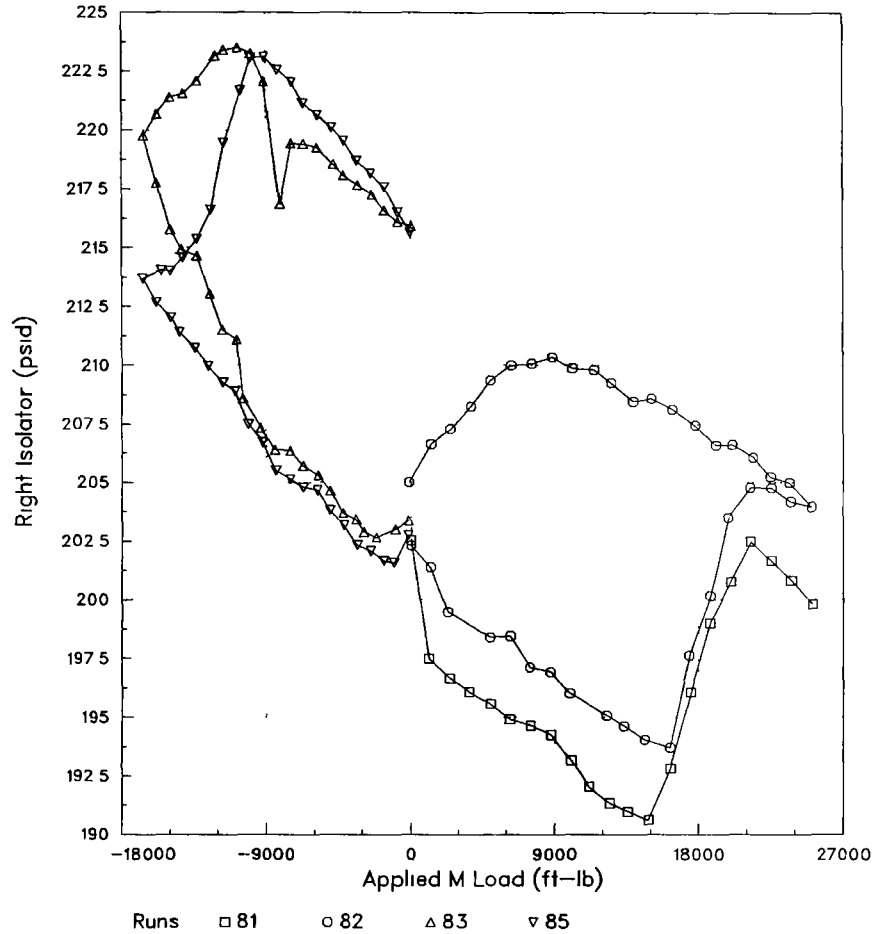

RSRA 741 1983 ROTOR CALIBRATION

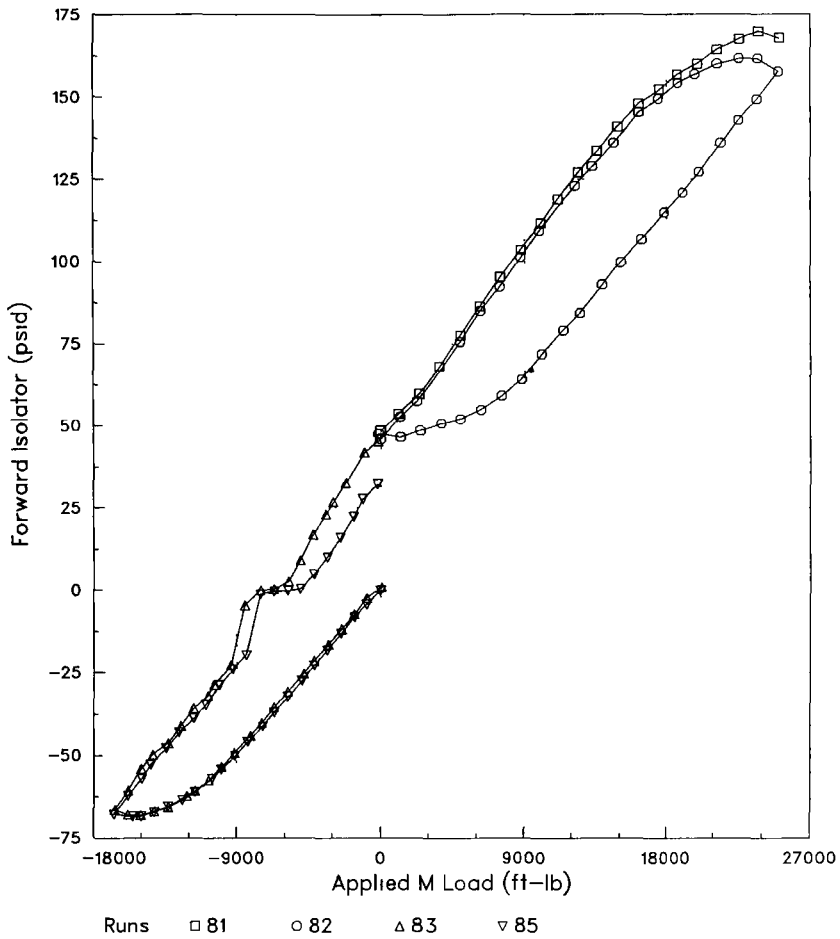

RSRA 741 1983 ROTOR CALIBRATION

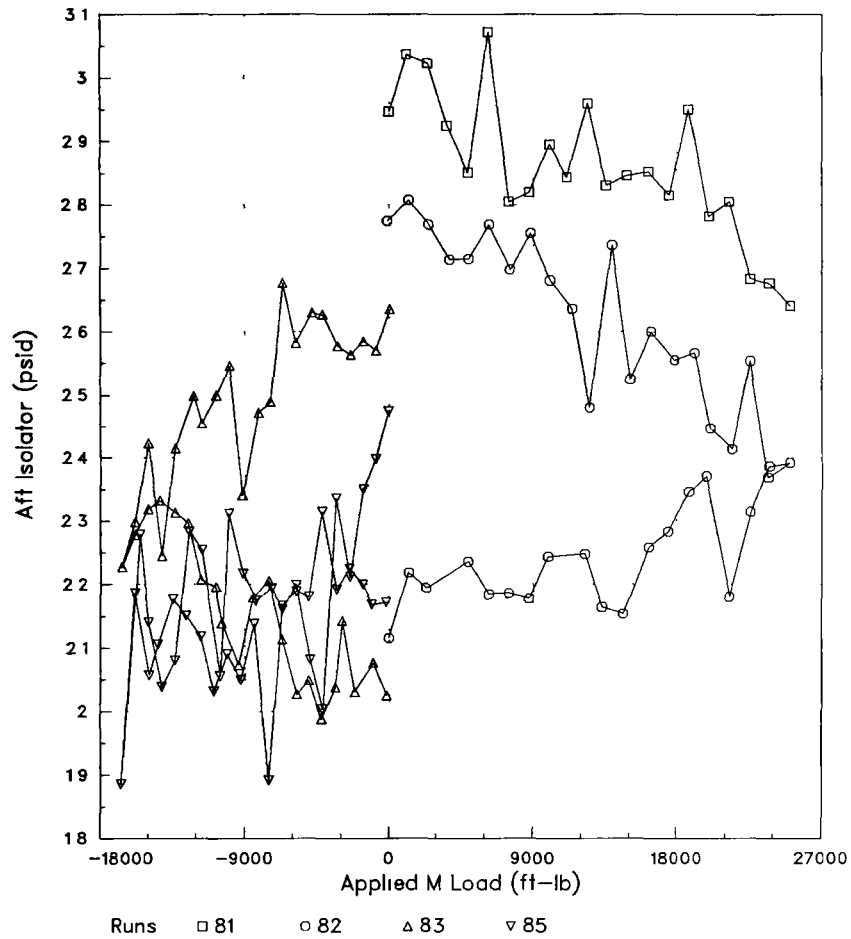

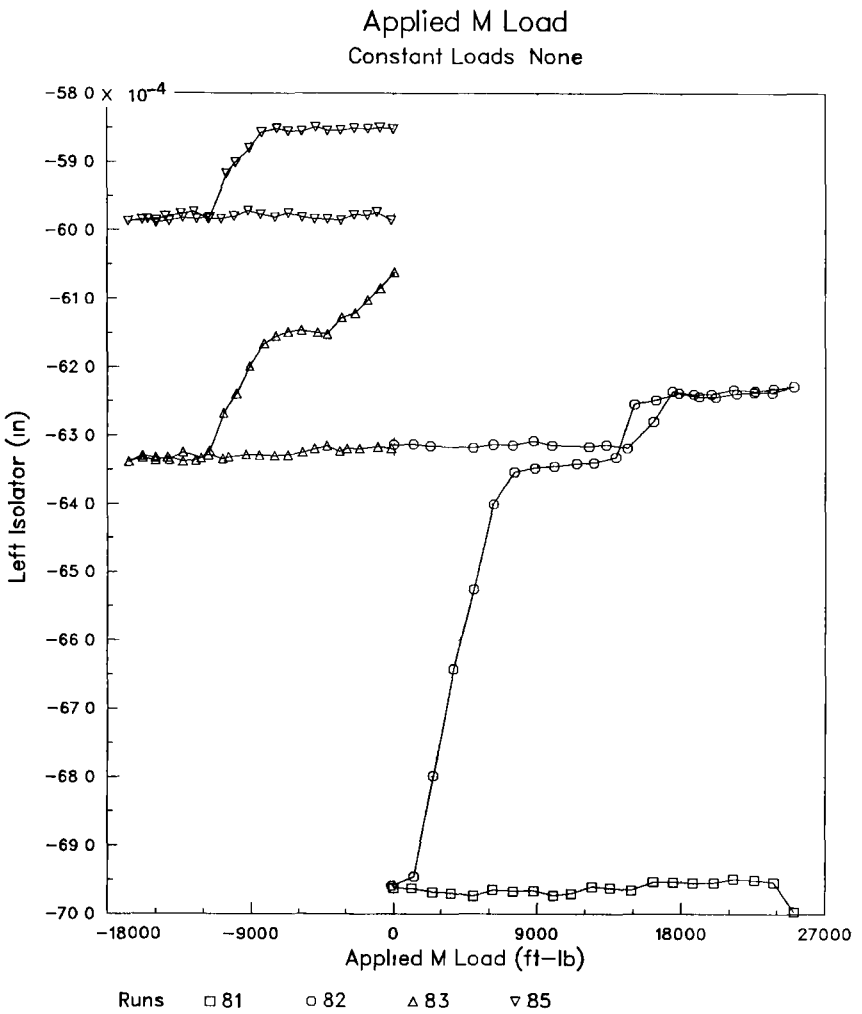

RSRA 741 1983 ROTOR CALIBRATION

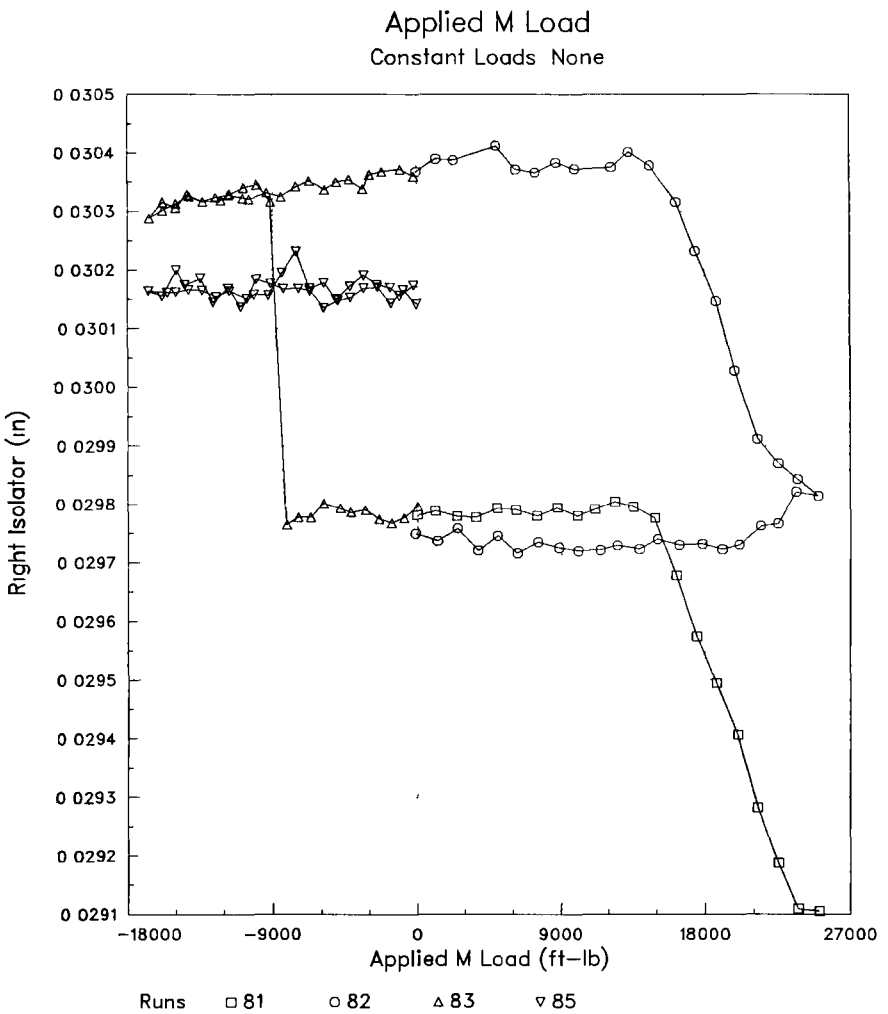

RSRA 741 1983 ROTOR CALIBRATION

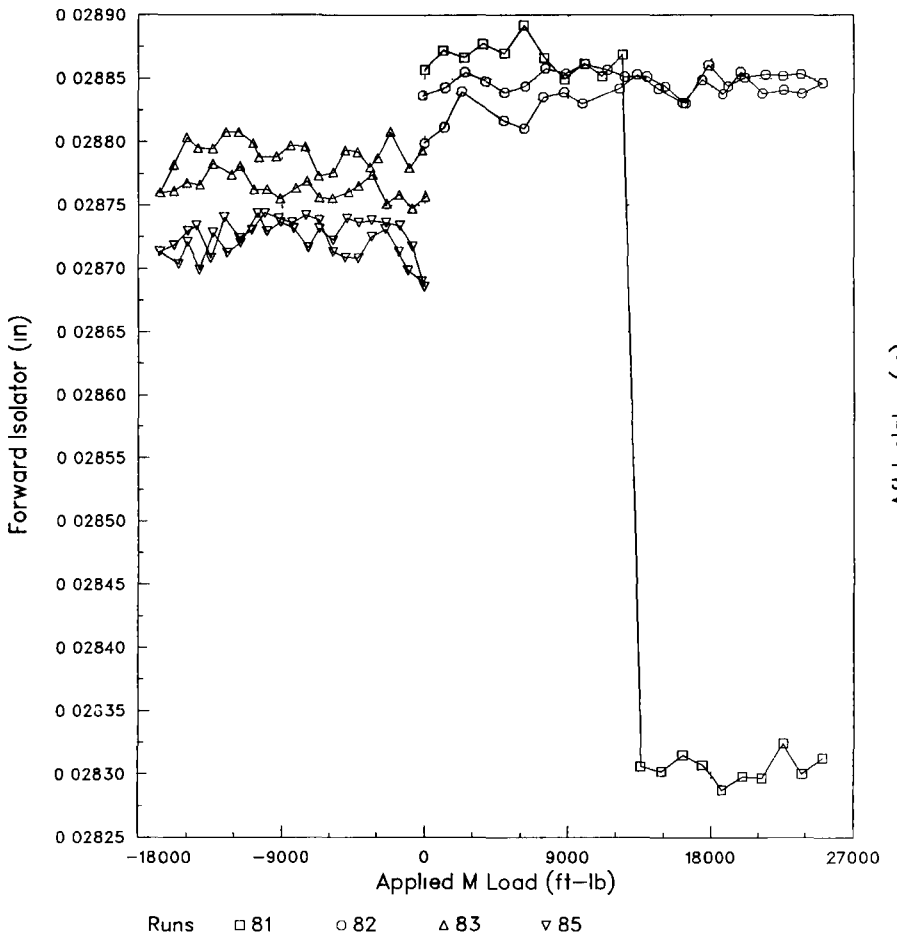

RSRA 741 1983 ROTOR CALIBRATION

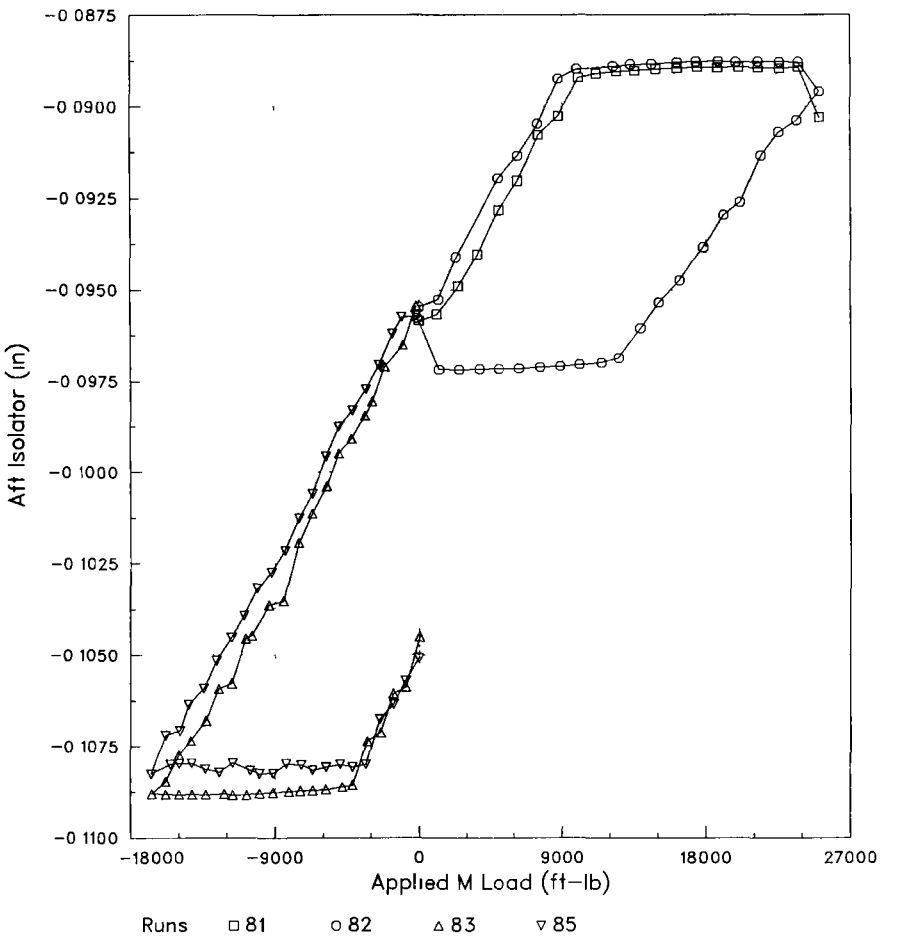

RSRA 741 1983 ROTOR CALIBRATION

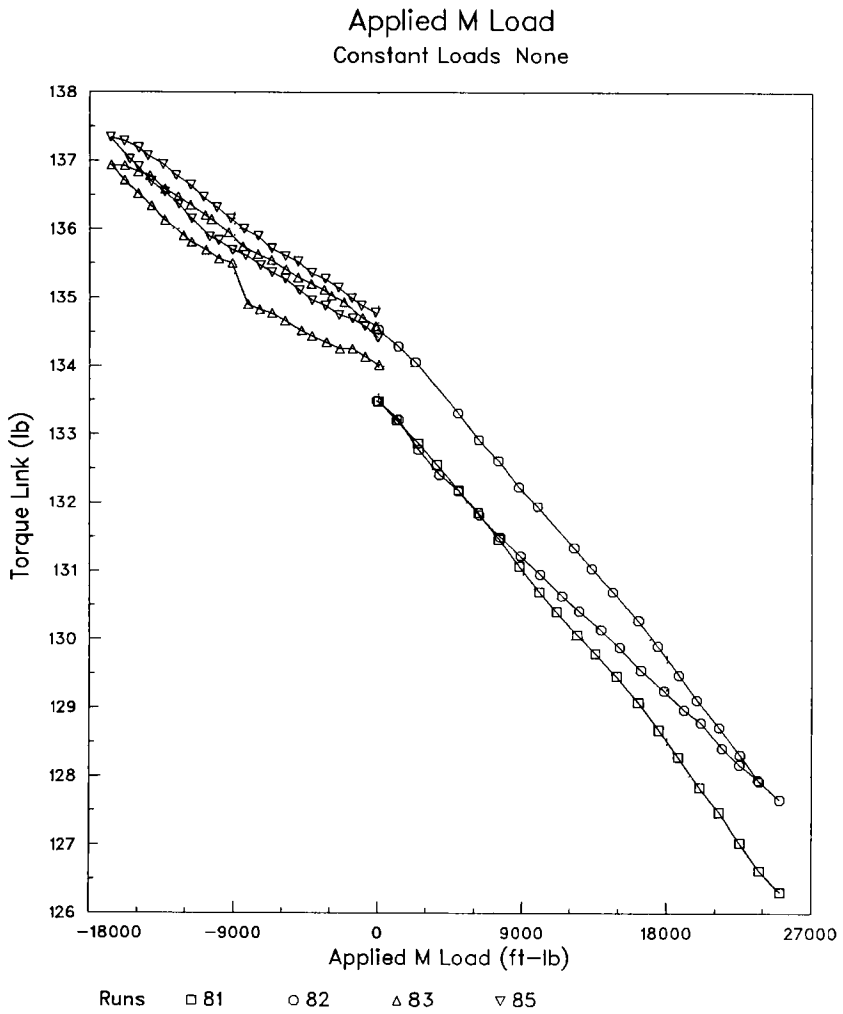

RSRA 741 1983 ROTOR CALIBRATION

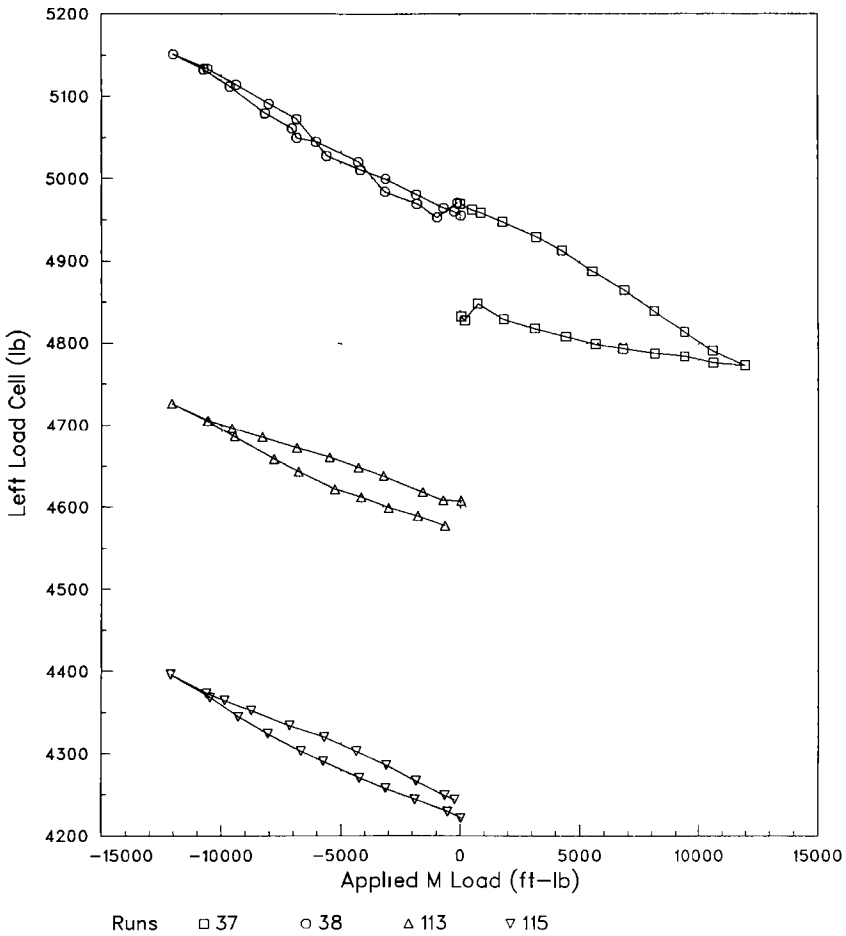

RSRA 741 1983 ROTOR CALIBRATION

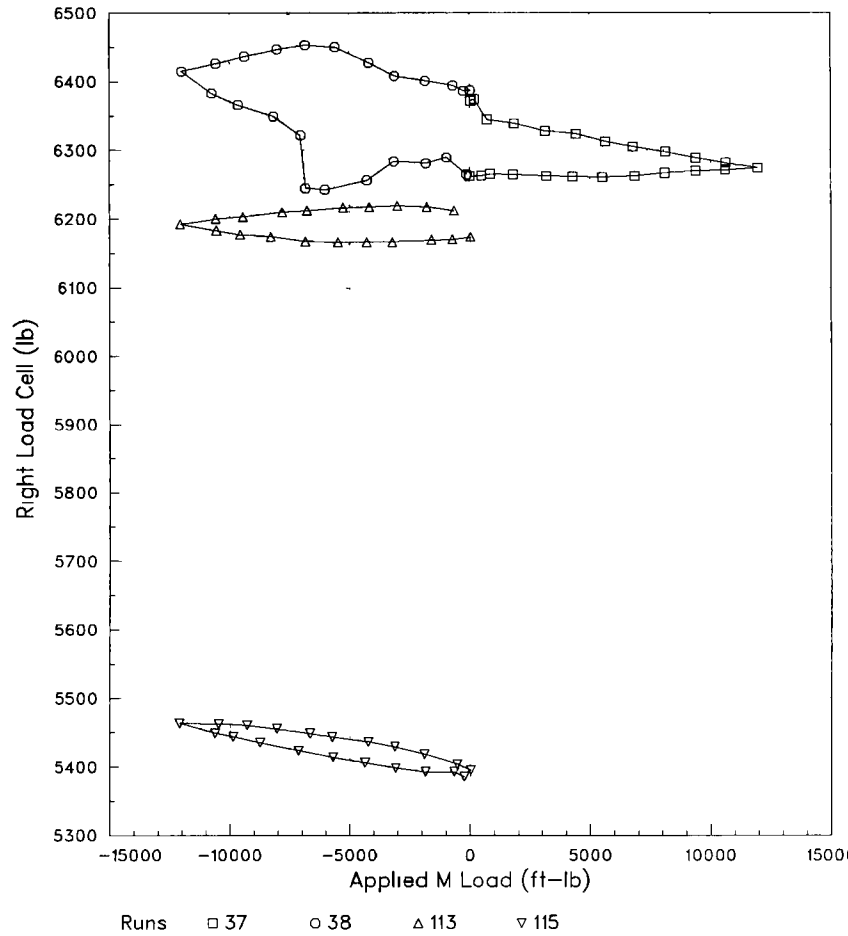

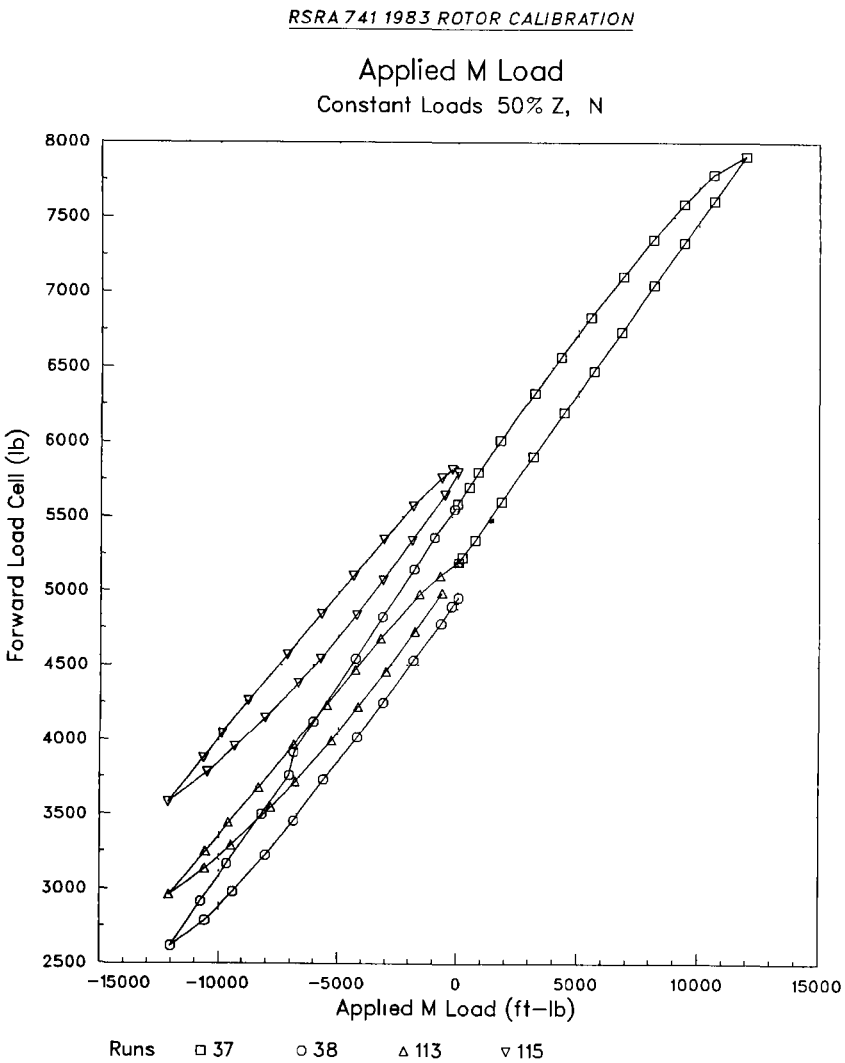
RSRA 741 1983 ROTOR CALIBRATION
Applied M Load
Constant Loads 50% Z, N
Forward Load Cell (lb)
8000
7500
7000
6500
6000
5500
5000
4500
4000
3500
3000
2500
−15000
−10000
−5000
0
5000
10000
15000
Applied M Load (ft−lb)
Runs □ 37 ○ 38 △ 113 ▽ 115

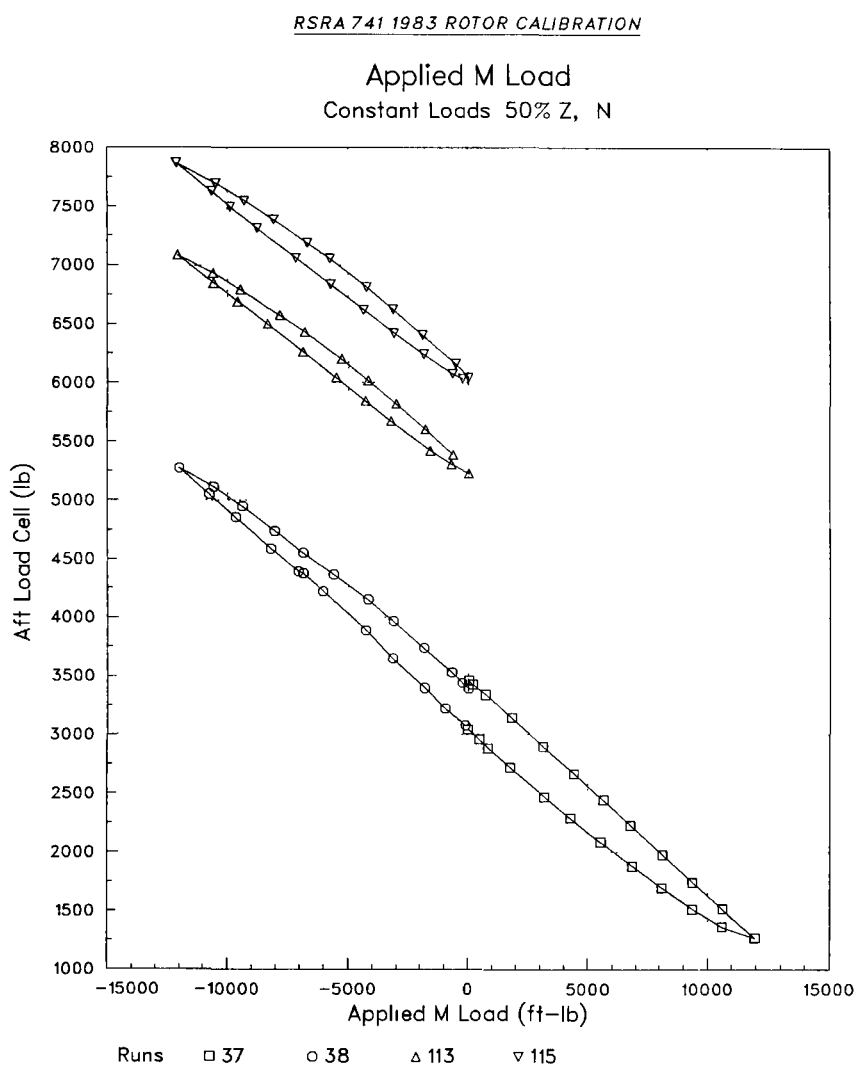
RSRA 741 1983 ROTOR CALIBRATION
Applied M Load
Constant Loads 50% Z, N
Aft Load Cell (lb)
8000
7500
7000
6500
6000
5500
5000
4500
4000
3500
3000
2500
2000
1500
1000
−15000
−10000
−5000
0
5000
10000
15000
Applied M Load (ft−lb)
Runs □ 37 ○ 38 △ 113 ▽ 115

RSRA 741 1983 ROTOR CALIBRATION

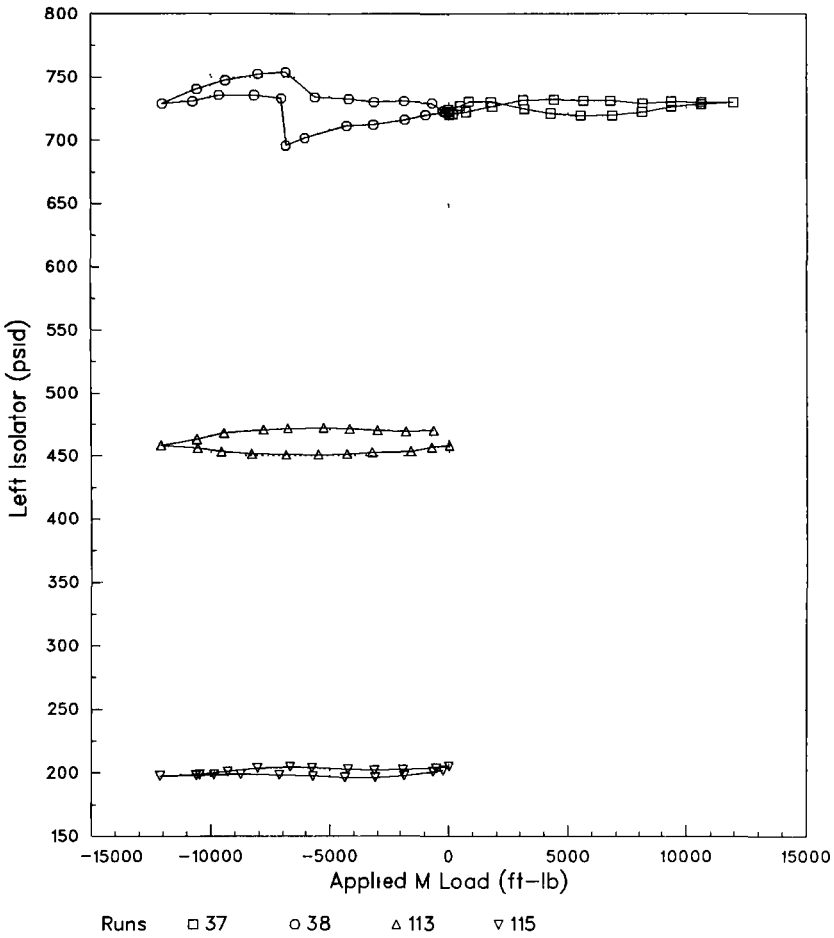

RSRA 741 1983 ROTOR CALIBRATION

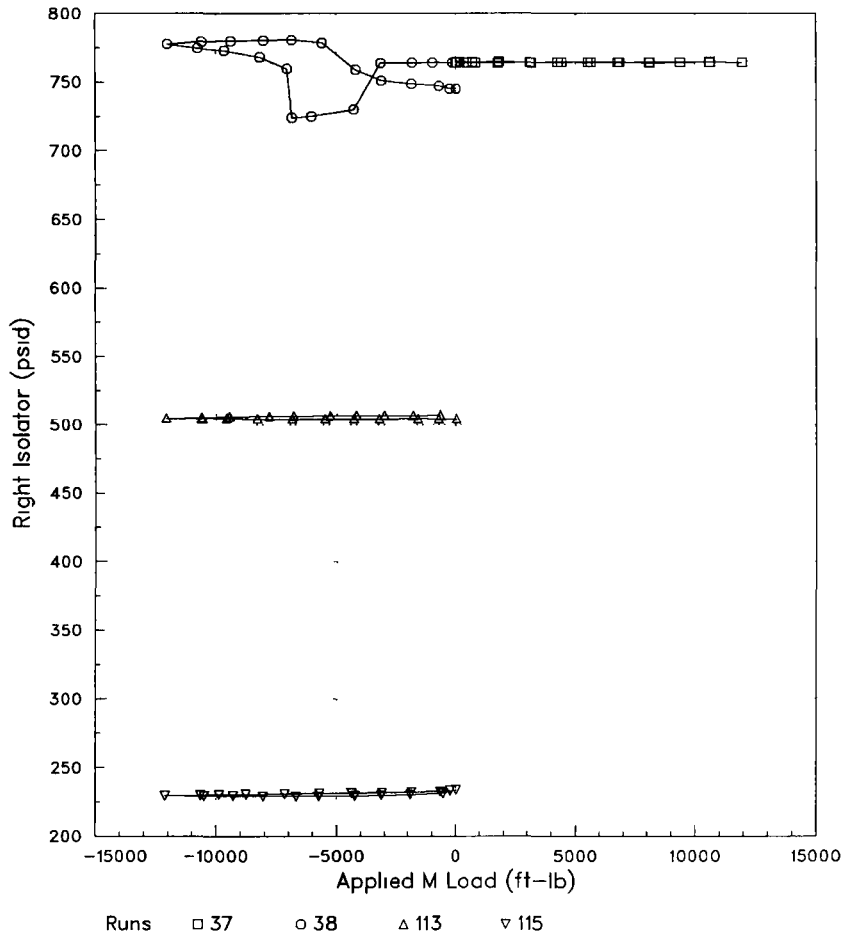

RSRA 741 1983 ROTOR CALIBRATION

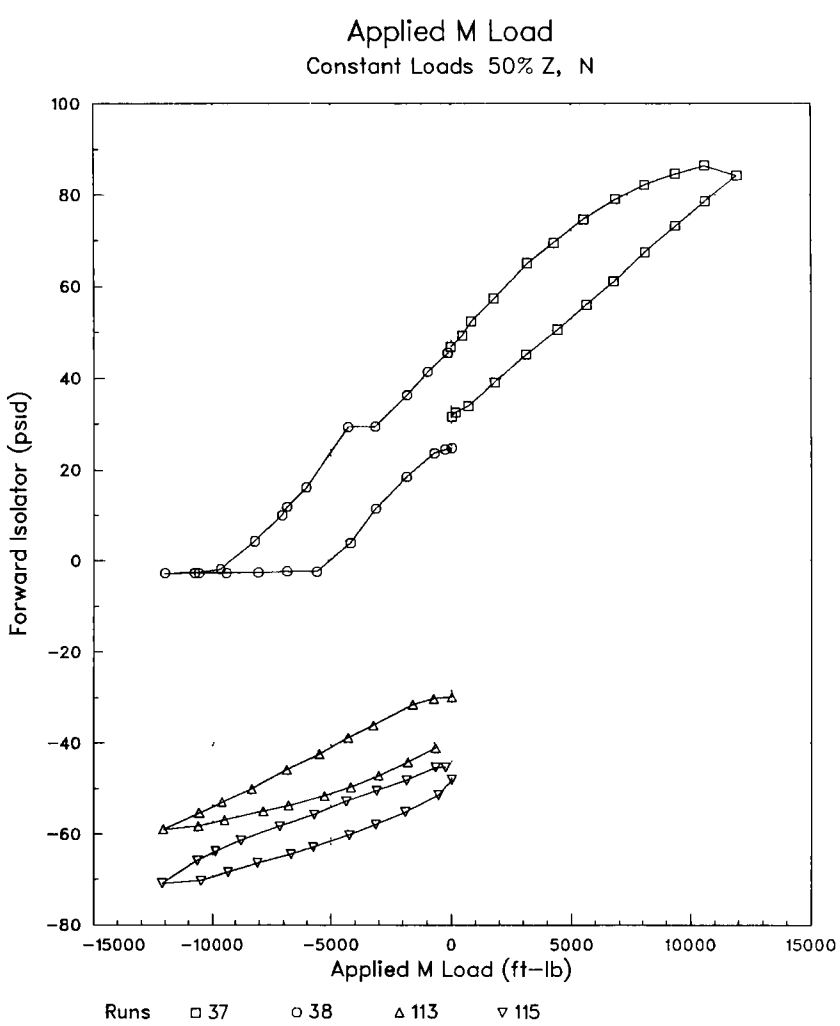

RSRA 741 1983 ROTOR CALIBRATION

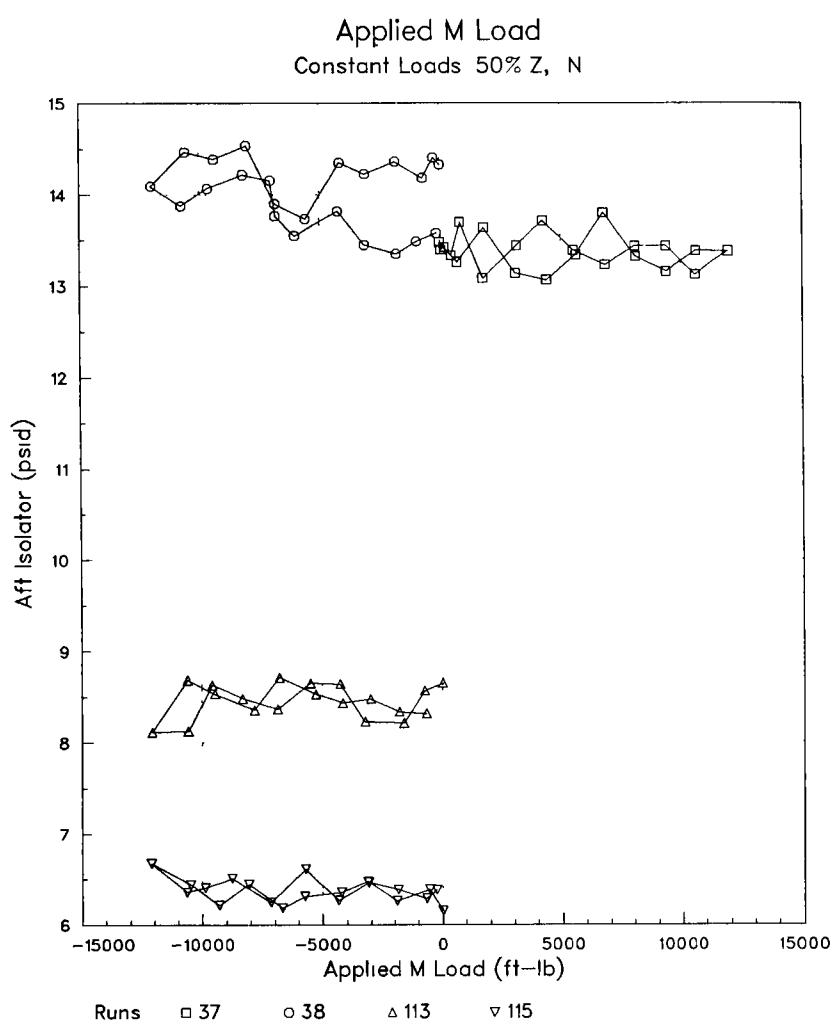

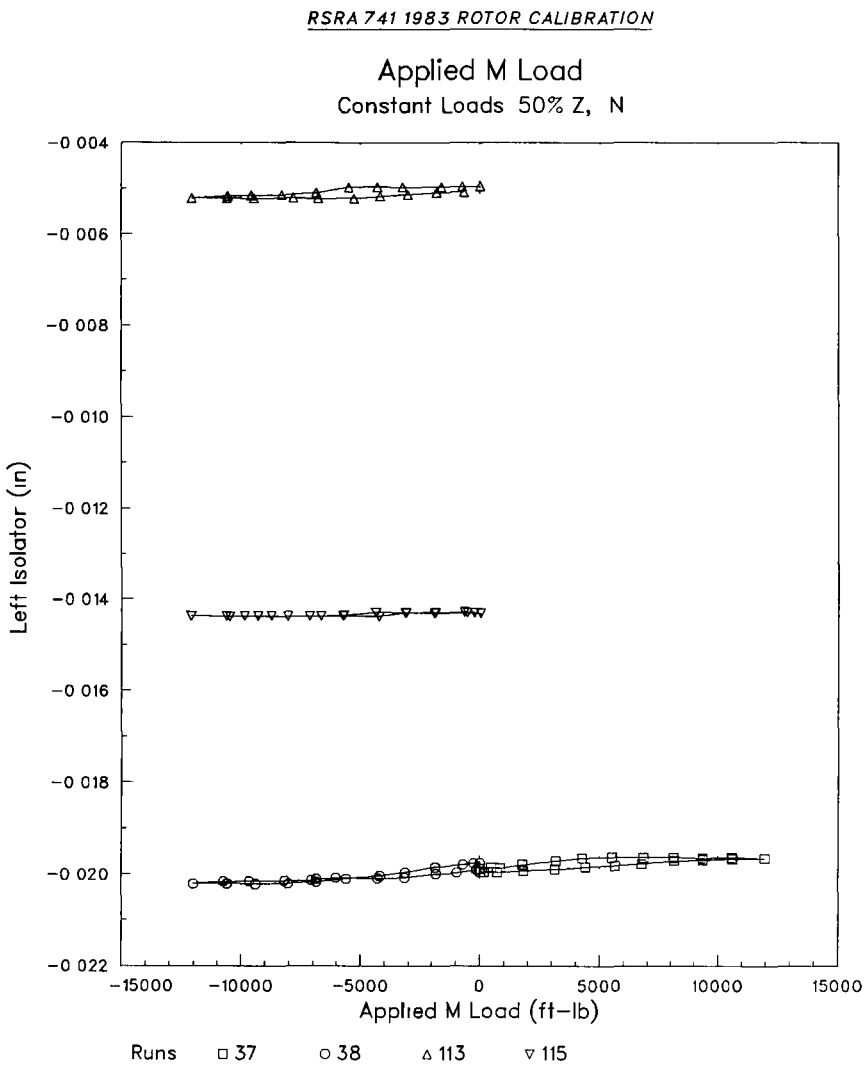
RSRA 741 1983 ROTOR CALIBRATION
Applied M Load
Constant Loads 50% Z, N
Left Isolator (in)
-0 004
-0 006
-0 008
-0 010
-0 012
-0 014
-0 016
-0 018
-0 020
-0 022
-15000
-10000
-5000
0
5000
10000
15000
Applied M Load (ft-lb)
Runs □ 37 ○ 38 △ 113 ▽ 115

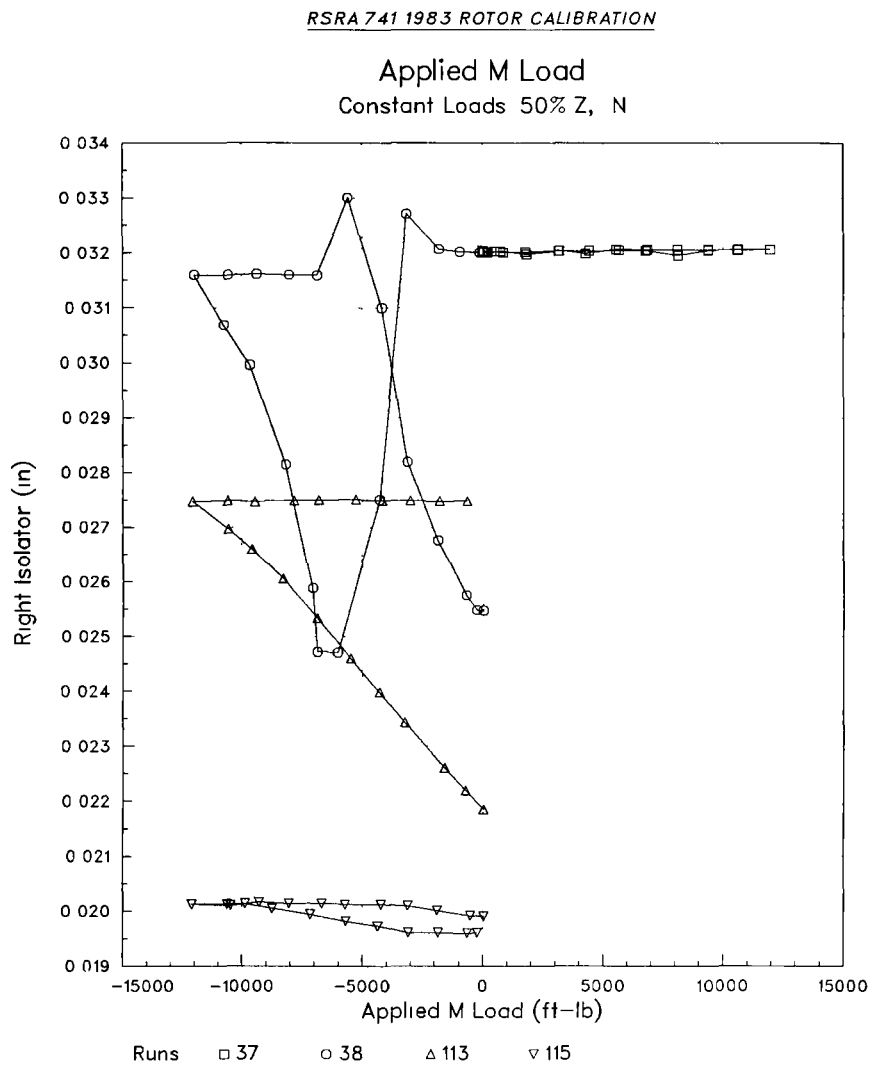
RSRA 741 1983 ROTOR CALIBRATION
Applied M Load
Constant Loads 50% Z, N
Right Isolator (in)
0 034
0 033
0 032
0 031
0 030
0 029
0 028
0 027
0 026
0 025
0 024
0 023
0 022
0 021
0 020
0 019
-15000
-10000
-5000
0
5000
10000
15000
Applied M Load (ft-lb)
Runs □ 37 ○ 38 △ 113 ▽ 115

RSRA 741 1983 ROTOR CALIBRATION

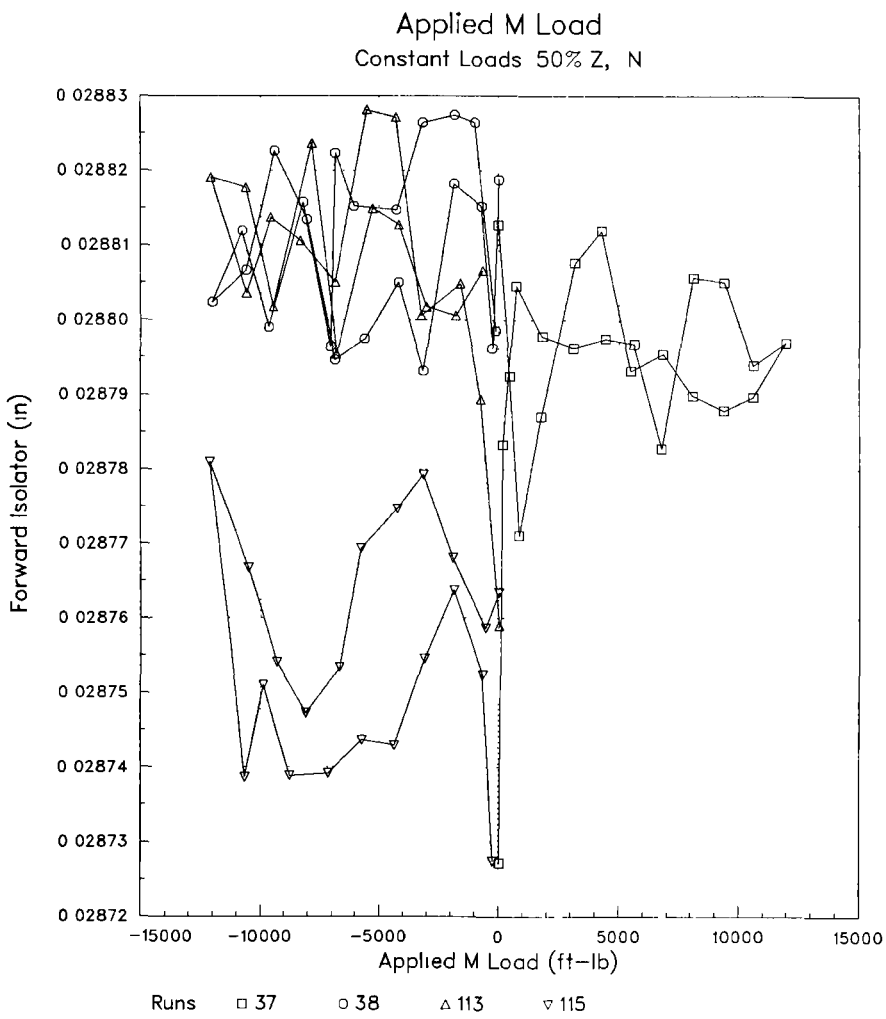

RSRA 741 1983 ROTOR CALIBRATION

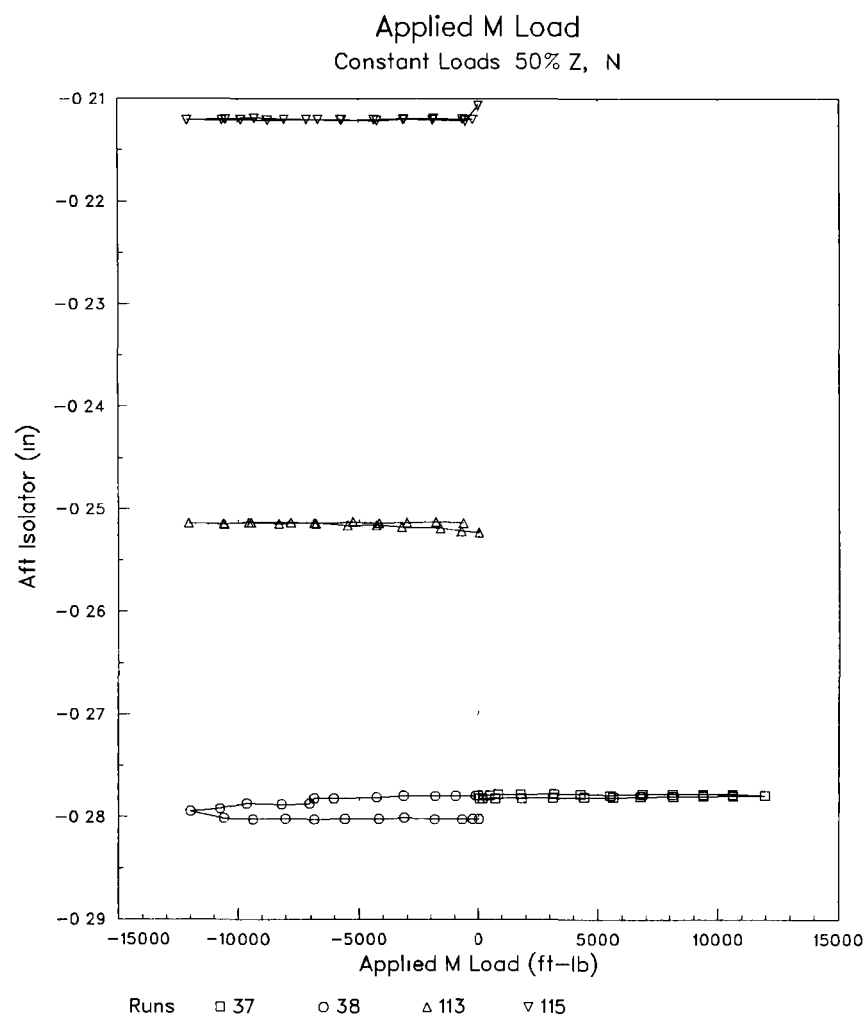

RSRA 741 1983 ROTOR CALIBRATION

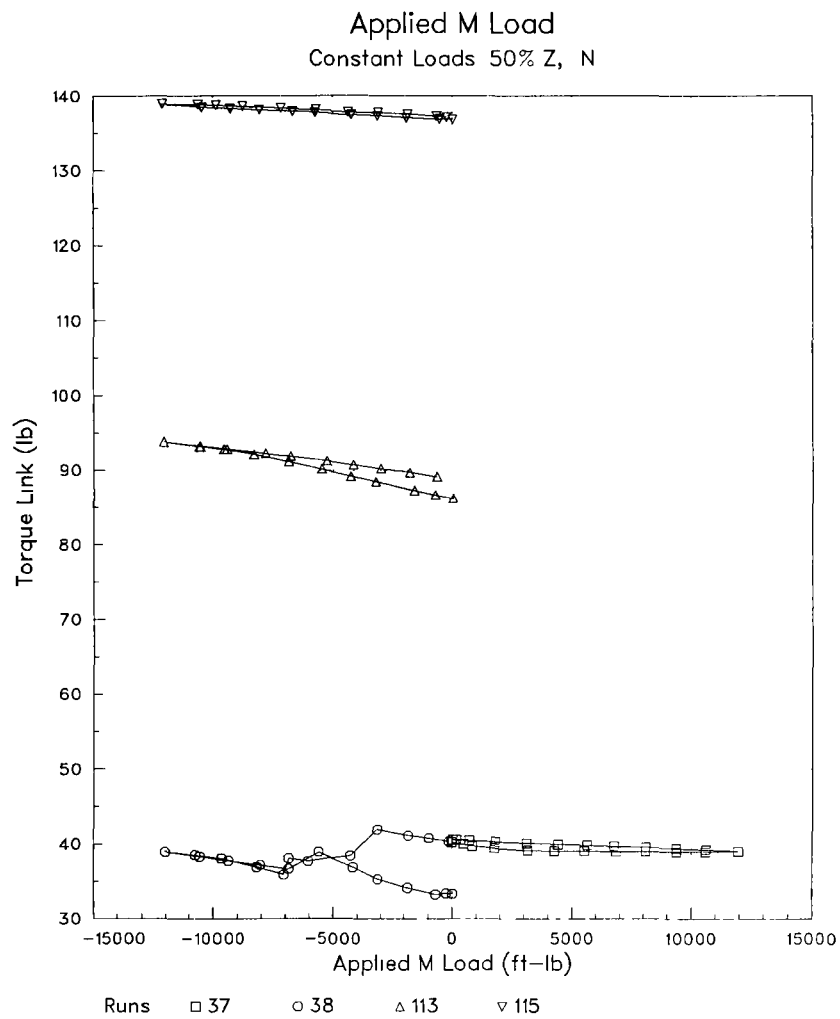

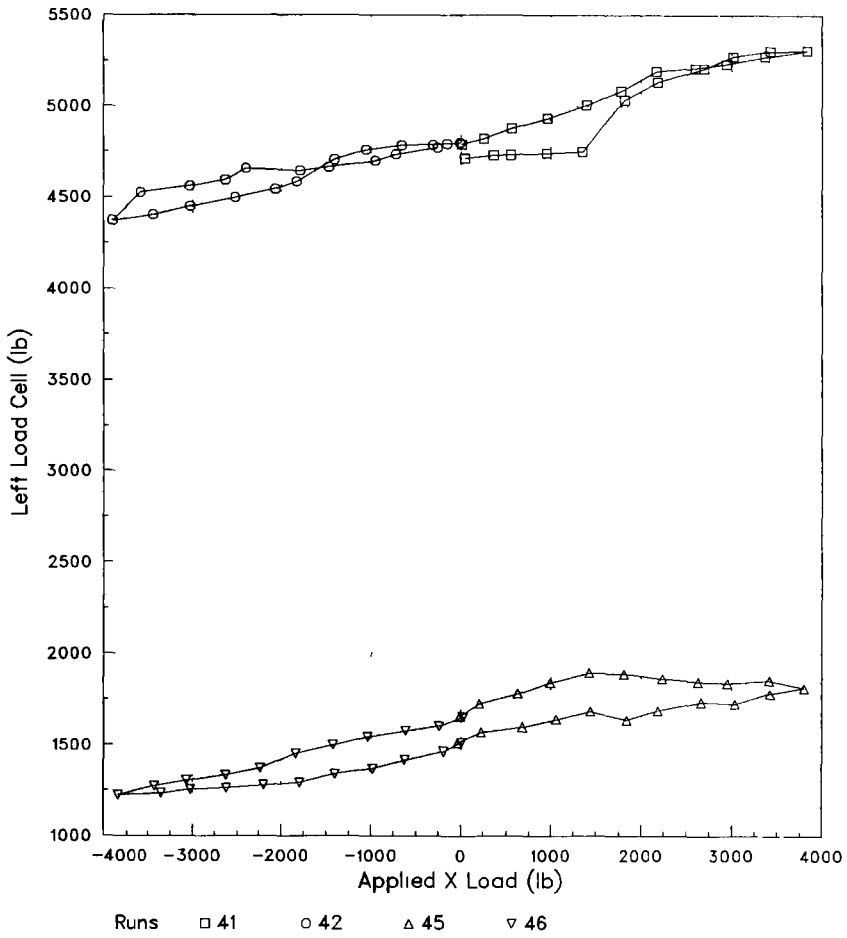

RSRA 741 1983 ROTOR CALIBRATION

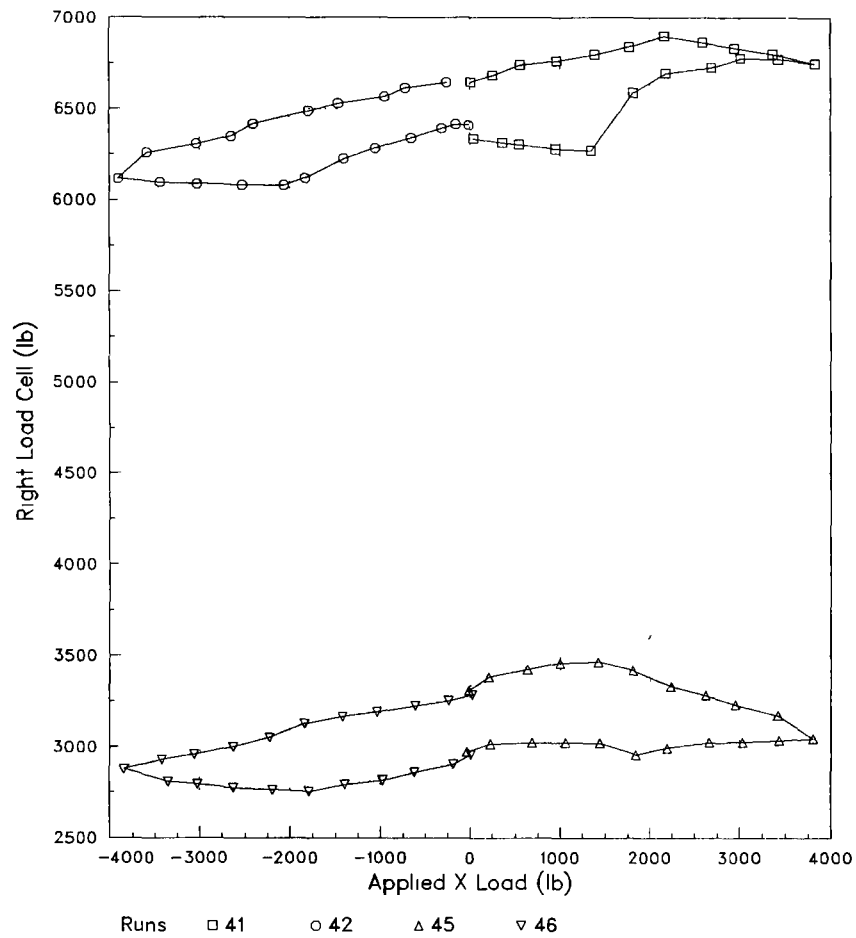

RSRA 741 1983 ROTOR CALIBRATION

Applied X Load
Constant Loads Z & N

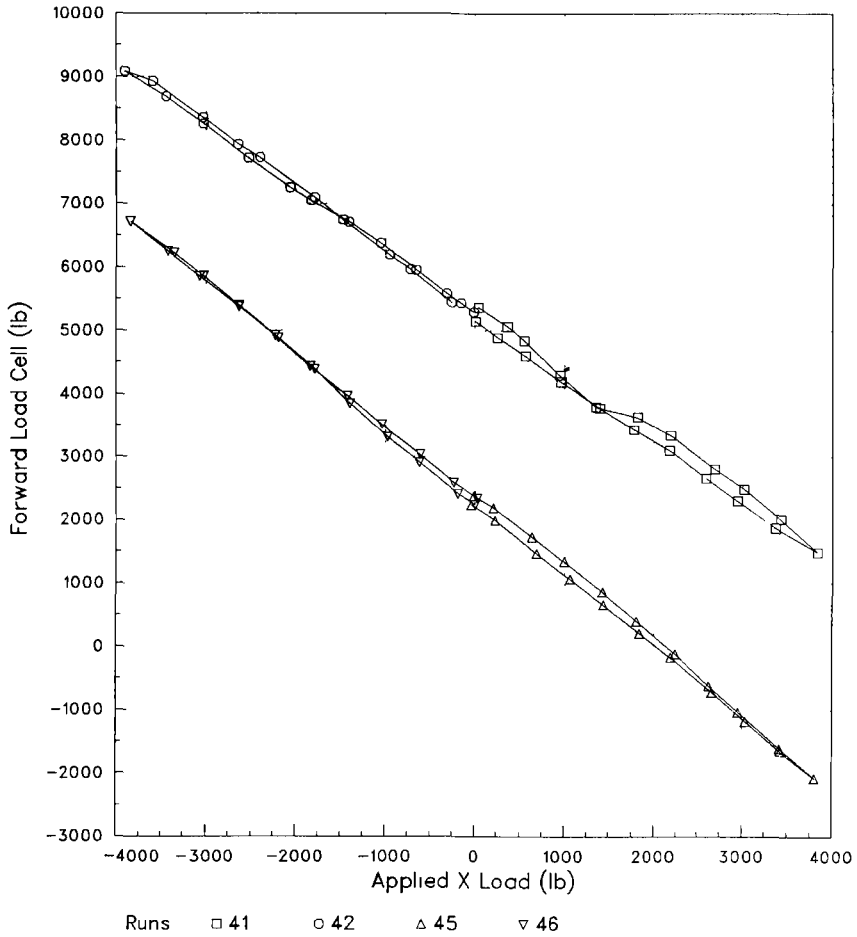

RSRA 741 1983 ROTOR CALIBRATION

Applied X Load
Constant Loads Z & N

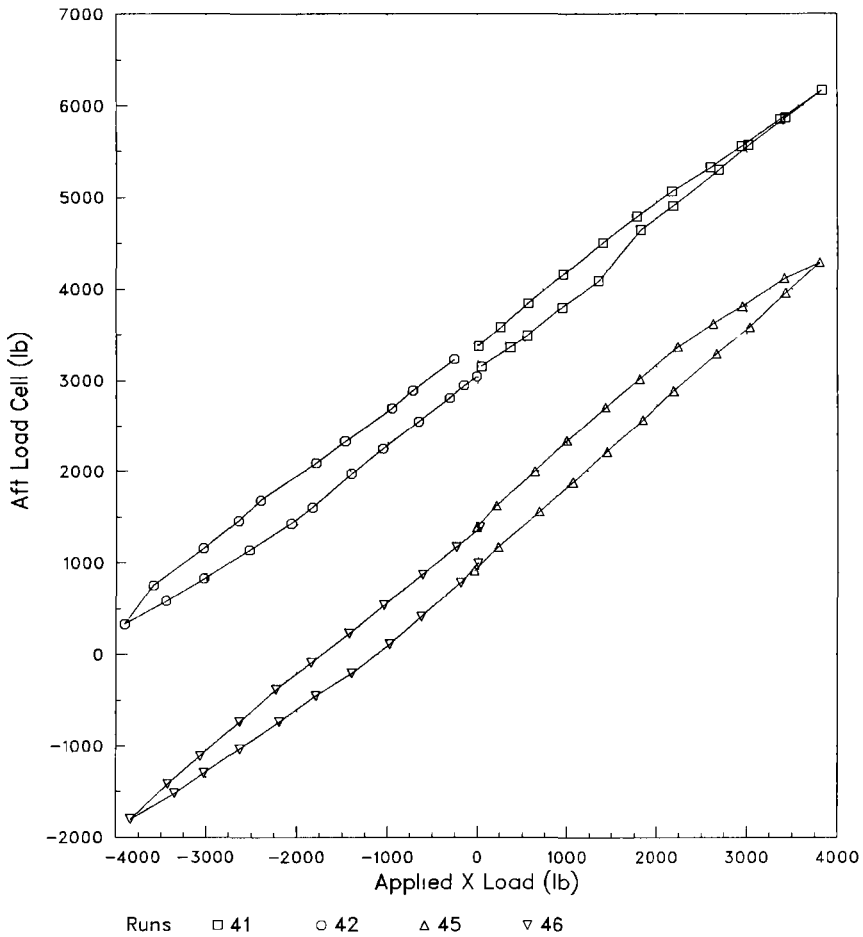

RSRA 741 1983 ROTOR CALIBRATION

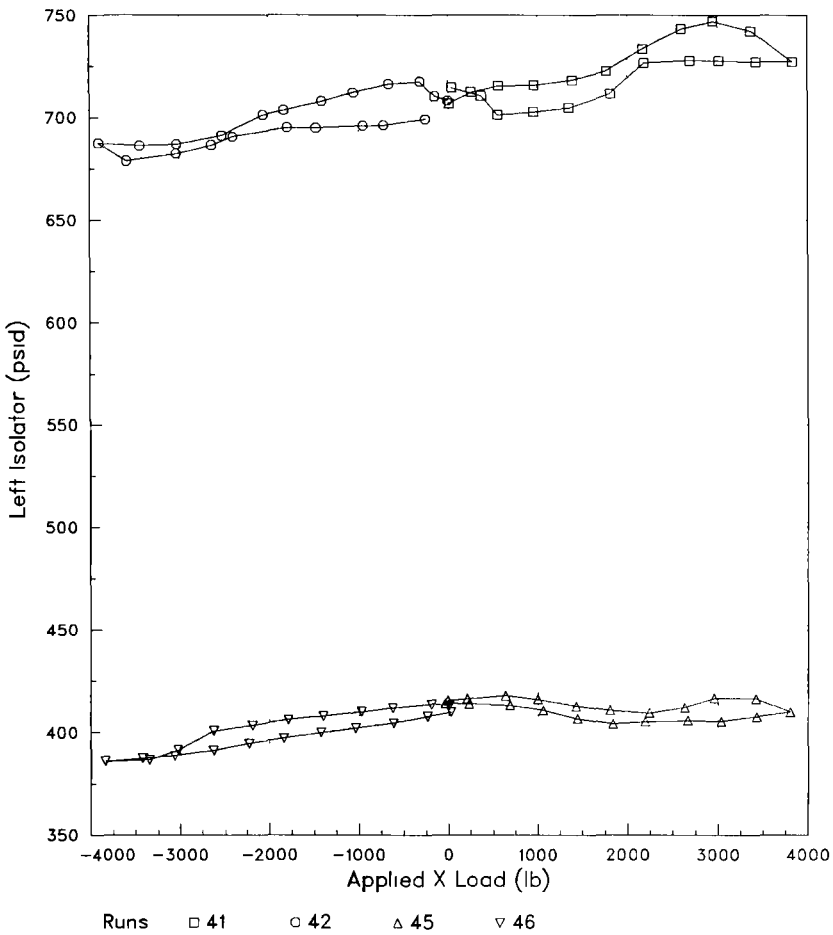

RSRA 741 1983 ROTOR CALIBRATION

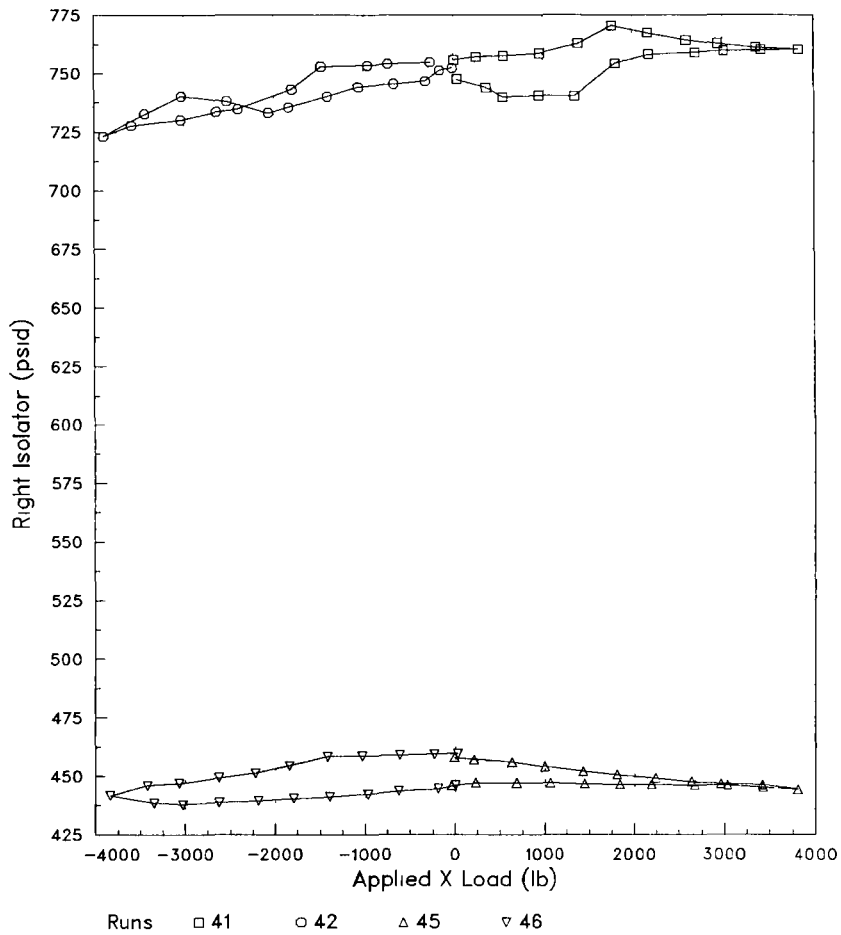

RSRA 741 1983 ROTOR CALIBRATION

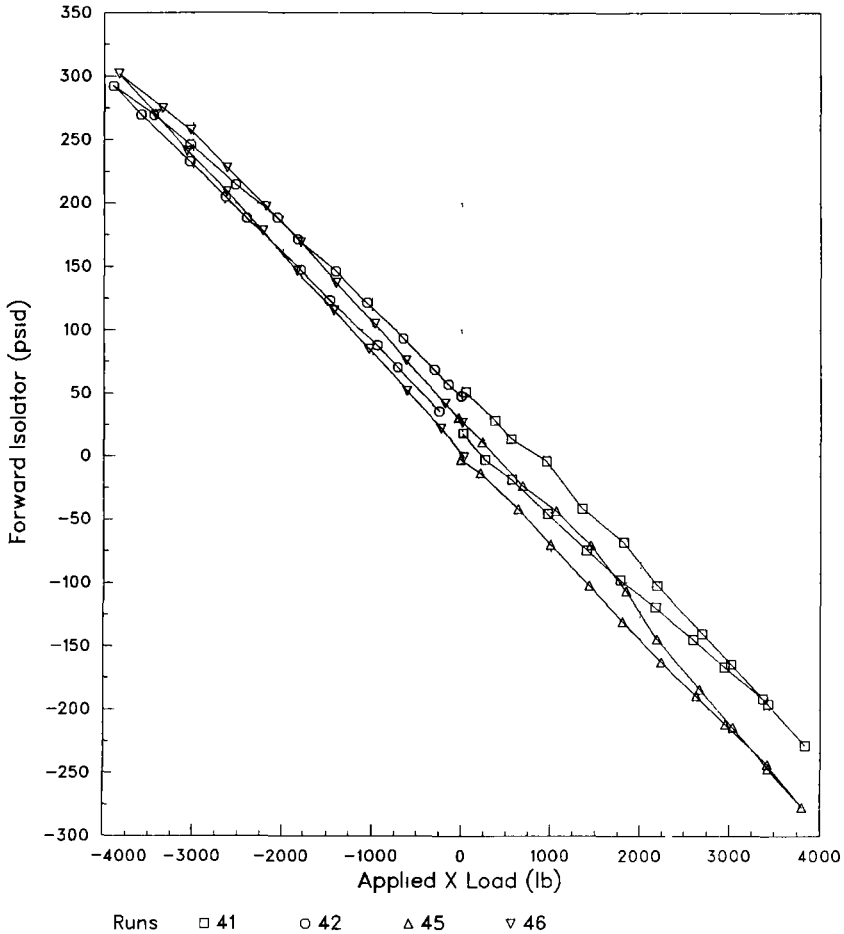

RSRA 741 1983 ROTOR CALIBRATION

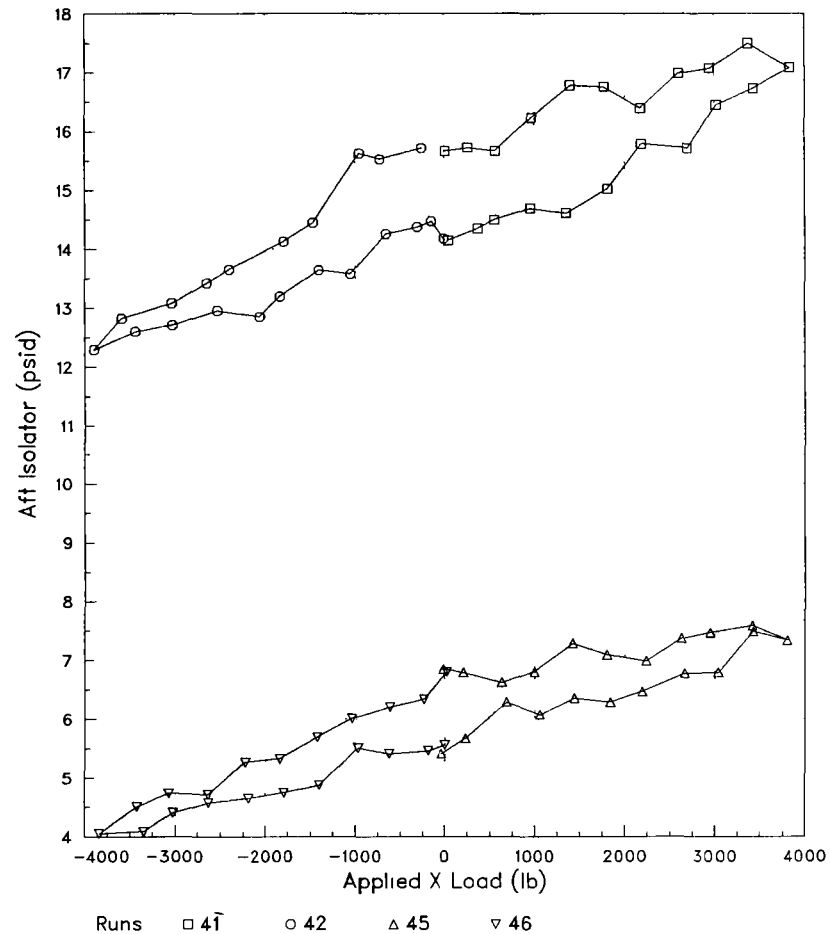

RSRA 741 1983 ROTOR CALIBRATION

Applied X Load

Constant Loads Z & N

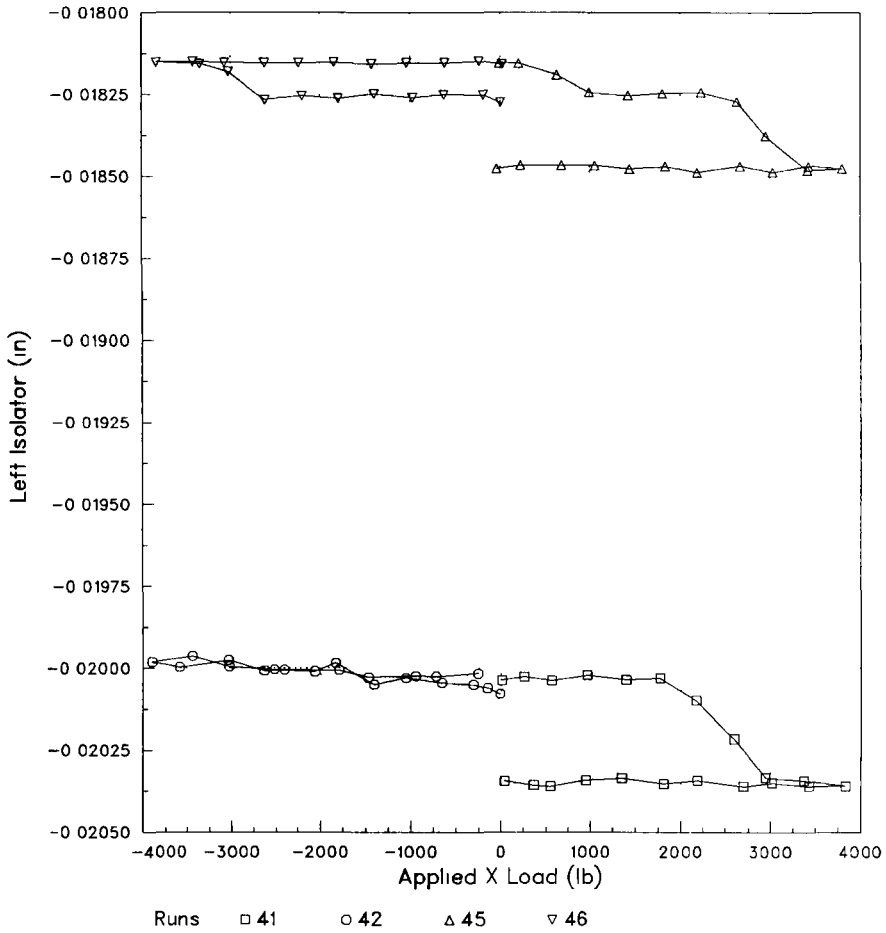

RSRA 741 1983 ROTOR CALIBRATION

Applied X Load

Constant Loads Z & N

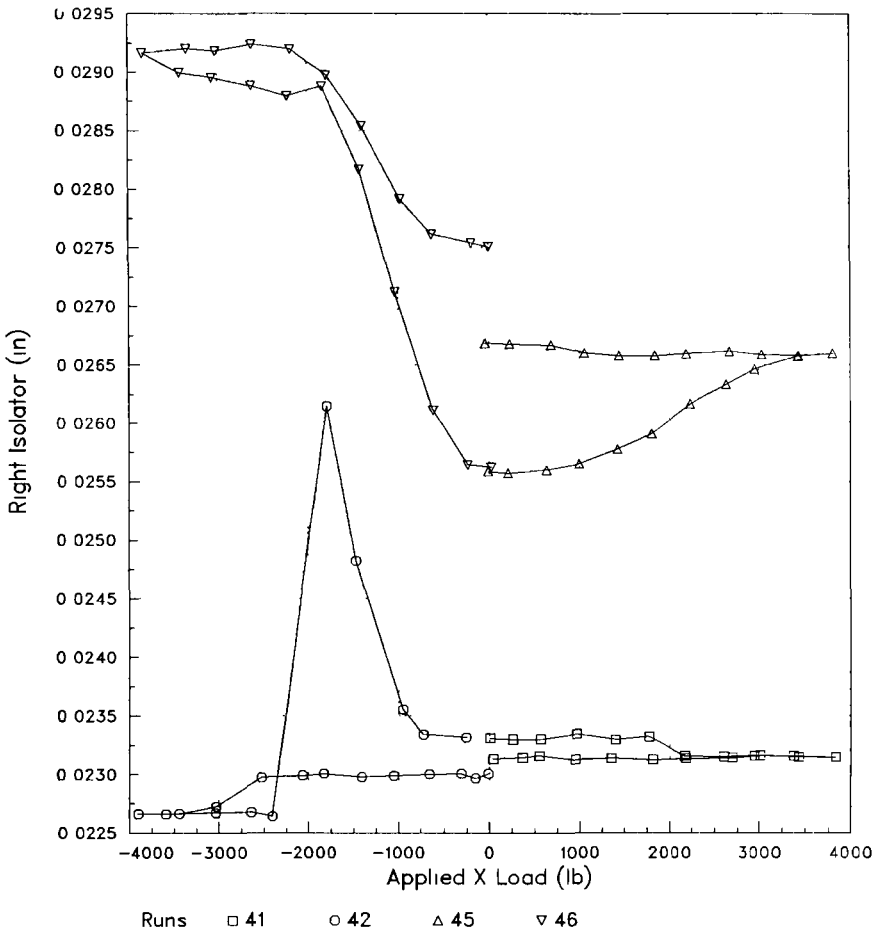

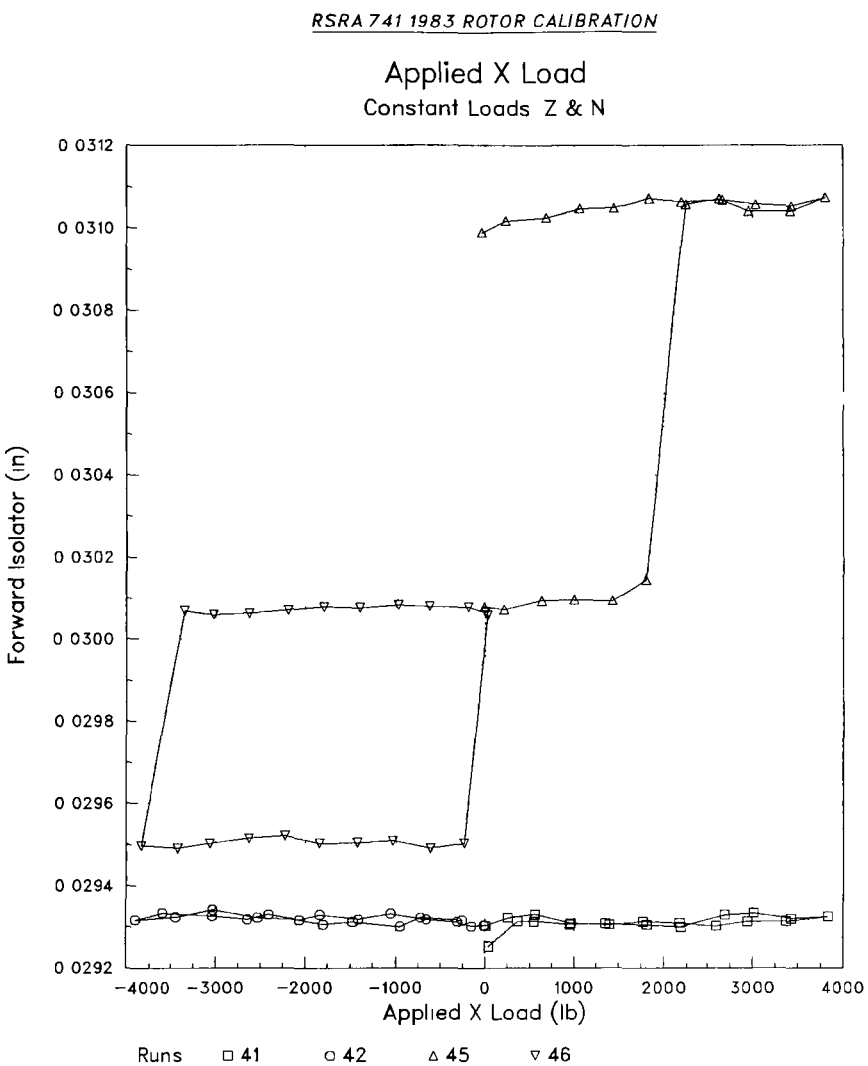
RSRA 741 1983 ROTOR CALIBRATION
Applied X Load
Constant Loads Z & N
Forward Isolator (in)
0 0312
0 0310
0 0308
0 0306
0 0304
0 0302
0 0300
0 0298
0 0296
0 0294
0 0292
−4000 −3000 −2000 −1000 0 1000 2000 3000 4000
Applied X Load (lb)
Runs □ 41 ○ 42 △ 45 ▽ 46

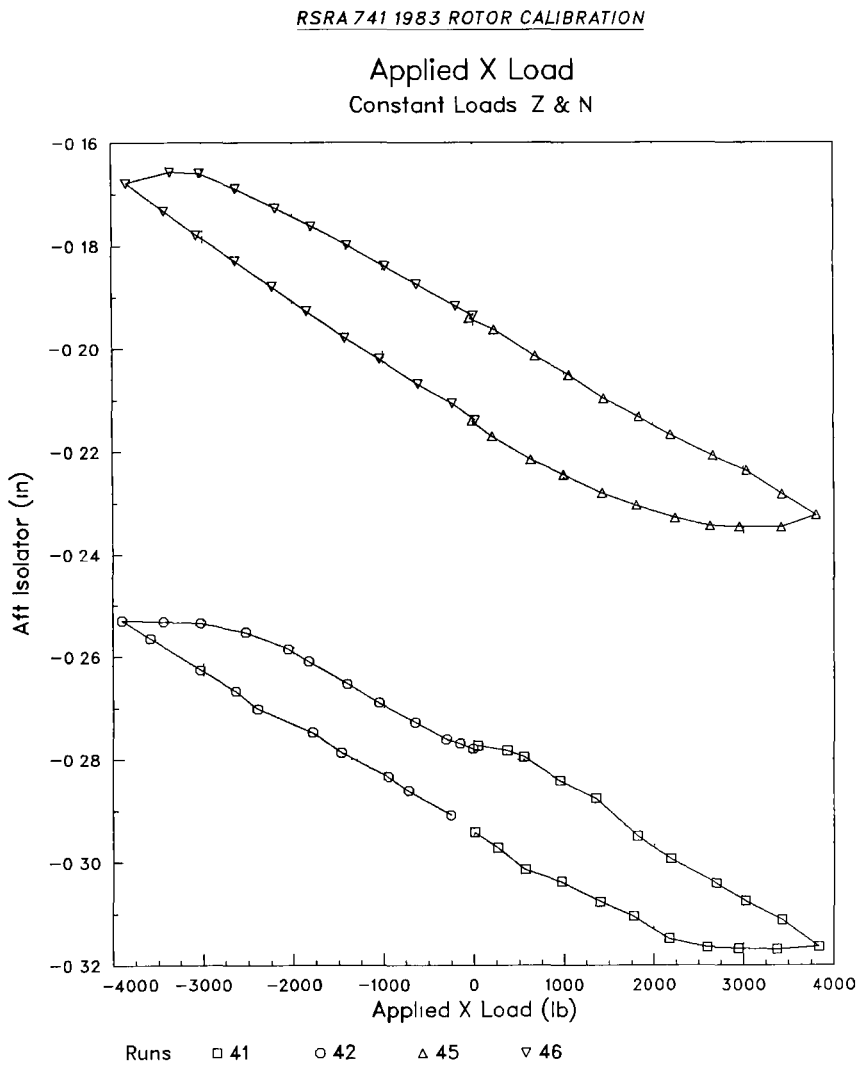
RSRA 741 1983 ROTOR CALIBRATION
Applied X Load
Constant Loads Z & N
Aft Isolator (in)
−0 16
−0 18
−0 20
−0 22
−0 24
−0 26
−0 28
−0 30
−0 32
−4000 −3000 −2000 −1000 0 1000 2000 3000 4000
Applied X Load (lb)
Runs □ 41 ○ 42 △ 45 ▽ 46

RSRA 741 1983 ROTOR CALIBRATION

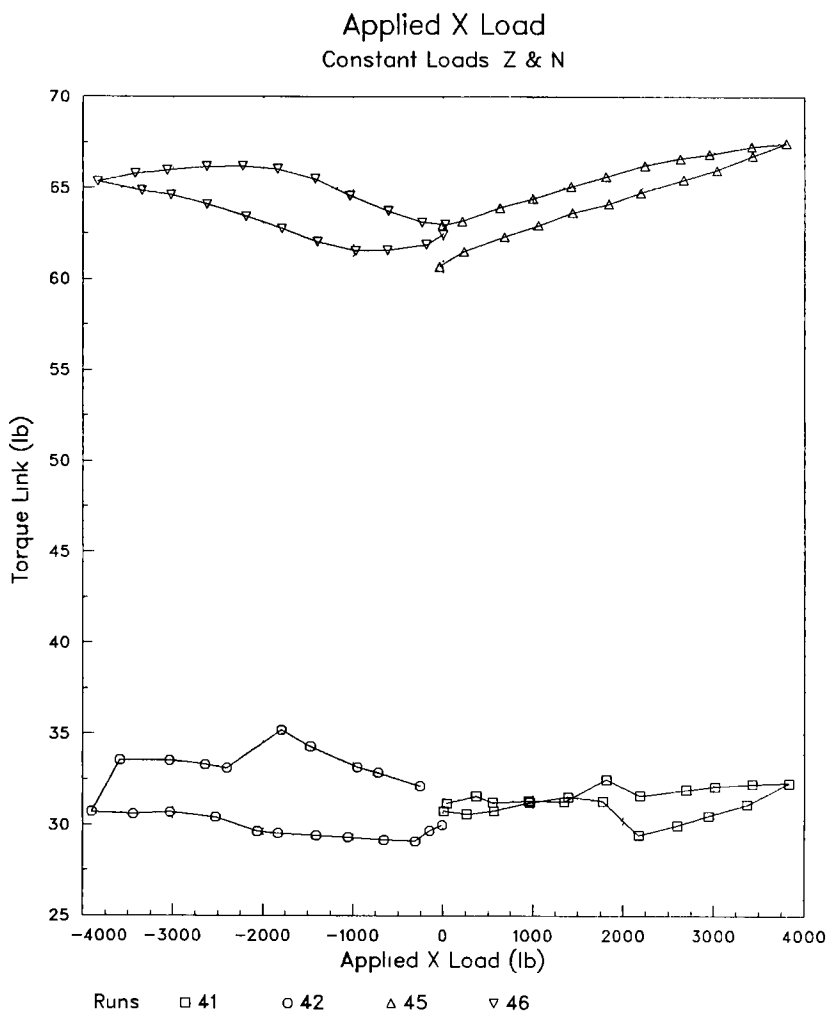

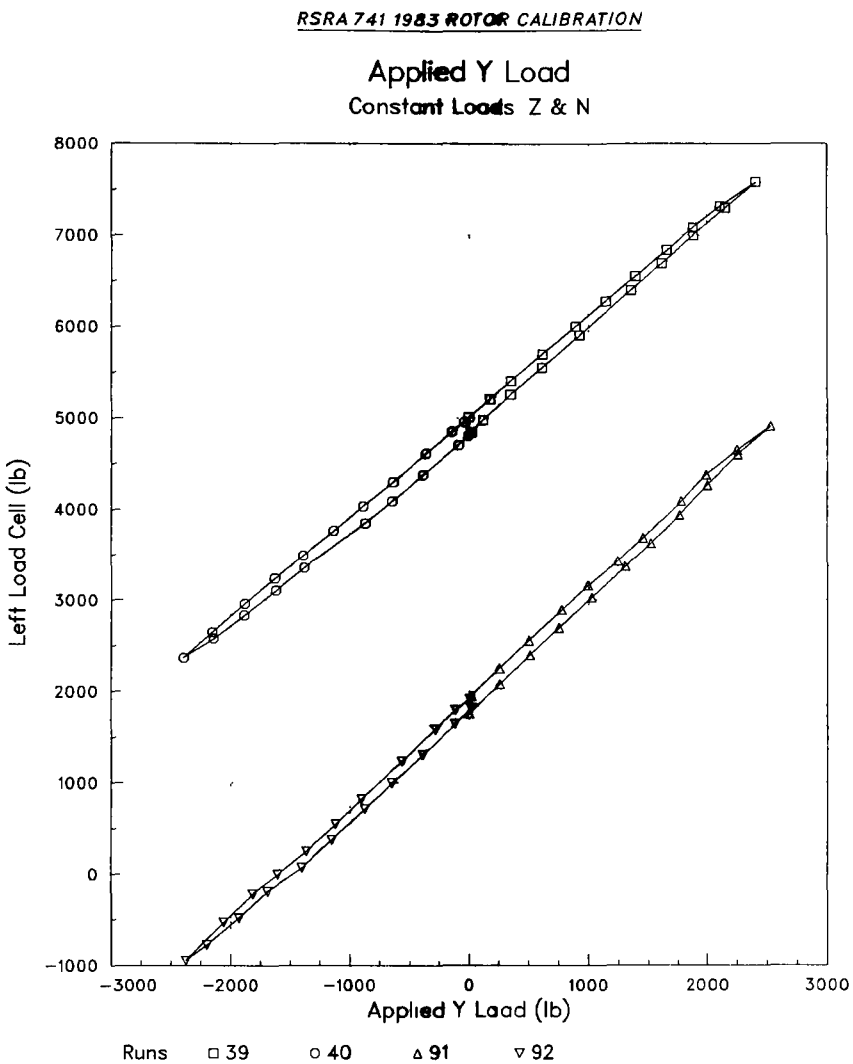
RSRA 741 1983 ROTOR CALIBRATION
Applied Y Load
Constant Loads Z & N
Left Load Cell (lb)
8000
7000
6000
5000
4000
3000
2000
1000
0
-1000
-3000
-2000
-1000
0
1000
2000
3000
Applied Y Load (lb)
Runs □ 39 ○ 40 △ 91 ▽ 92

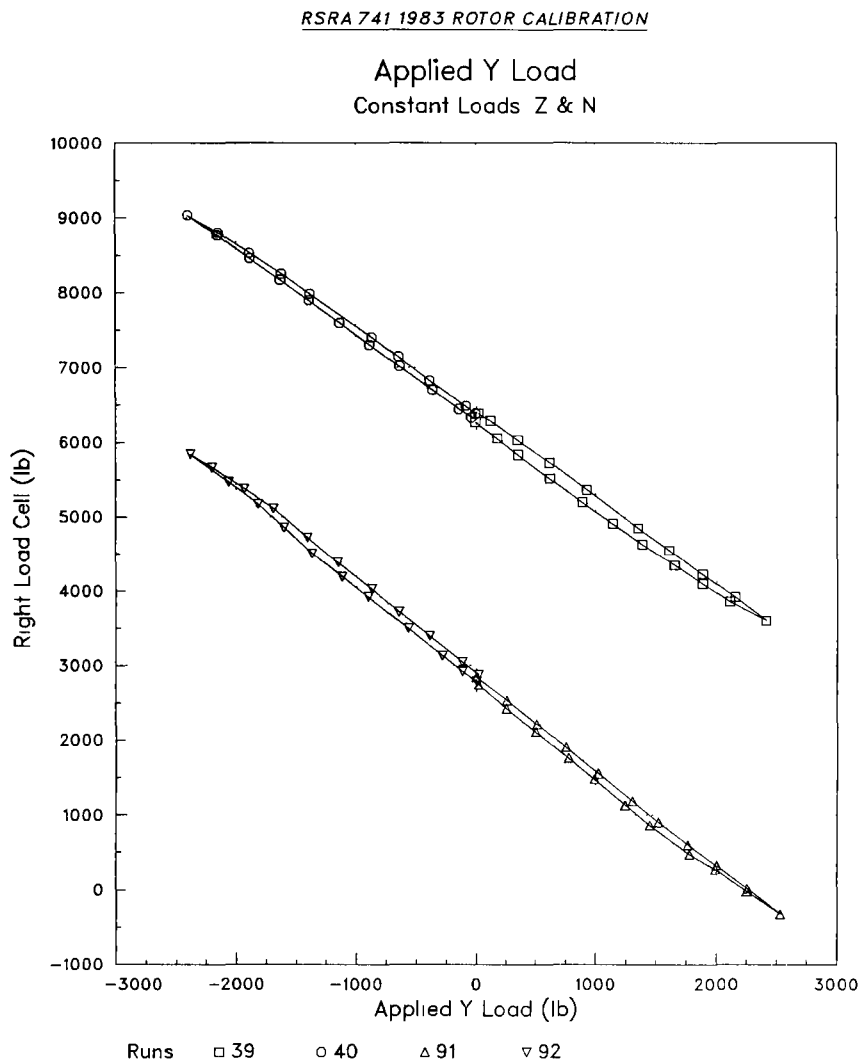
RSRA 741 1983 ROTOR CALIBRATION
Applied Y Load
Constant Loads Z & N
Right Load Cell (lb)
10000
9000
8000
7000
6000
5000
4000
3000
2000
1000
0
-1000
-3000
-2000
-1000
0
1000
2000
3000
Applied Y Load (lb)
Runs □ 39 ○ 40 △ 91 ▽ 92

RSRA 741 1983 ROTOR CALIBRATION

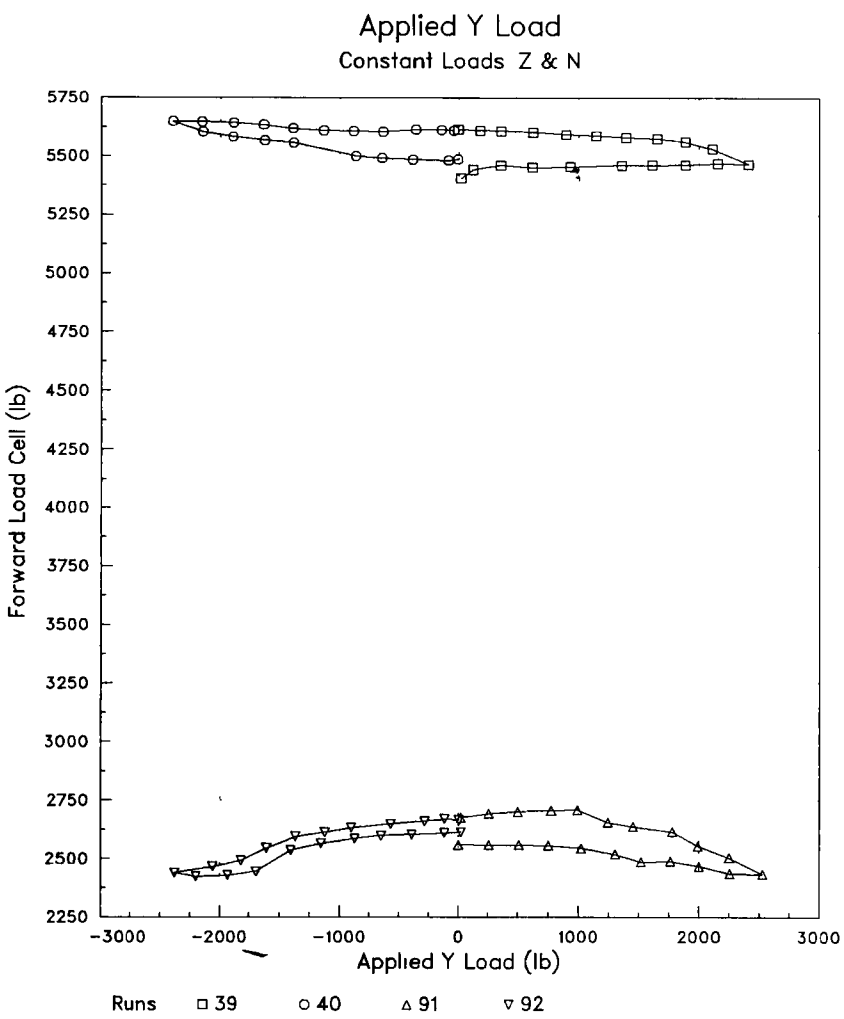

RSRA 741 1983 ROTOR CALIBRATION

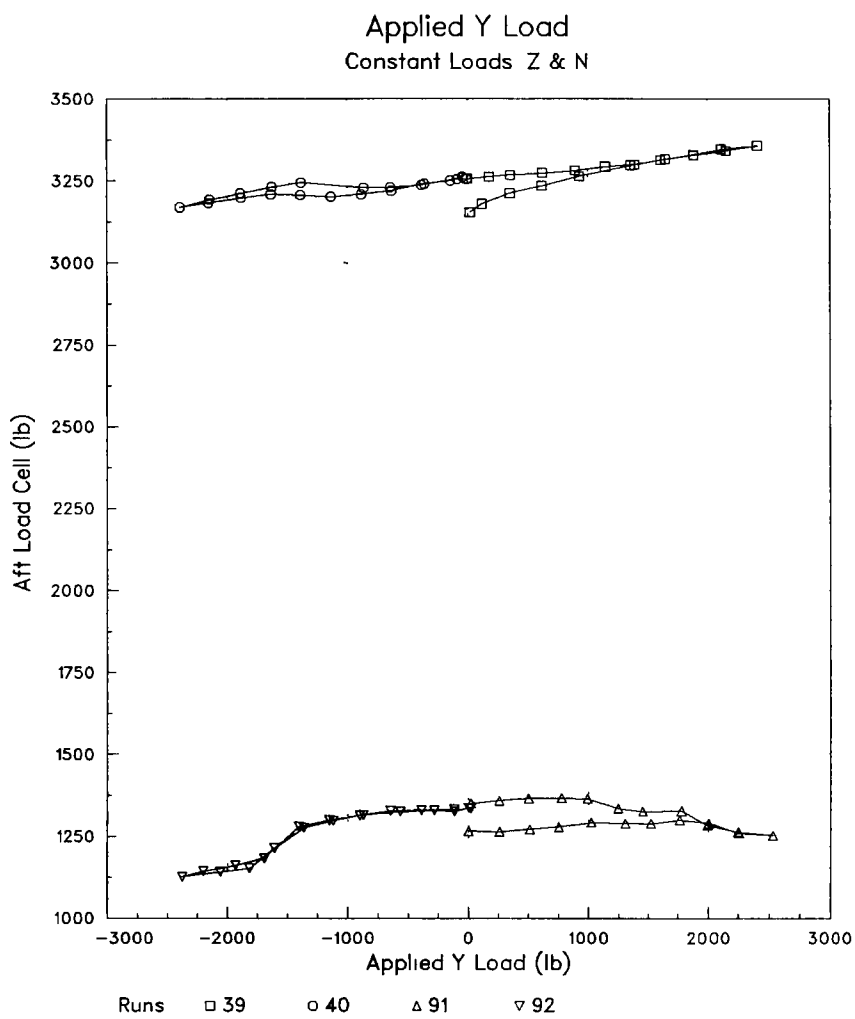

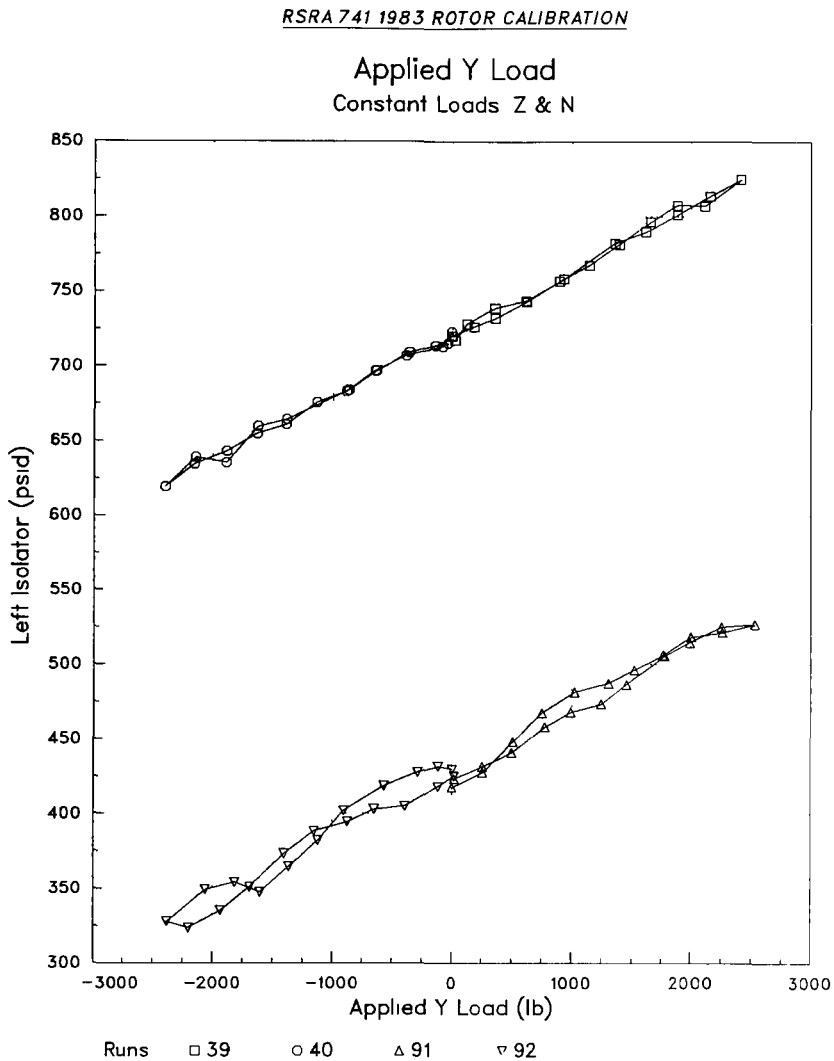
RSRA 741 1983 ROTOR CALIBRATION
Applied Y Load
Constant Loads Z & N
Left Isolator (psid)
850
800
750
700
650
600
550
500
450
400
350
300
−3000
−2000
−1000
0
1000
2000
3000
Applied Y Load (lb)
Runs □ 39 ○ 40 △ 91 ▽ 92

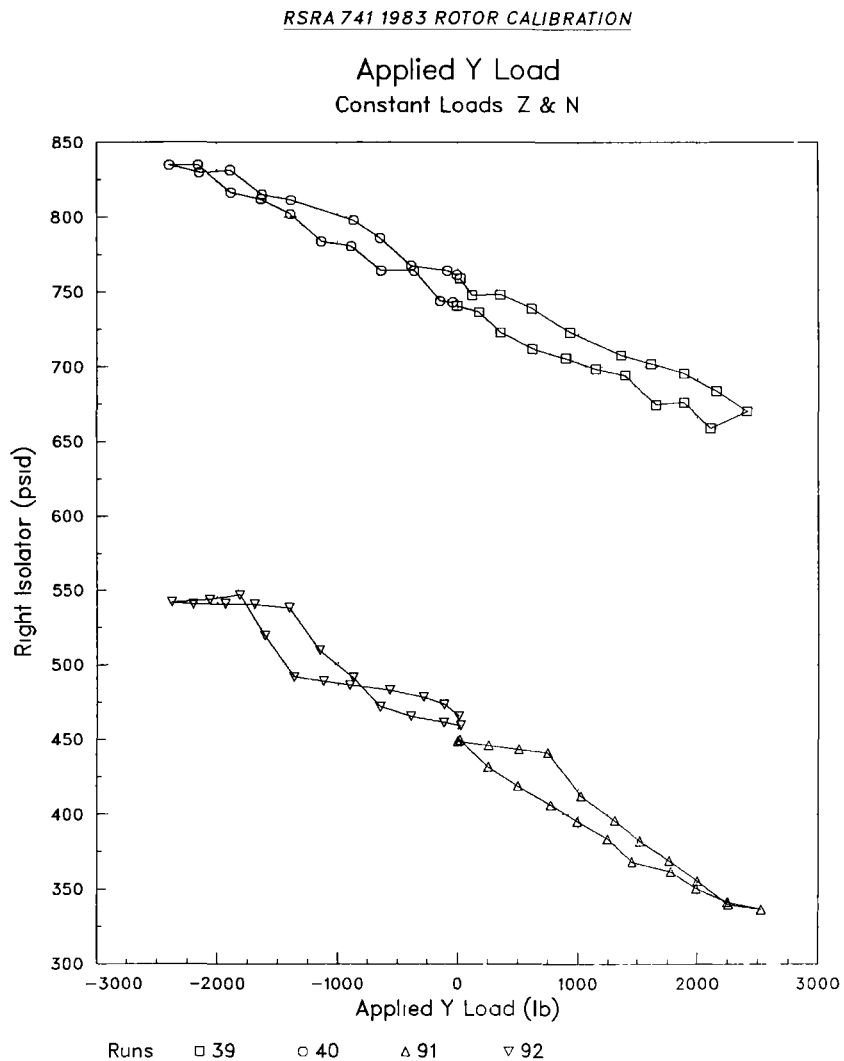
RSRA 741 1983 ROTOR CALIBRATION
Applied Y Load
Constant Loads Z & N
Right Isolator (psid)
850
800
750
700
650
600
550
500
450
400
350
300
−3000
−2000
−1000
0
1000
2000
3000
Applied Y Load (lb)
Runs □ 39 ○ 40 △ 91 ▽ 92

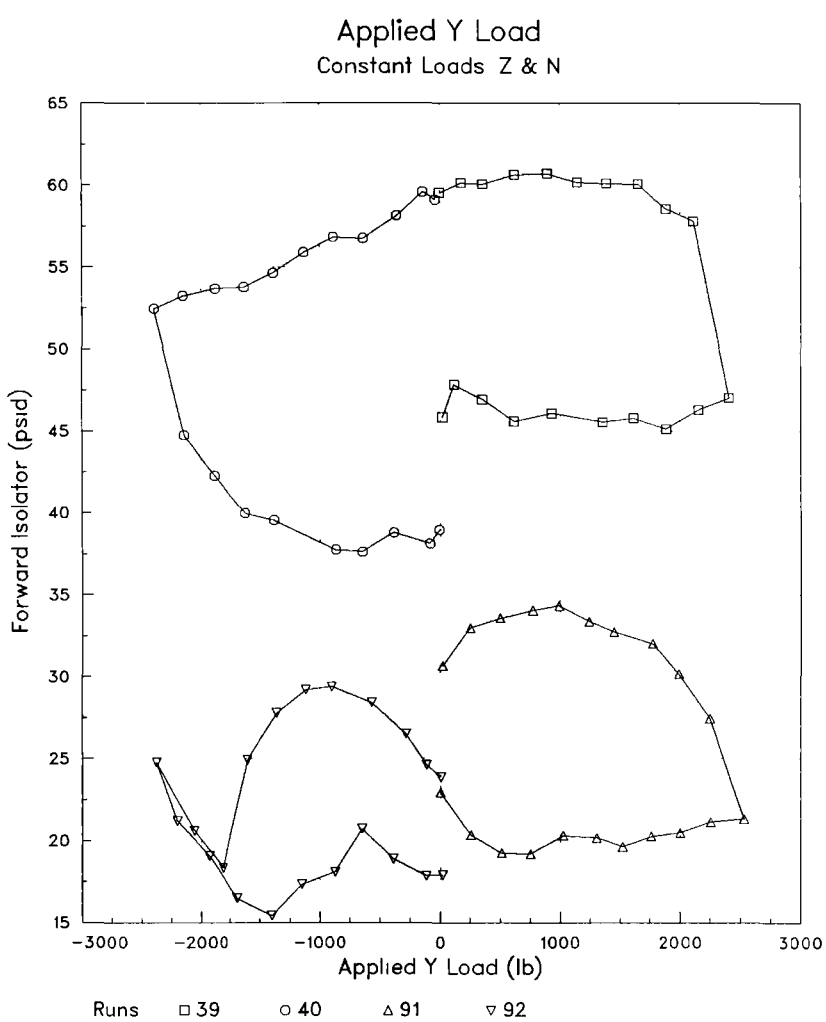

RSRA 741 1983 ROTOR CALIBRATION

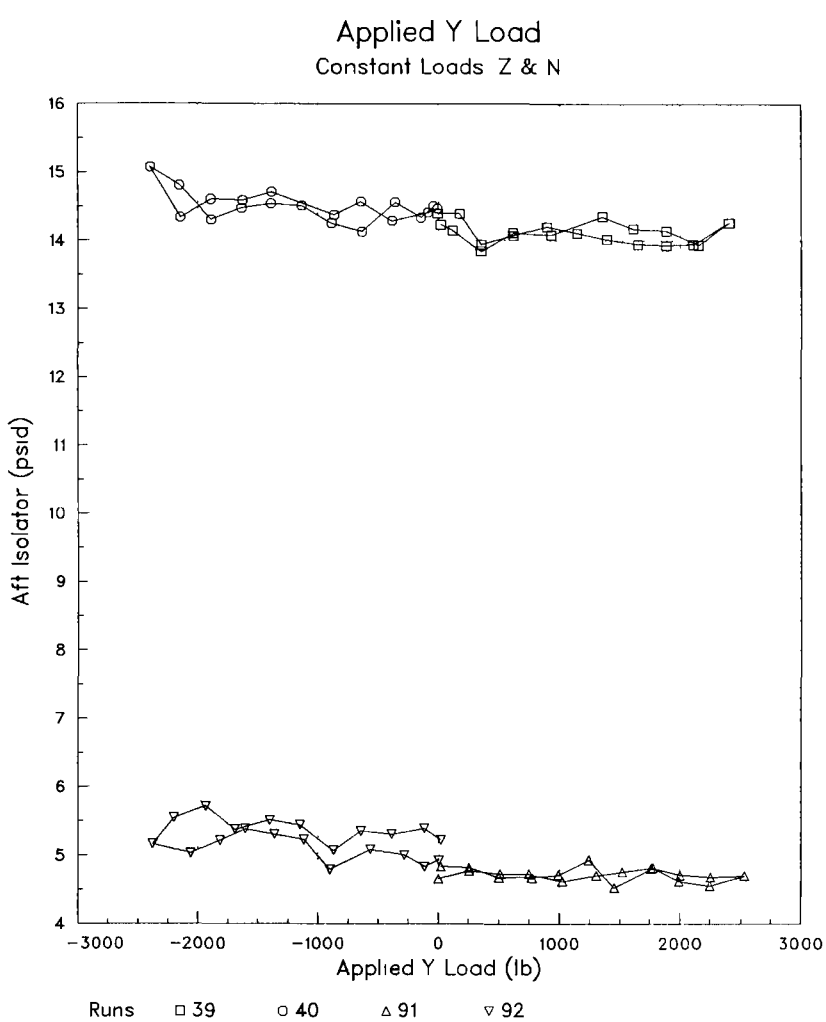

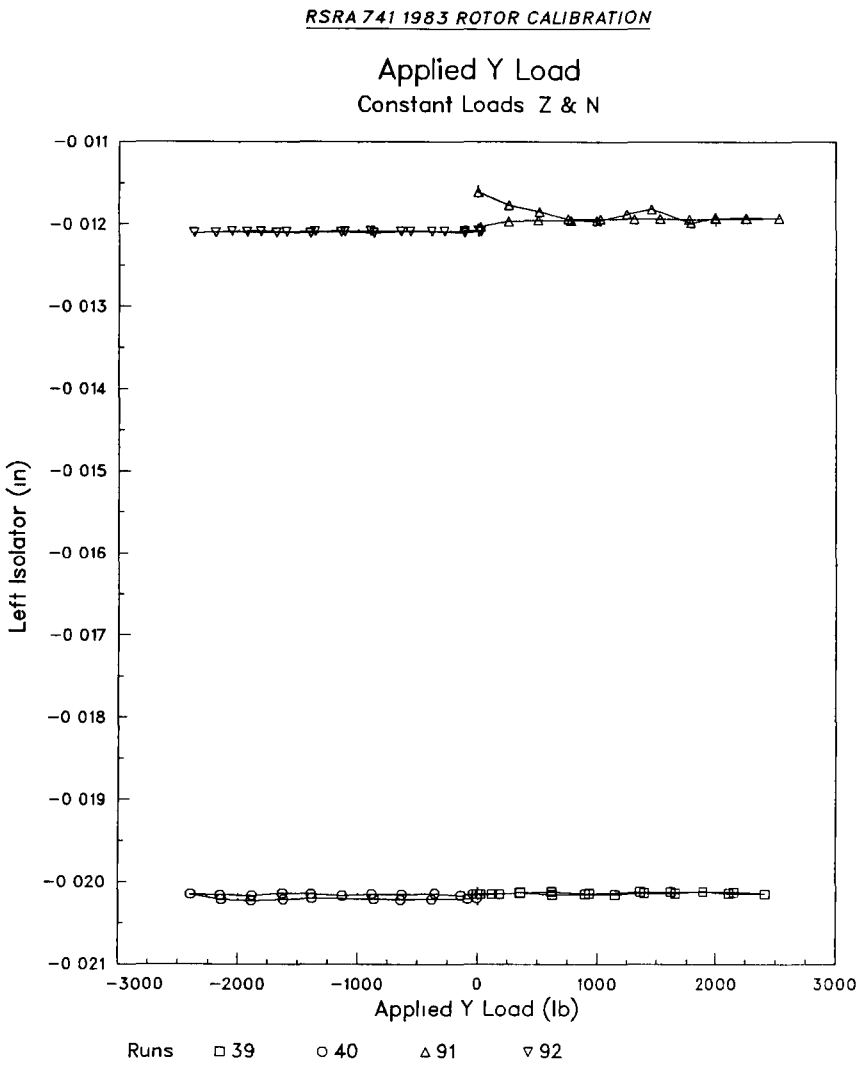
RSRA 741 1983 ROTOR CALIBRATION
Applied Y Load
Constant Loads Z & N
Left Isolator (in)
-0 011
-0 012
-0 013
-0 014
-0 015
-0 016
-0 017
-0 018
-0 019
-0 020
-0 021
-3000
-2000
-1000
0
1000
2000
3000
Applied Y Load (lb)
Runs □ 39 ○ 40 △ 91 ▽ 92

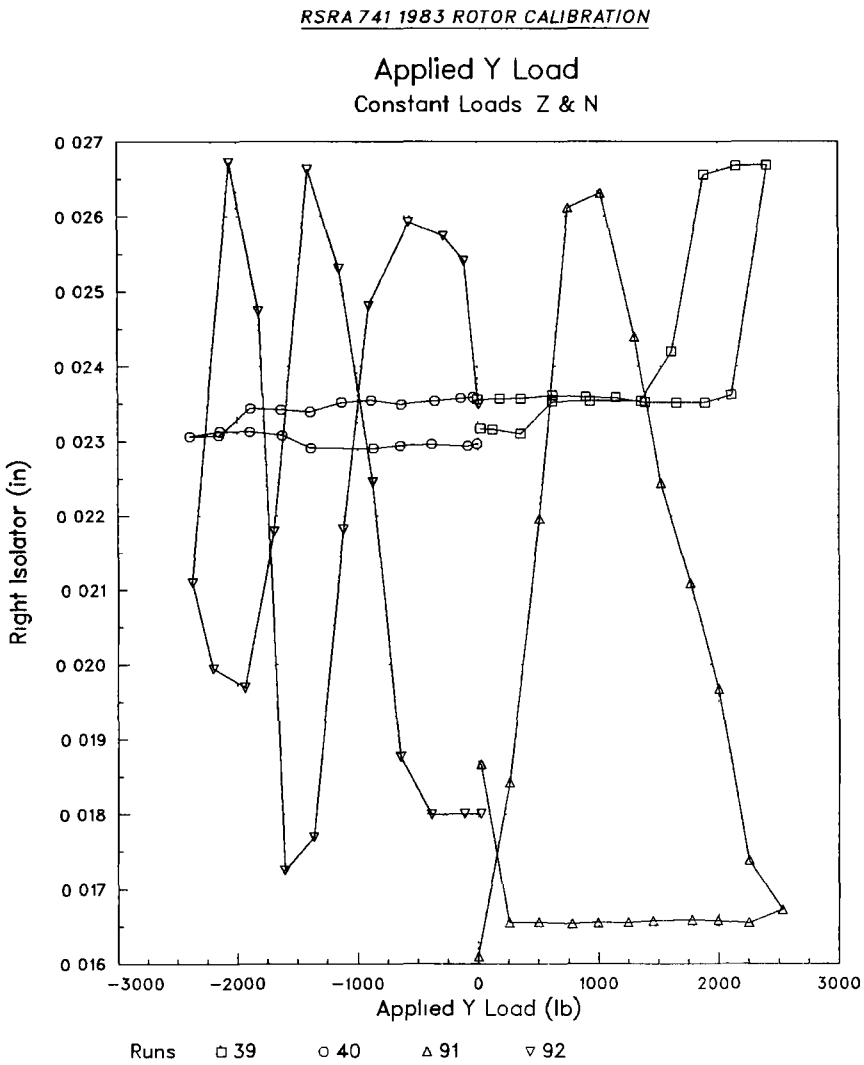
RSRA 741 1983 ROTOR CALIBRATION
Applied Y Load
Constant Loads Z & N
Right Isolator (in)
0 027
0 026
0 025
0 024
0 023
0 022
0 021
0 020
0 019
0 018
0 017
0 016
-3000
-2000
-1000
0
1000
2000
3000
Applied Y Load (lb)
Runs □ 39 ○ 40 △ 91 ▽ 92

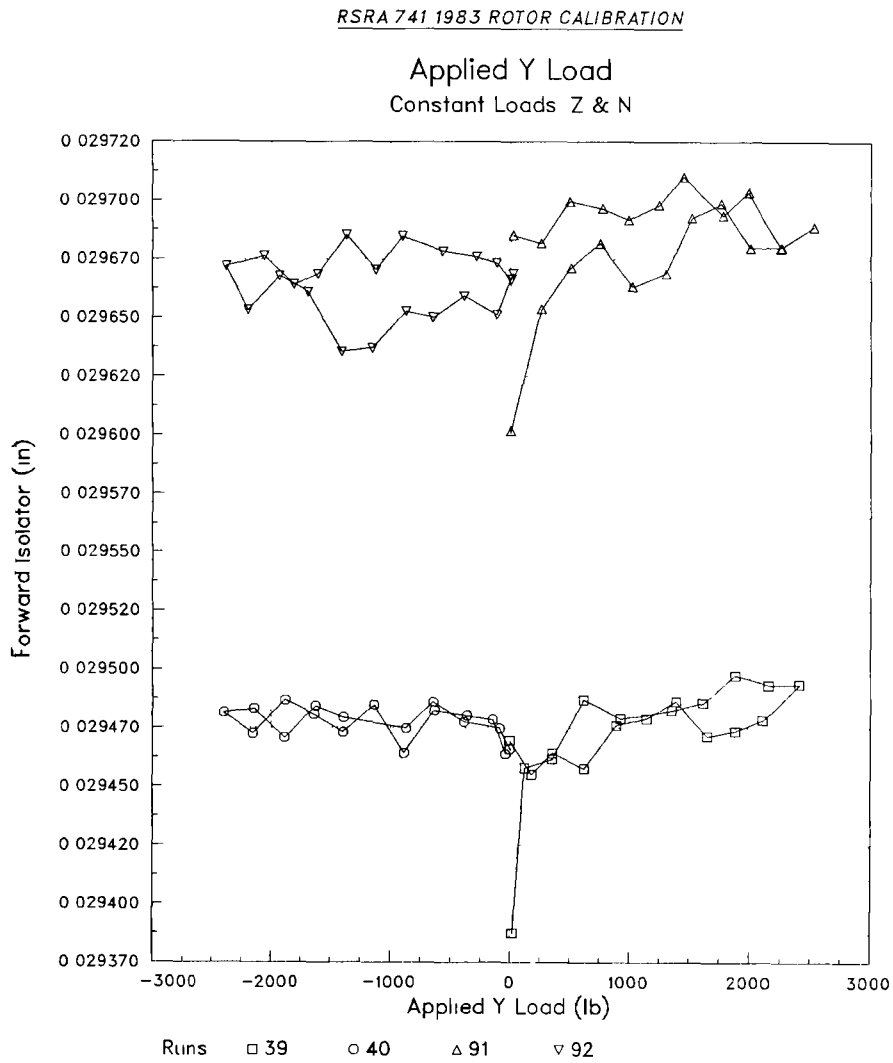
RSRA 741 1983 ROTOR CALIBRATION
Applied Y Load
Constant Loads Z & N
Forward Isolator (in)
0 029720
0 029700
0 029670
0 029650
0 029620
0 029600
0 029570
0 029550
0 029520
0 029500
0 029470
0 029450
0 029420
0 029400
0 029370
-3000
-2000
-1000
0
1000
2000
3000
Applied Y Load (lb)
Runs □ 39 ○ 40 △ 91 ▽ 92

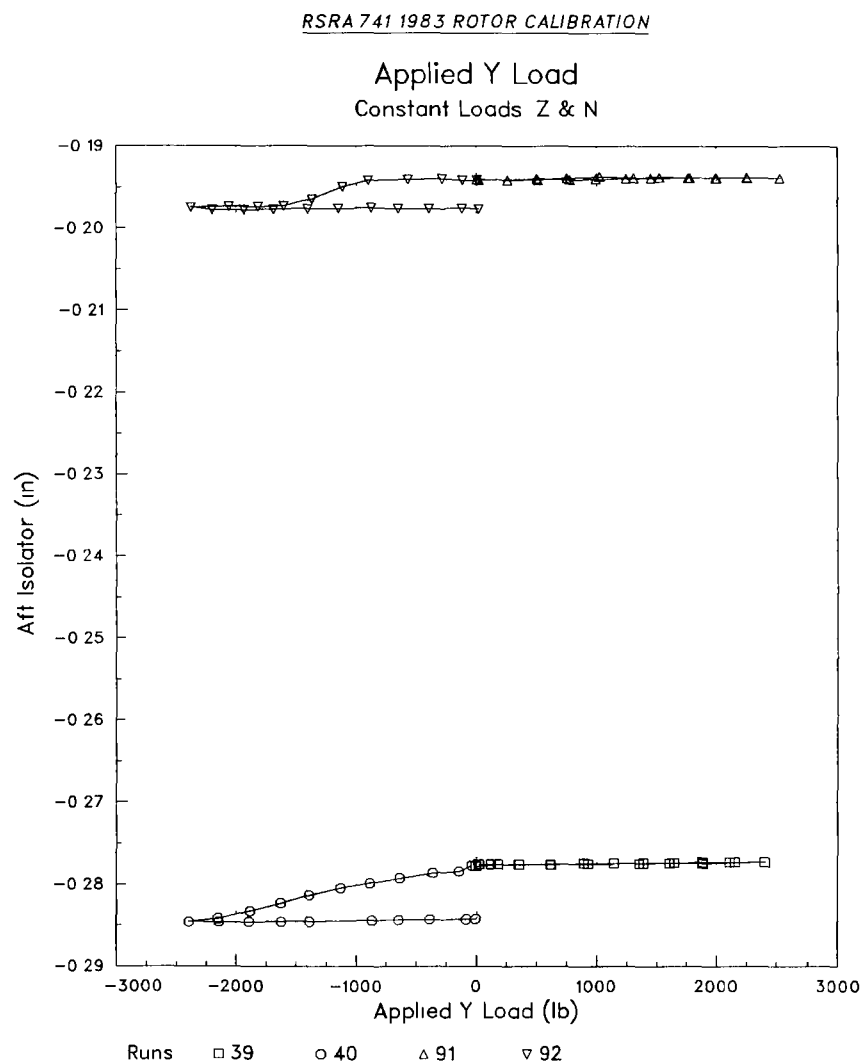
RSRA 741 1983 ROTOR CALIBRATION
Applied Y Load
Constant Loads Z & N
Aft Isolator (in)
-0 19
-0 20
-0 21
-0 22
-0 23
-0 24
-0 25
-0 26
-0 27
-0 28
-0 29
-3000
-2000
-1000
0
1000
2000
3000
Applied Y Load (lb)
Runs □ 39 ○ 40 △ 91 ▽ 92

RSRA 741 1983 ROTOR CALIBRATION

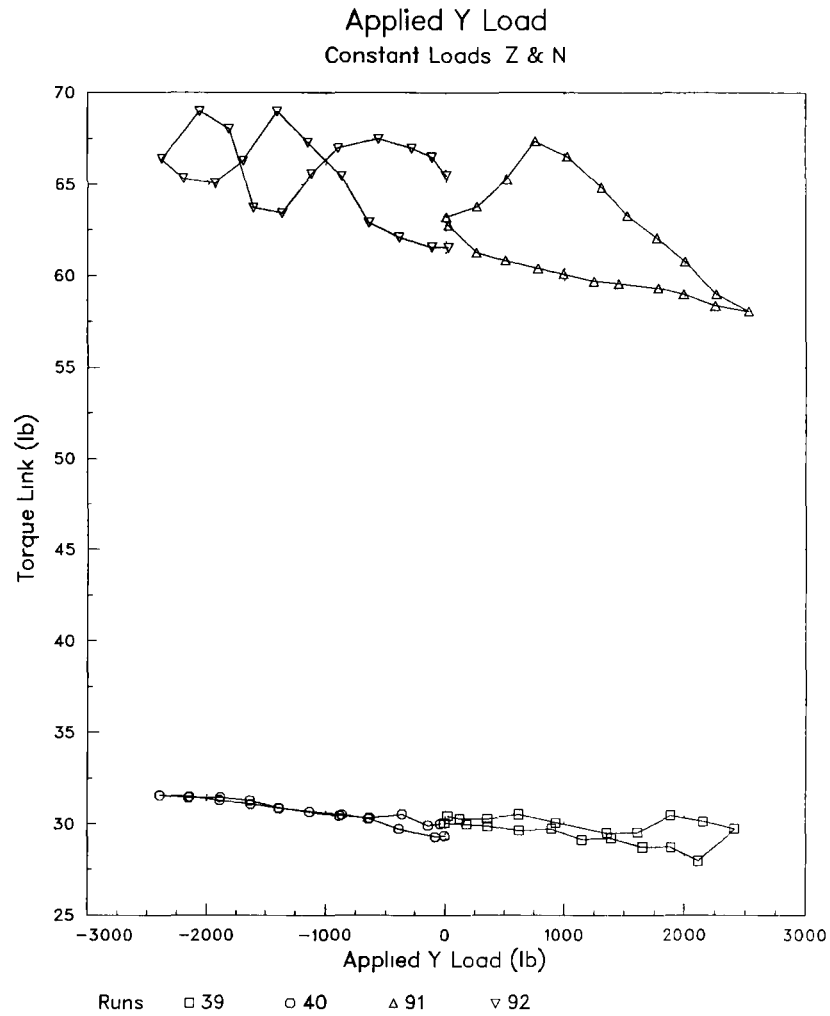

RSRA 741 1983 ROTOR CALIBRATION

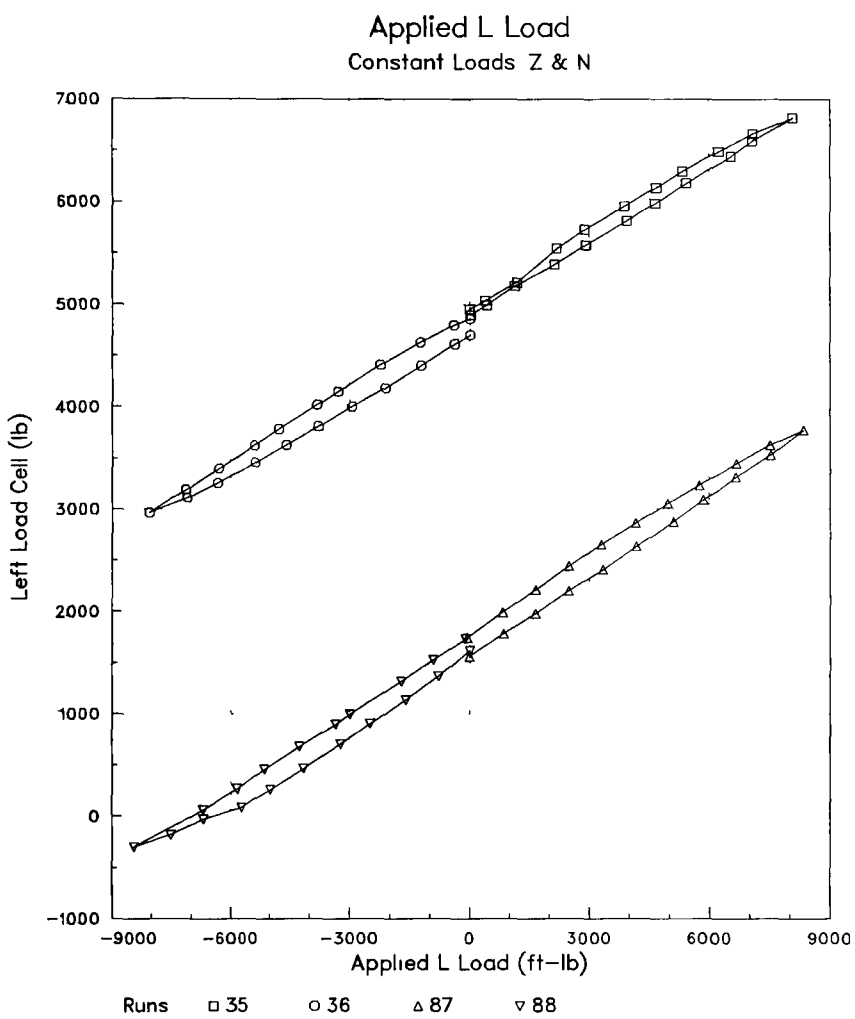

RSRA 741 1983 ROTOR CALIBRATION

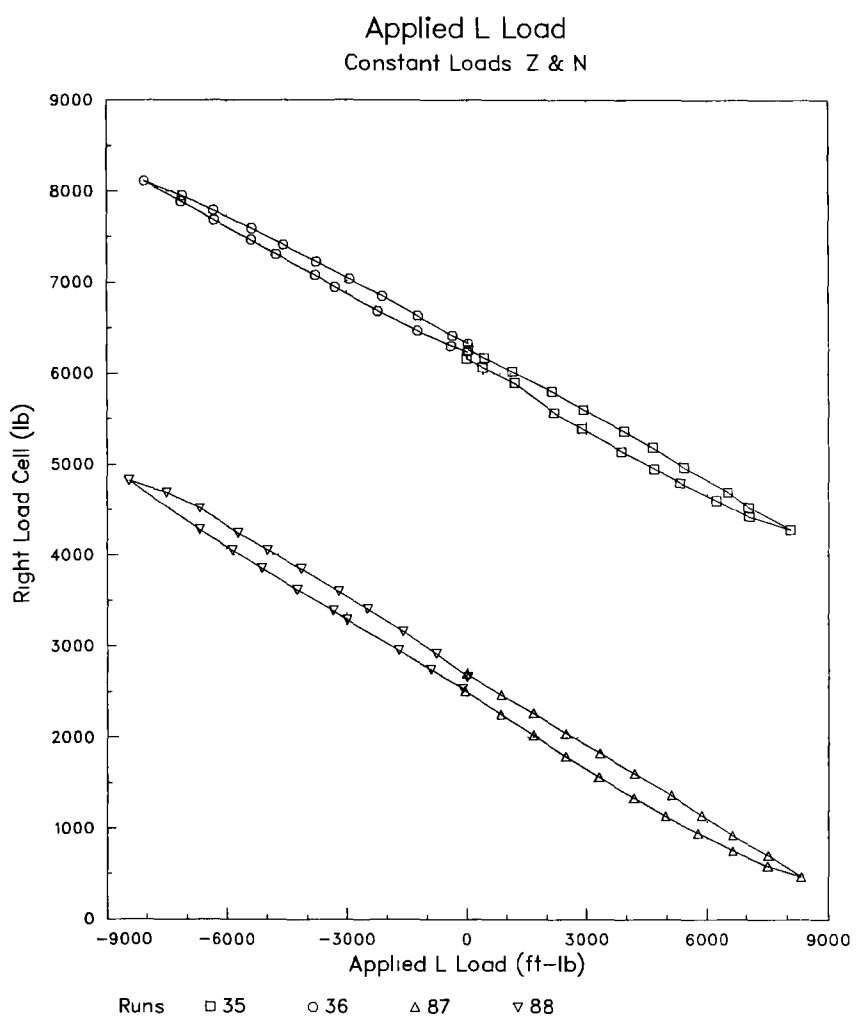

RSRA 741 1983 ROTOR CALIBRATION

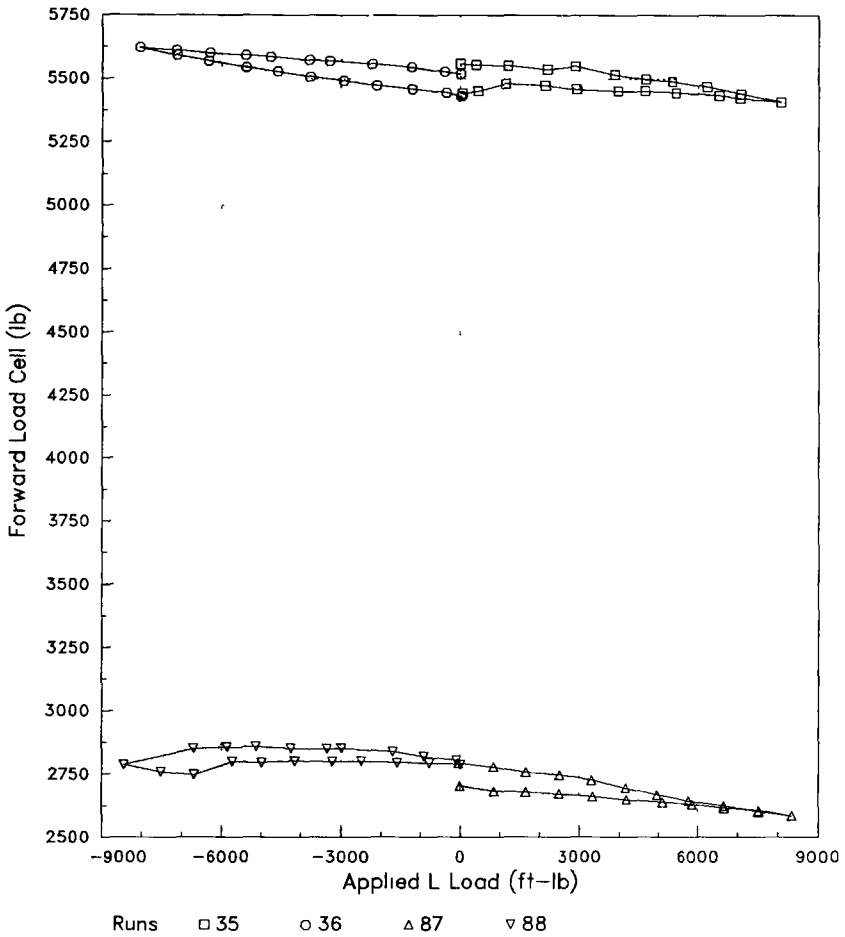

RSRA 741 1983 ROTOR CALIBRATION

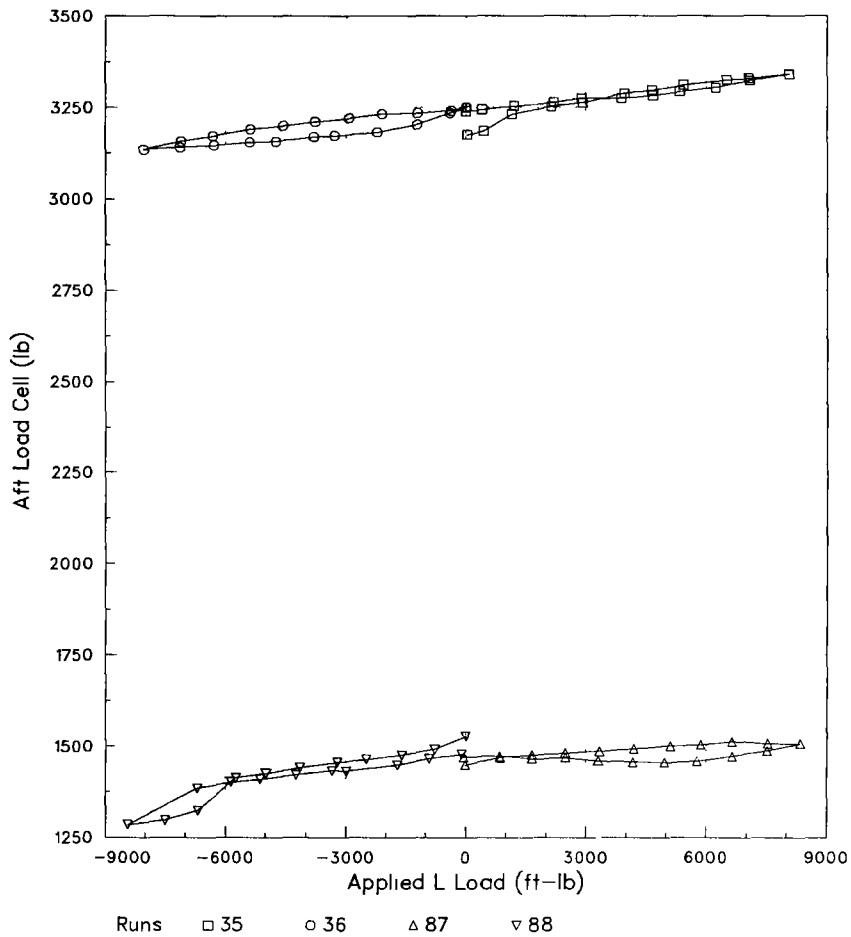

RSRA 741 1983 ROTOR CALIBRATION

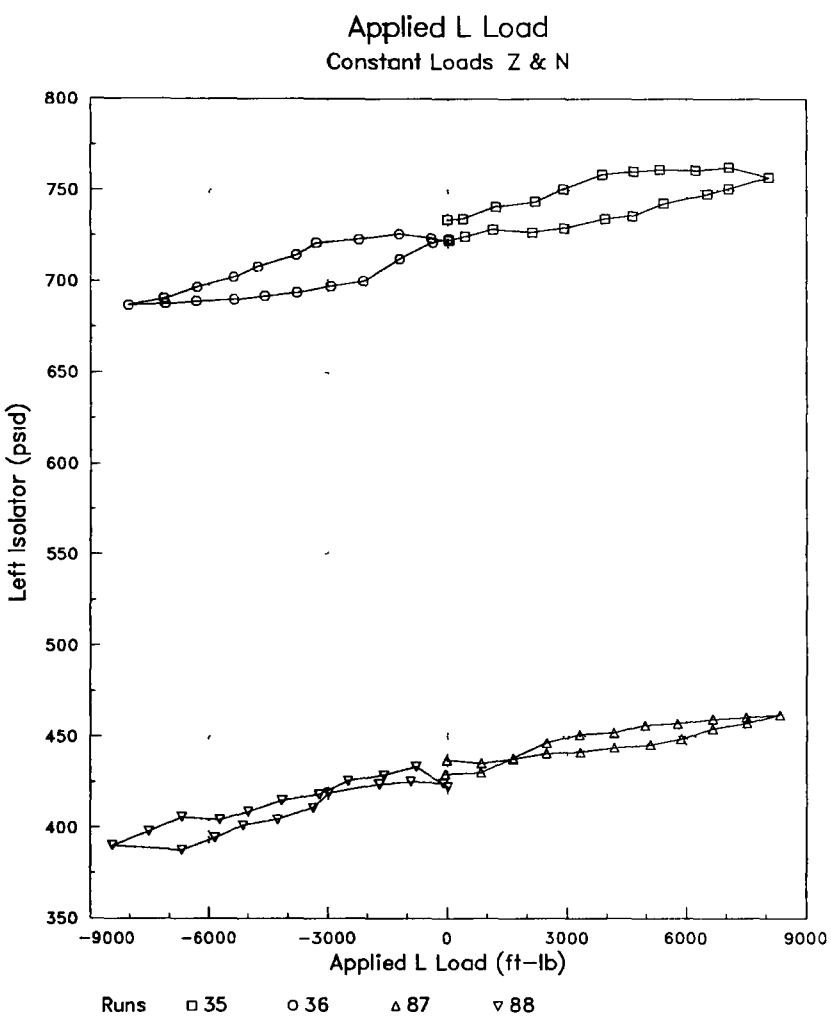

RSRA 741 1983 ROTOR CALIBRATION

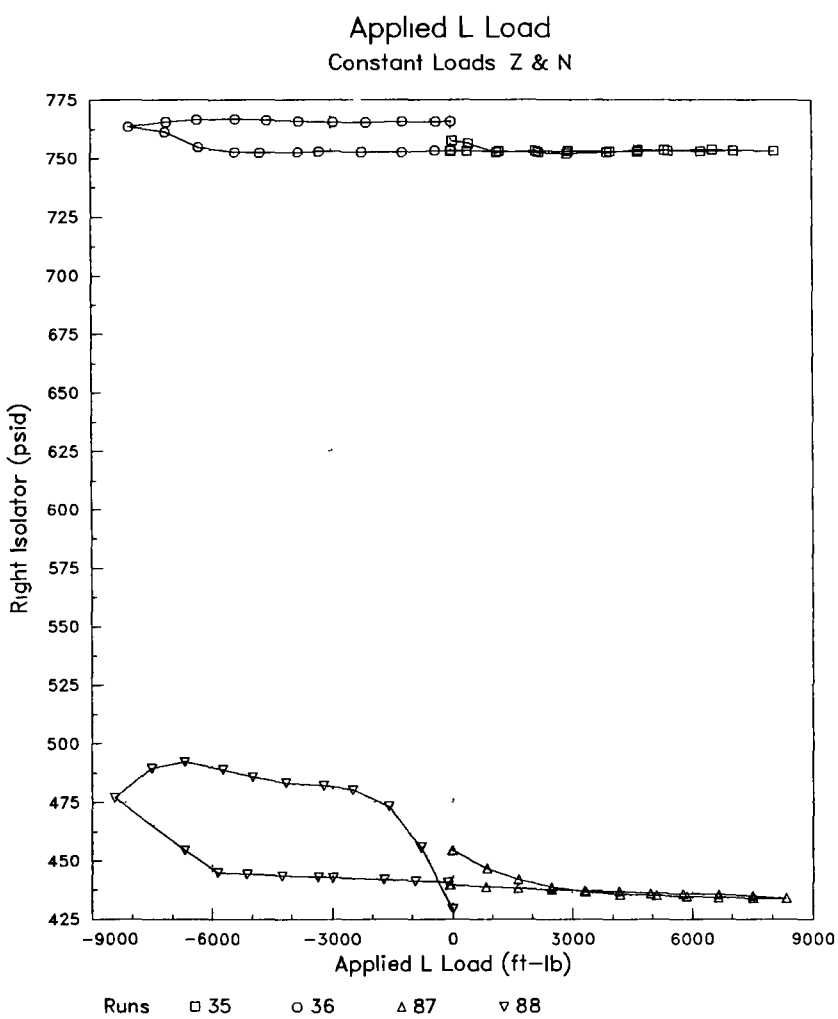

RSRA 741 1983 ROTOR CALIBRATION

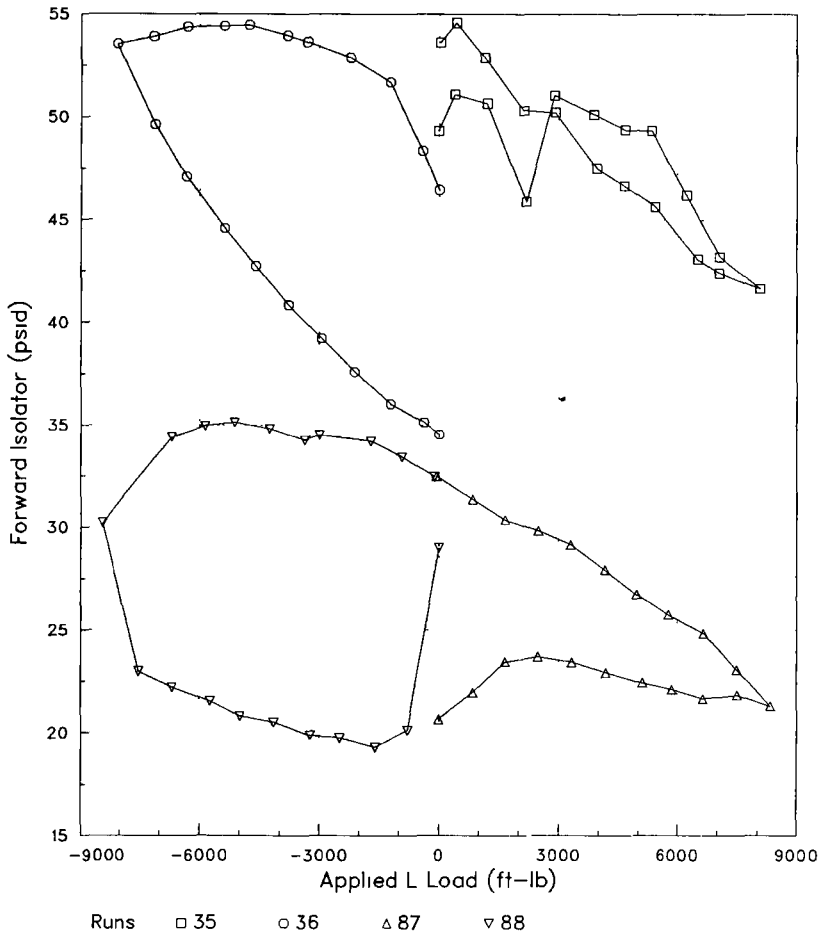

RSRA 741 1983 ROTOR CALIBRATION

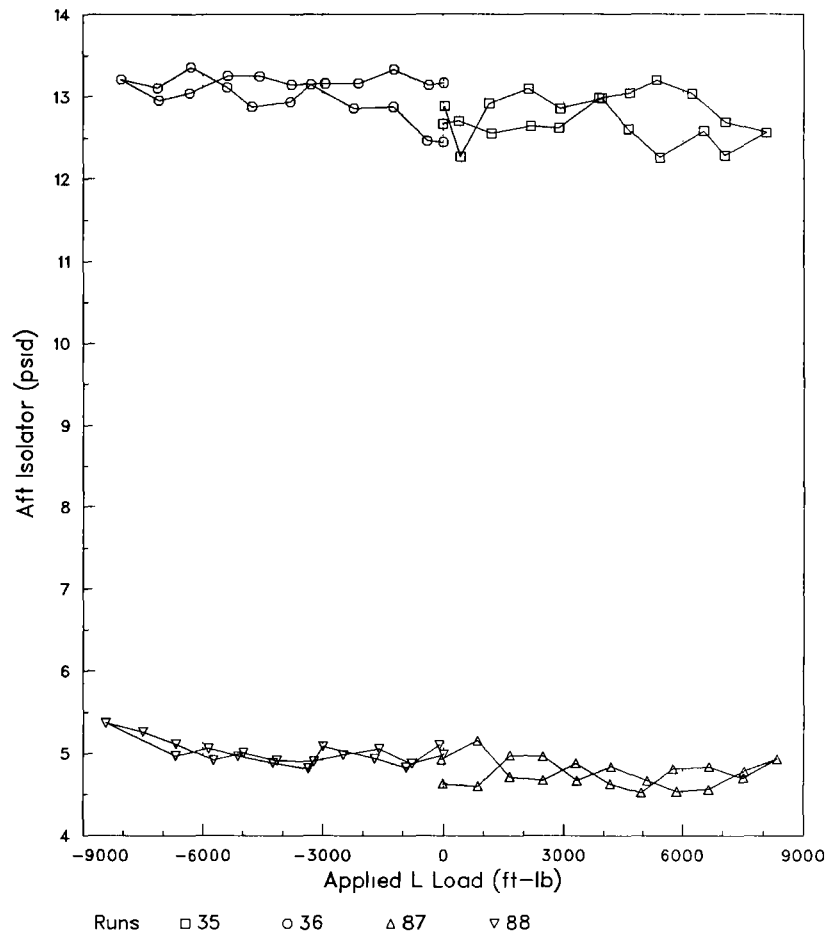

RSRA 741 1983 ROTOR CALIBRATION

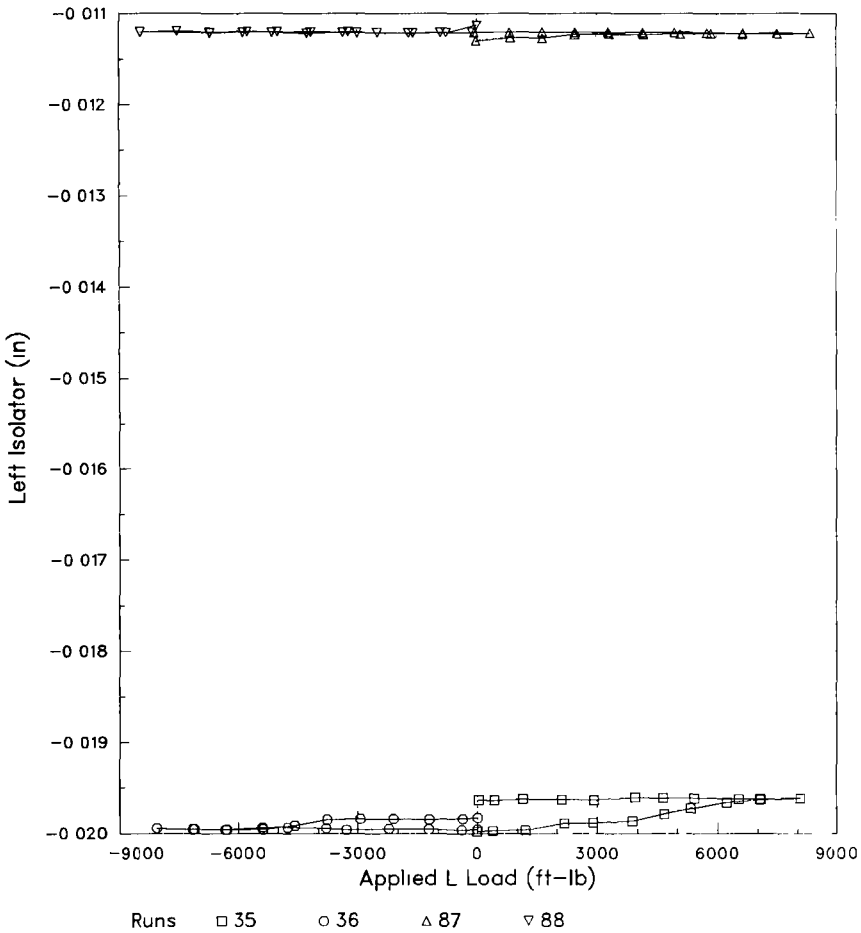

***RSRA 741** 1983 ROTOR CALIBRATION*

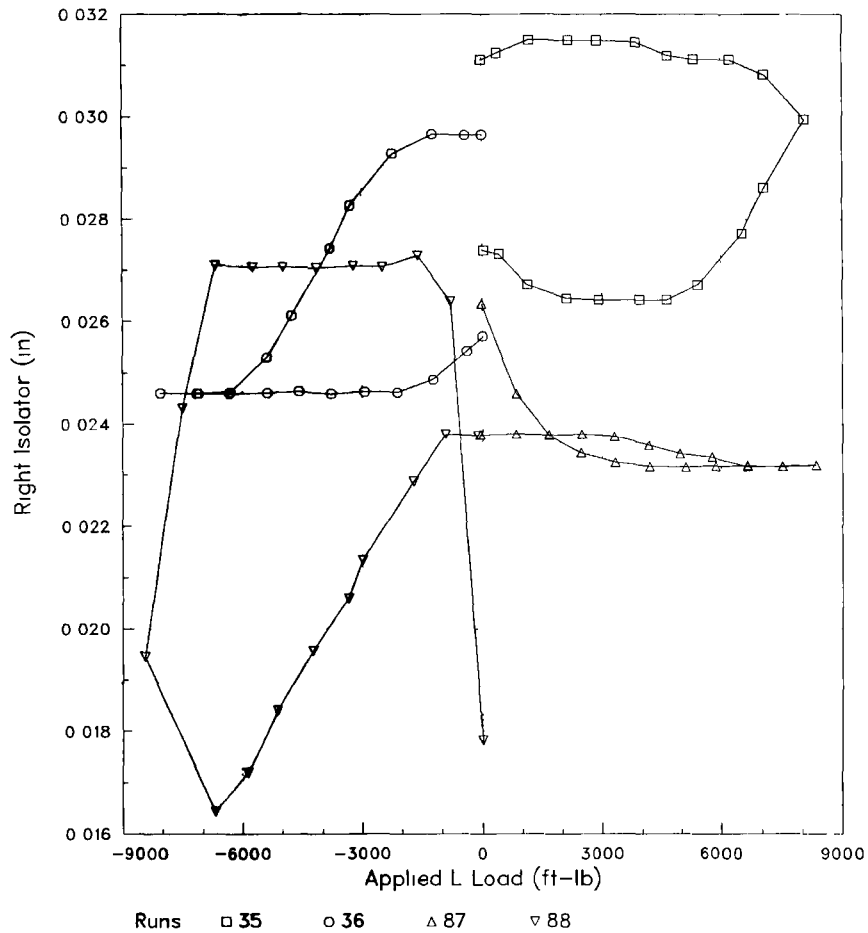

RSRA 741 1983 ROTOR CALIBRATION

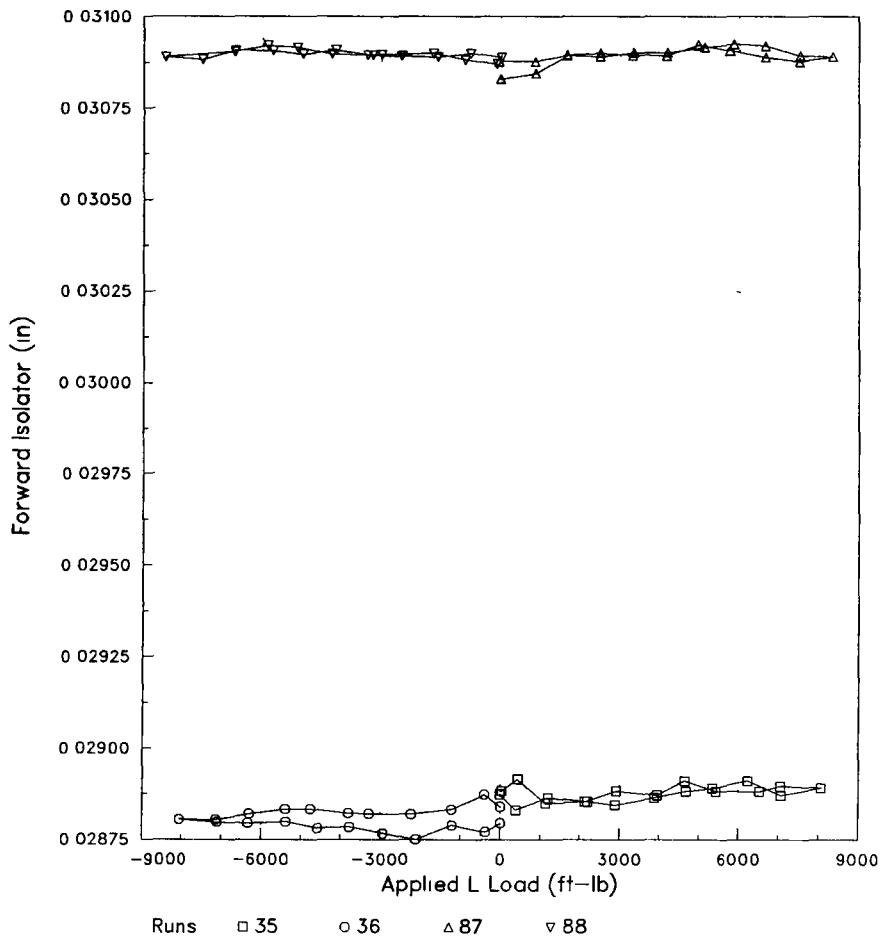

RSRA 741 1983 ROTOR CALIBRATION

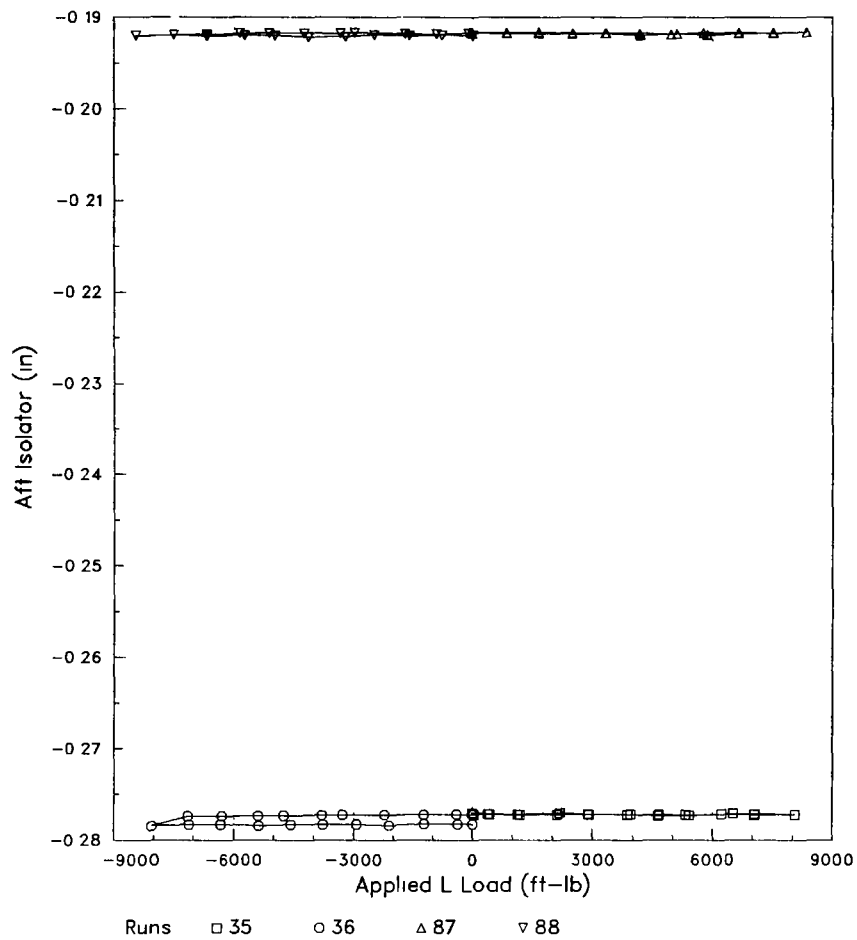

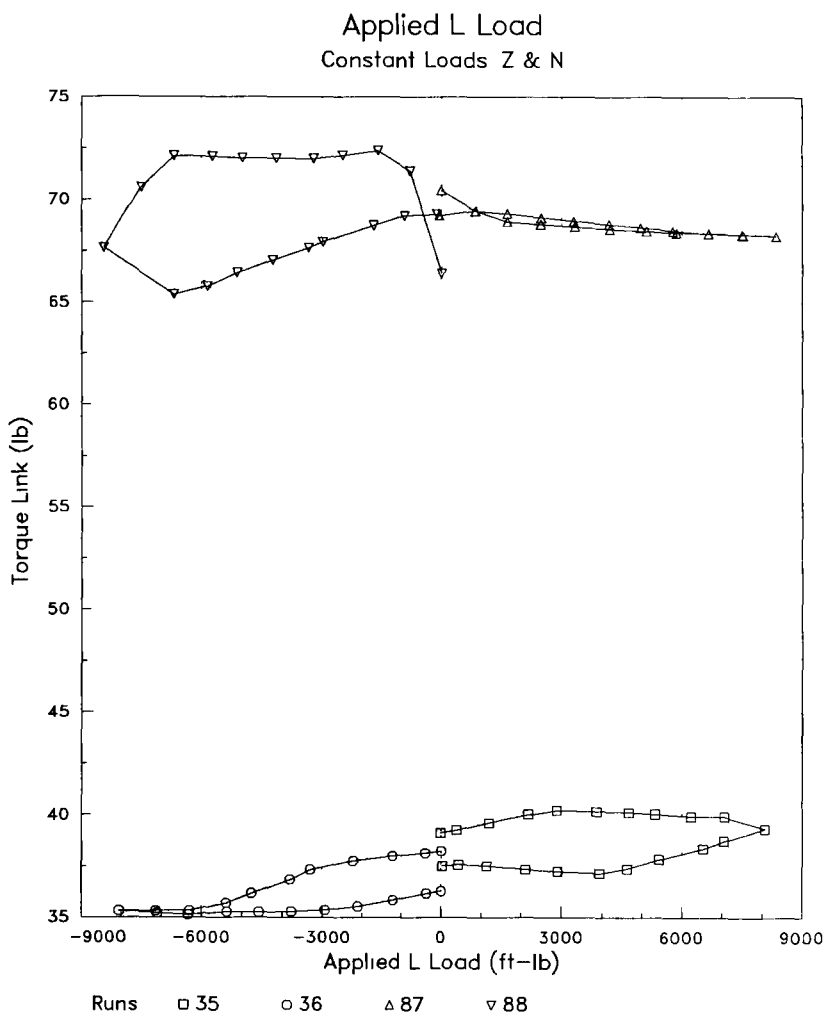
Applied L Load
Constant Loads Z & N
Torque Link (lb)
75
70
65
60
55
50
45
40
35
-9000
-6000
-3000
0
3000
6000
9000
Applied L Load (ft-lb)
Runs
□ 35
○ 36
△ 87
▽ 88

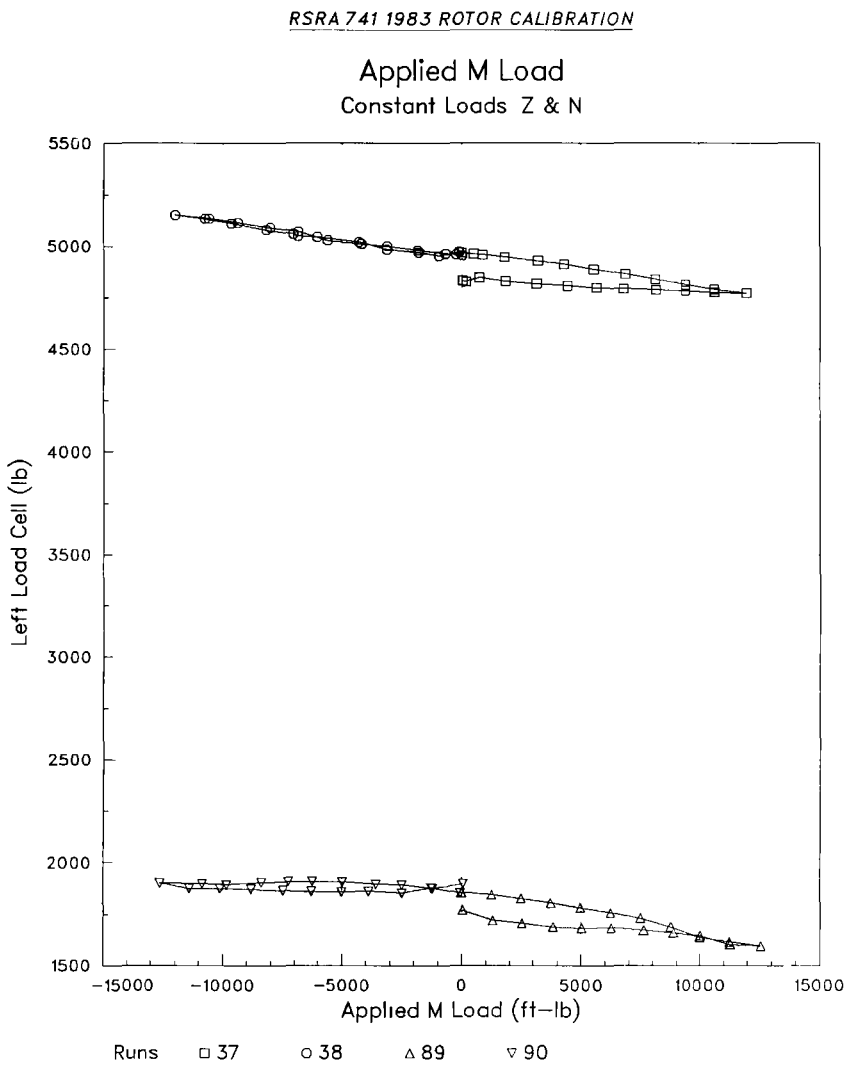
RSRA 741 1983 ROTOR CALIBRATION
Applied M Load
Constant Loads Z & N
Left Load Cell (lb)
5500
5000
4500
4000
3500
3000
2500
2000
1500
−15000
−10000
−5000
0
5000
10000
15000
Applied M Load (ft−lb)
Runs □ 37 ○ 38 △ 89 ▽ 90

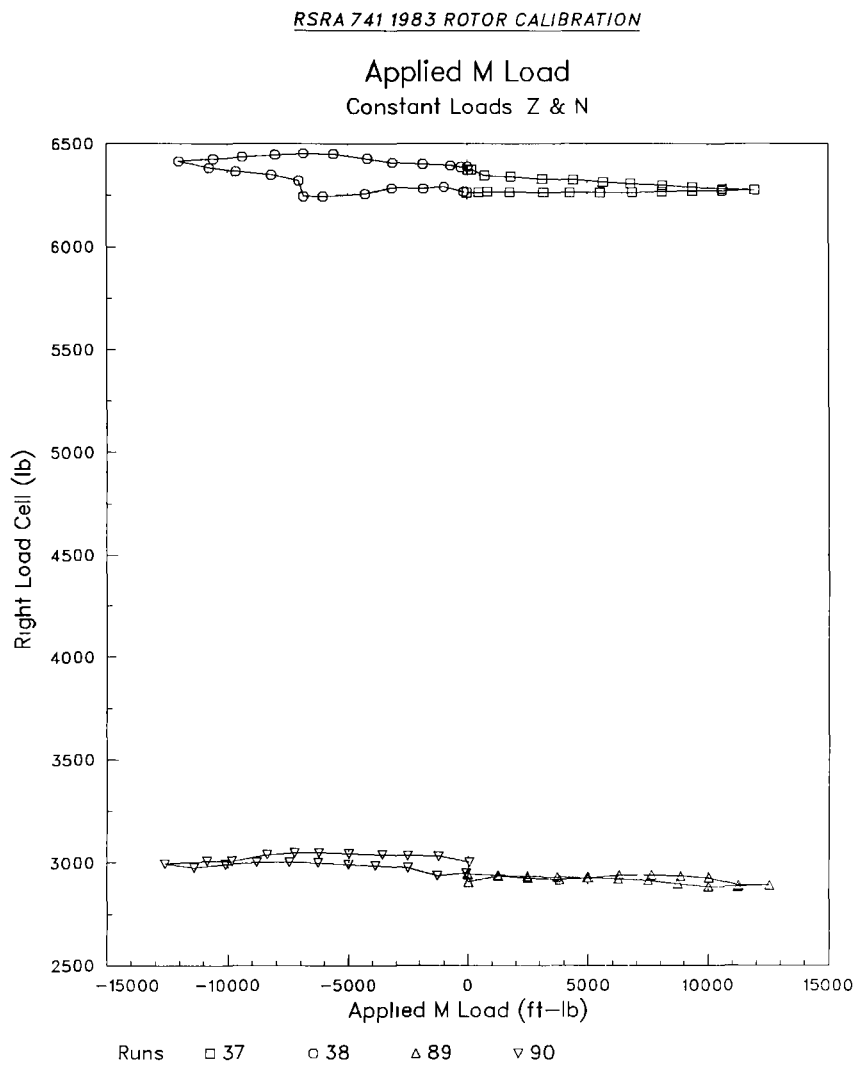
RSRA 741 1983 ROTOR CALIBRATION
Applied M Load
Constant Loads Z & N
Right Load Cell (lb)
6500
6000
5500
5000
4500
4000
3500
3000
2500
−15000
−10000
−5000
0
5000
10000
15000
Applied M Load (ft−lb)
Runs □ 37 ○ 38 △ 89 ▽ 90

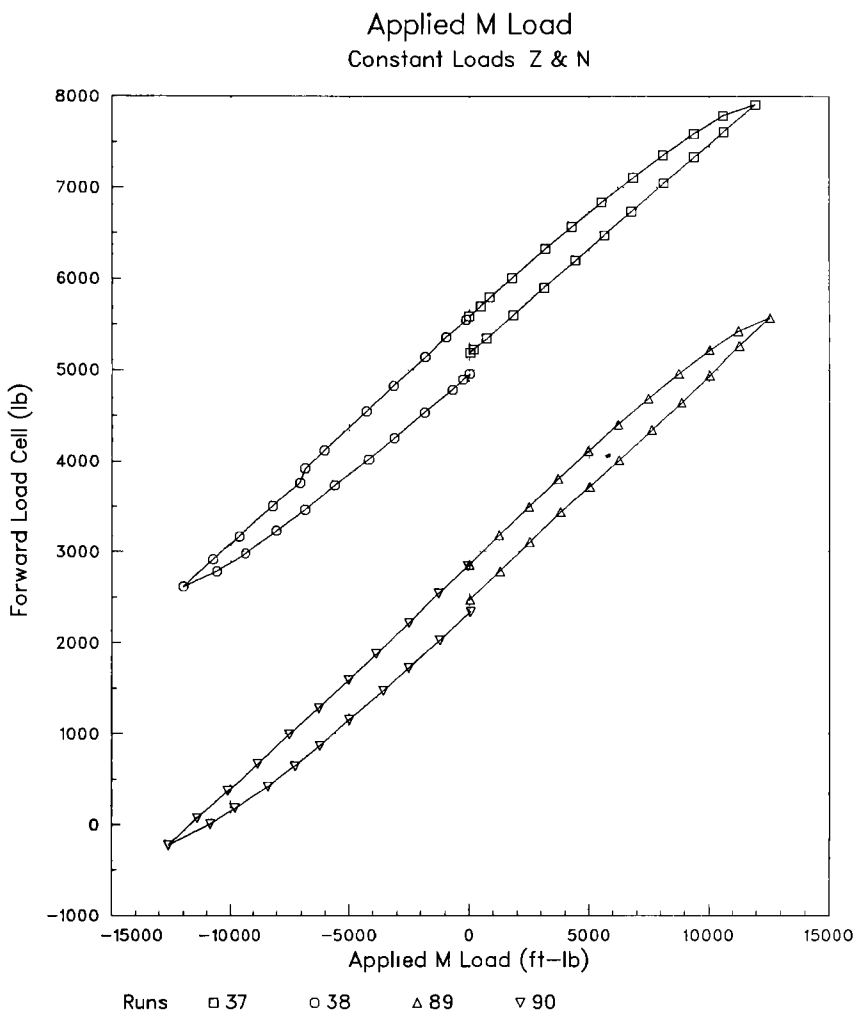

RSRA 741 1983 ROTOR CALIBRATION

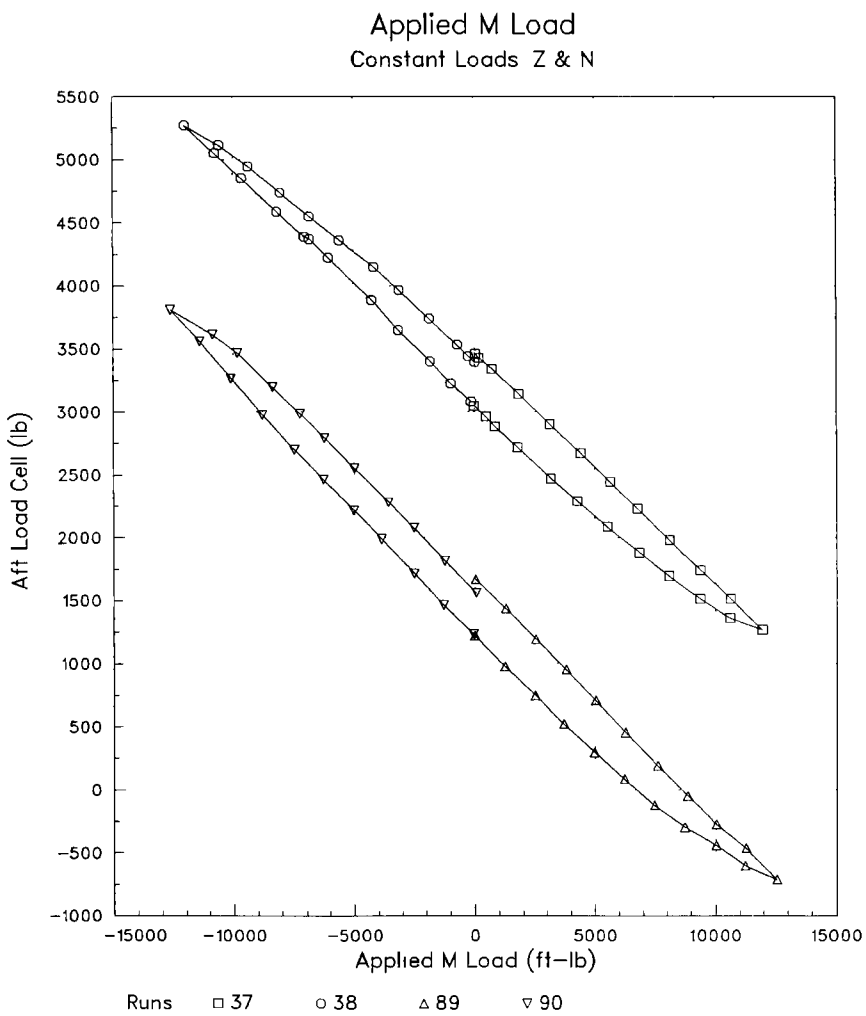

RSRA 741 1983 ROTOR CALIBRATION

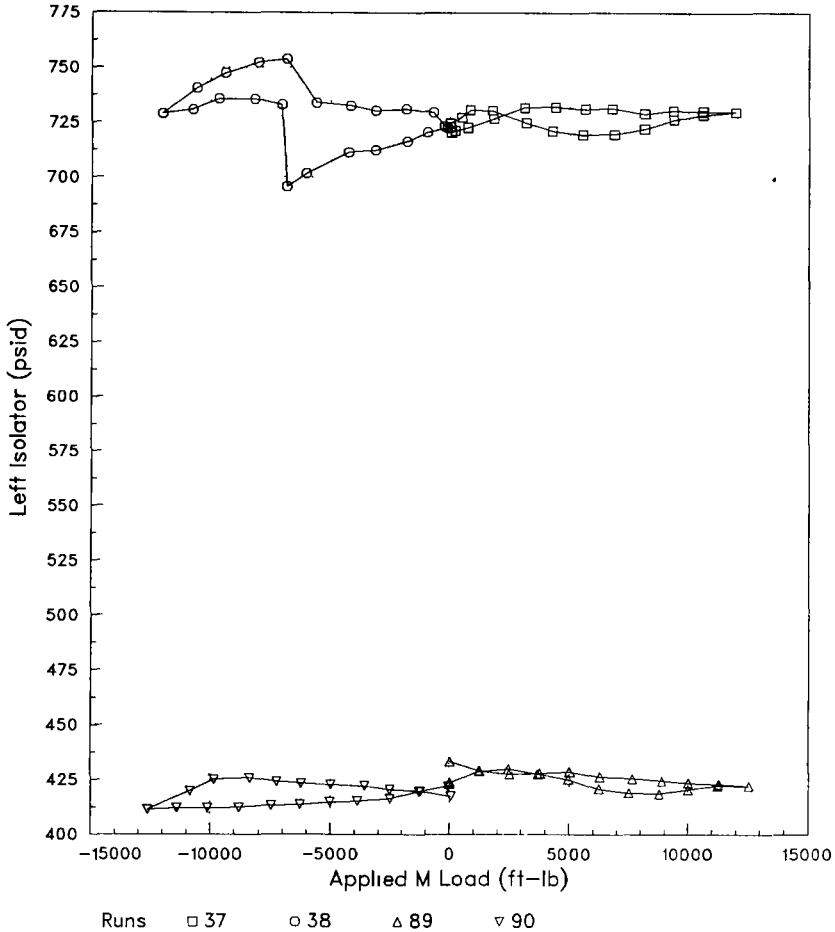

RSRA 741 1983 ROTOR CALIBRATION

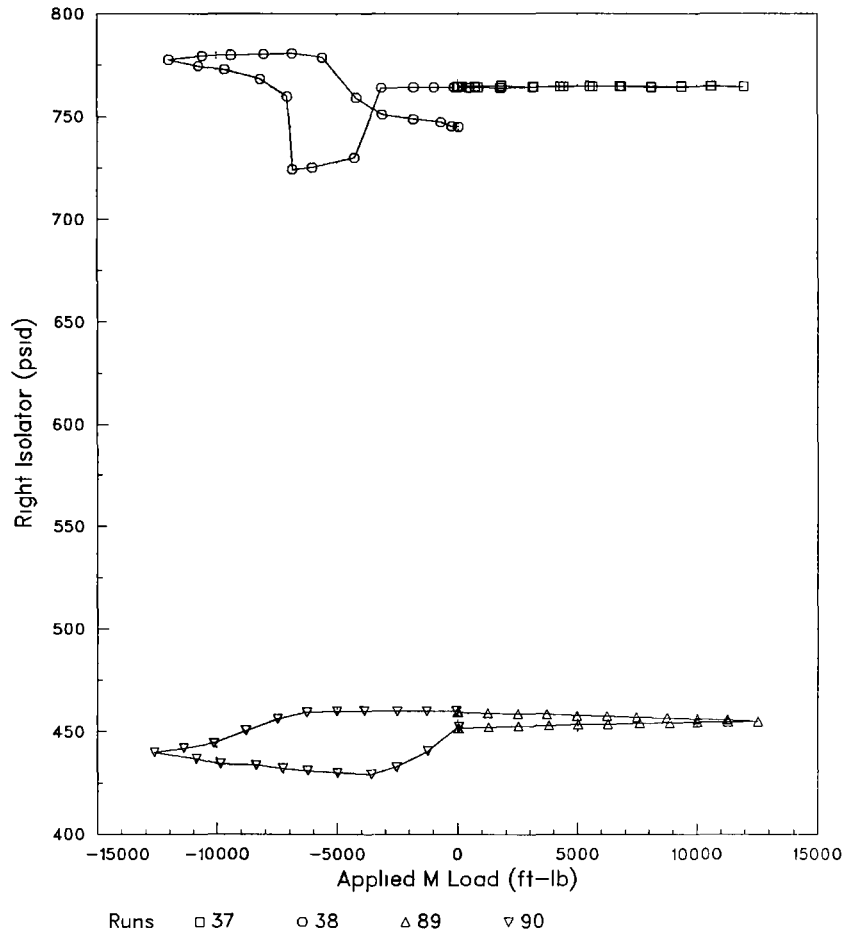

RSRA 741 1983 ROTOR CALIBRATION

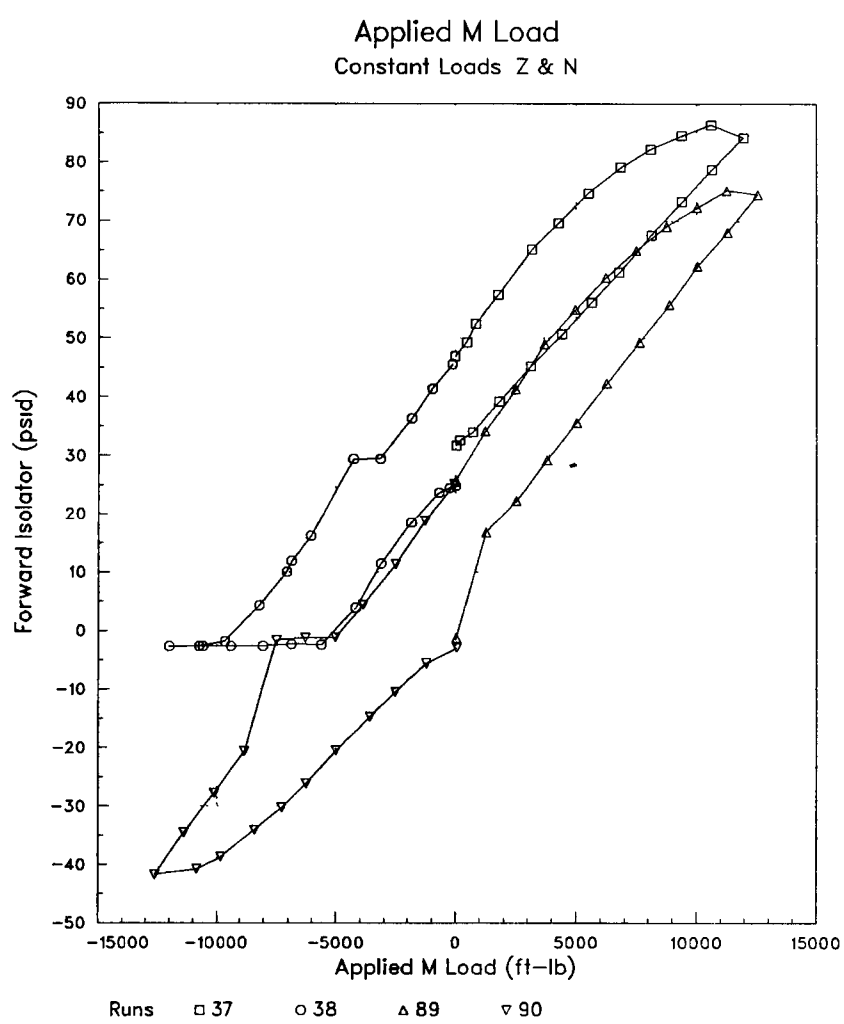

RSRA 741 1983 ROTOR CALIBRATION

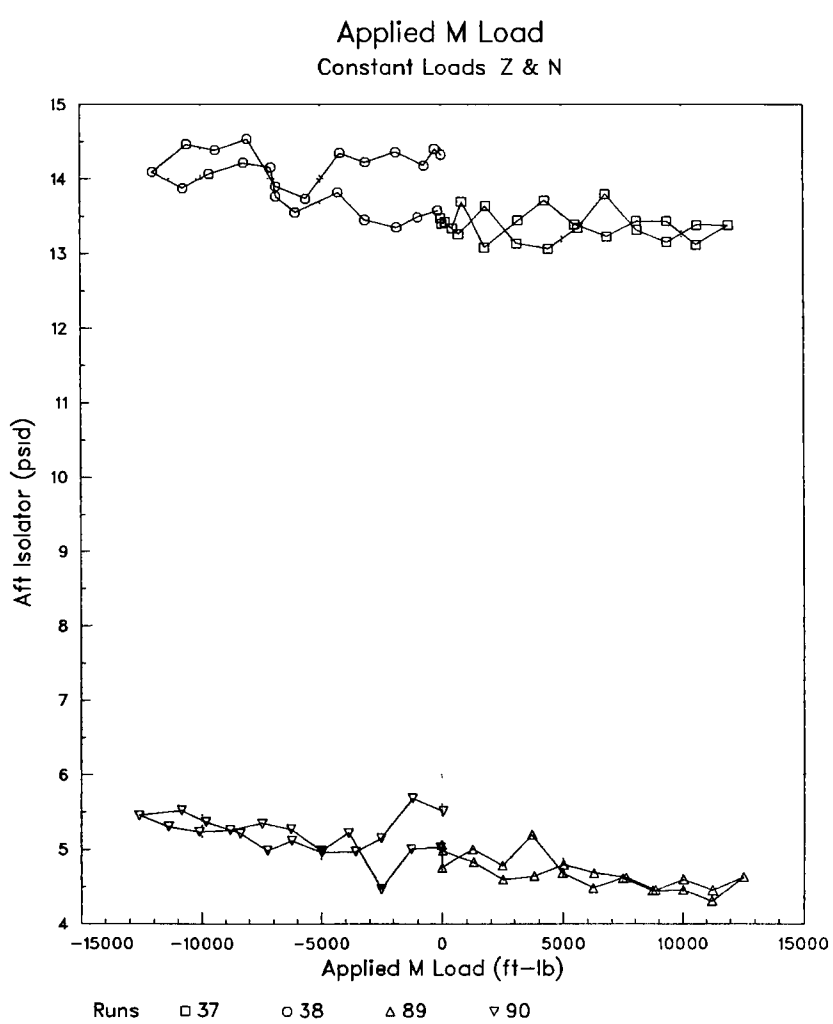

RSRA 741 1983 ROTOR CALIBRATION

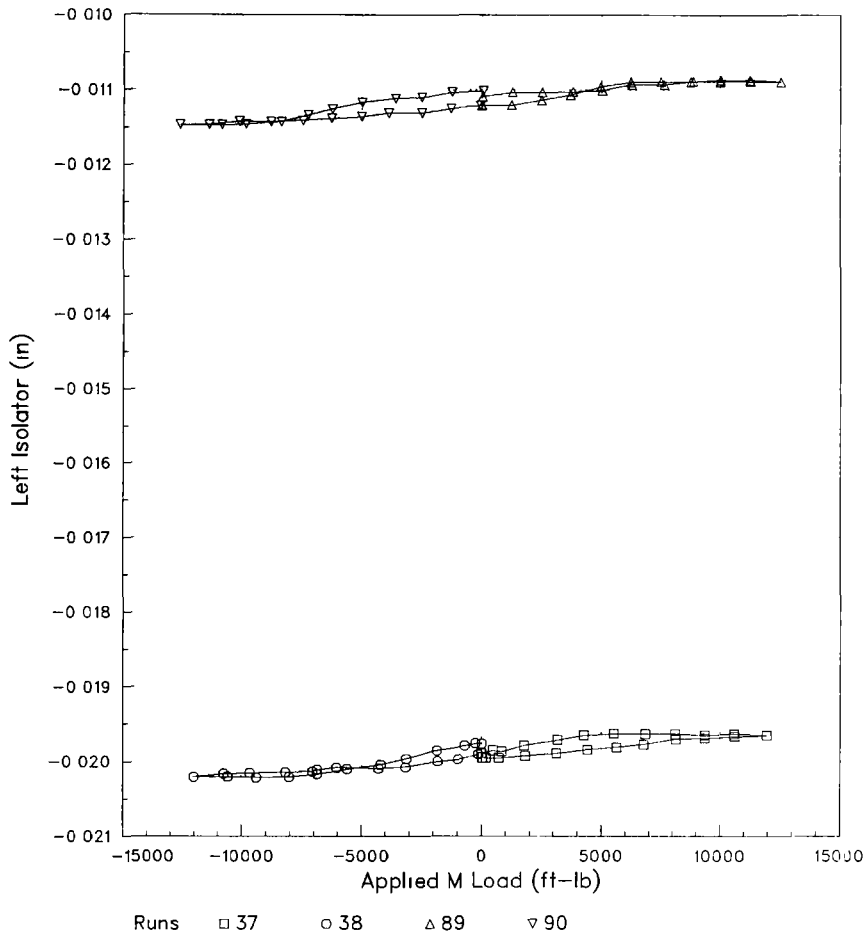

RSRA 741 1983 ROTOR CALIBRATION

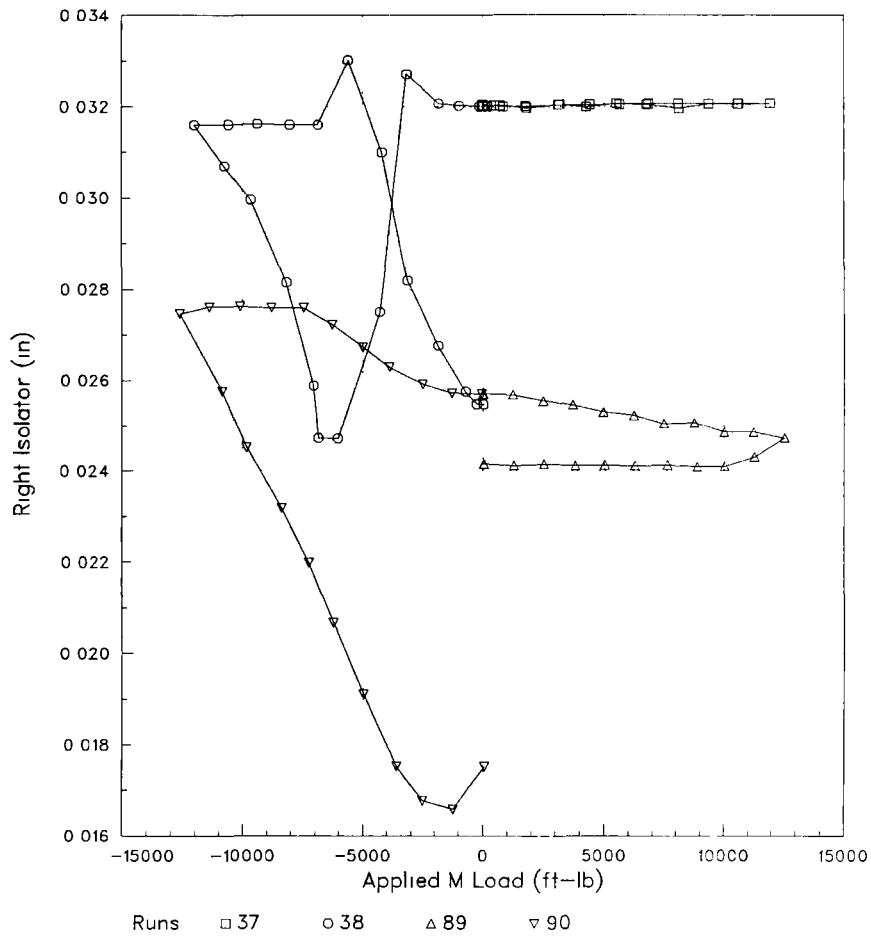

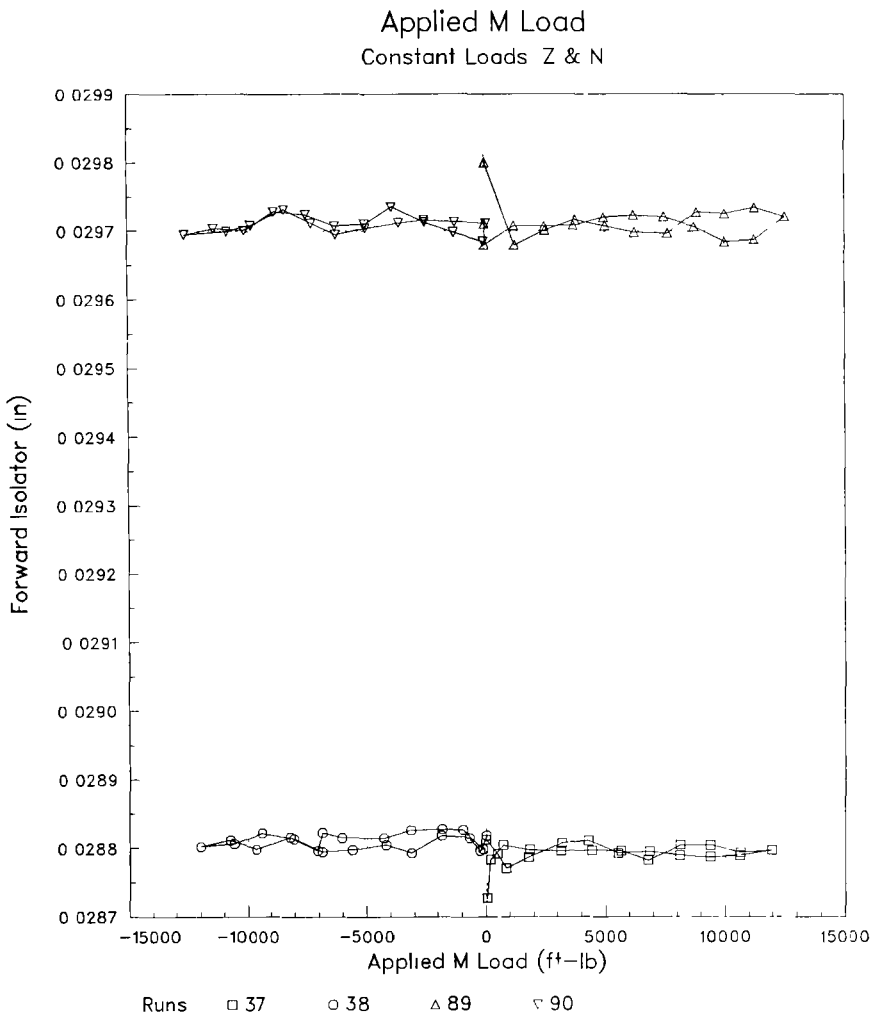

RSRA 741 1983 ROTOR CALIBRATION

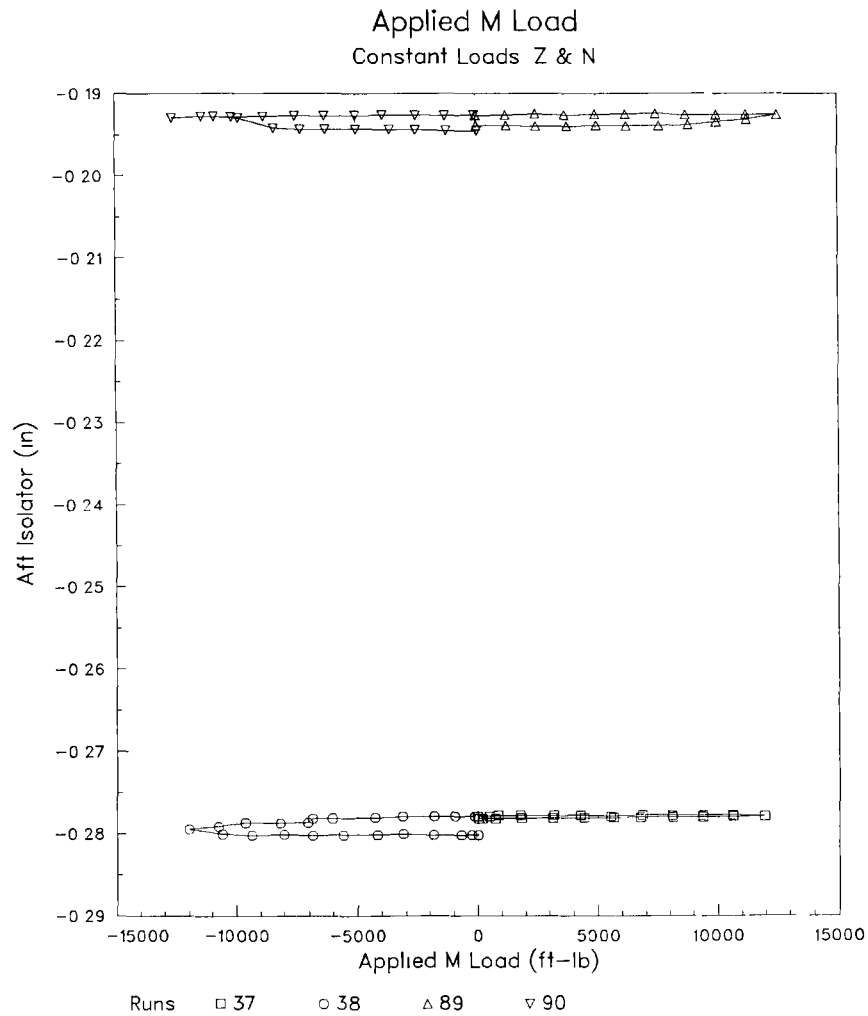

RSRA 741 1983 ROTOR CALIBRATION

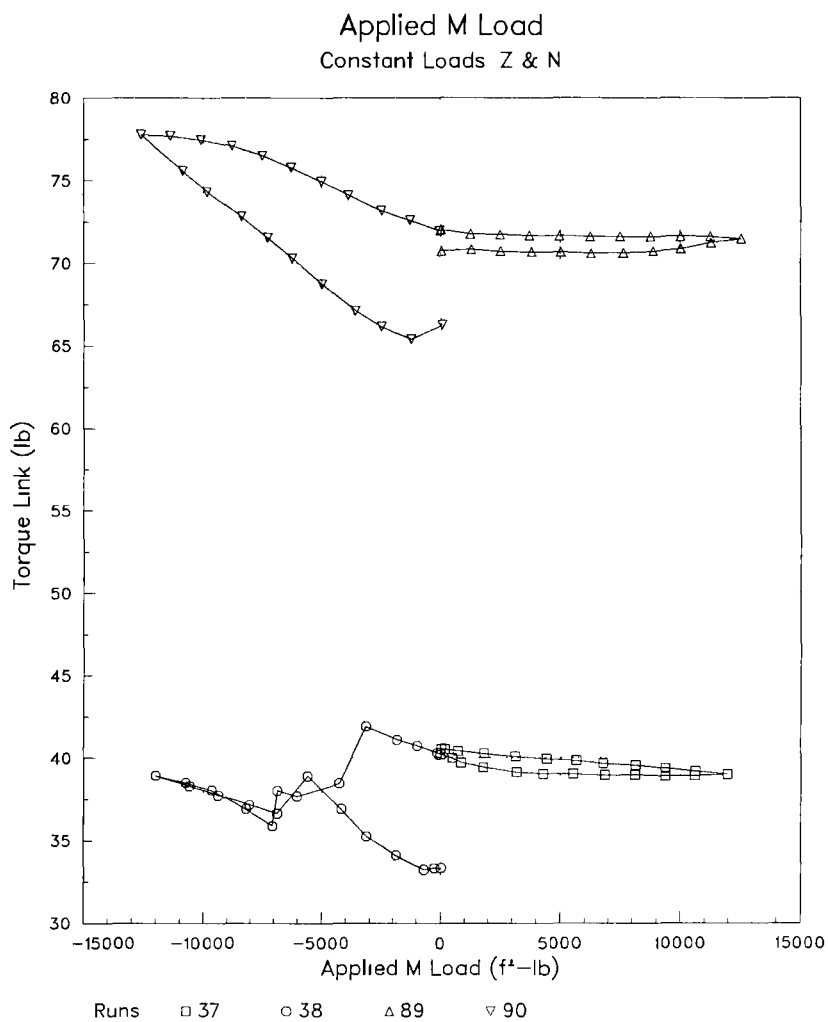

APPENDIX B

PRELIMINARY ANALYSES

The choices of analytical procedures and transducer data used in the main body of this paper were made after rejecting other approaches Inverse-regression analysis was eliminated first, then displacement-transducer data were deleted from the regression data sets Aft-isolator load data were also eliminated from the final analysis

REJECTION OF INVERSE REGRESSION

Inverse-regression analysis, used with success in earlier work (ref 2), could not be used here The problem results from nonlinear torque-linkage load response, shown for single N (torque) load in the figure included in this appendix In order to accommodate the large torque loads experienced in flight, the lateral isolators have opposing preloads The torque linkage also has a large preload, so that the resulting net preloads on the linkage bearings occur near the middle of the normal operating range As applied torque load increases through the preload range, bearing friction creates a kink in the strain-gage response curve The reverse of this kink shows up in almost all other transducer responses with varying severity

These nonlinear responses can be canceled out by a conventional direct regression, but not by an inverse regression During regression, all transducer data must be used together with the applied torque data to properly cancel out the kink in the torque-linkage response However, this is not possible with an inverse regression, which uses data from only one transducer at a time Nor can the torque linkage strain-gage data simply be deleted, because nonlinearities would remain uncanceled in the other transducer data The unsuitability of inverse-regression analysis caused no problem for this calibration, because the focused load-cell arrangment greatly reduced the problems with highly redundant data that led to the use of inverse regression in earlier work The present use of direct regression was also aided by changes in calibration-data distribution and organization (compare table 3 in the main body of the present paper to table 2 in ref 2)

The regression problems associated with the torque linkage would be ideally addressed by rebiasing the linkage and isolator preloads to locate the net preload outside of the normal operating load range This option is restricted by the requirements of new rotors and flight-test programs, and will have to be separately addressed for each individual case Any adjustments to the torque linkage will necessitate a new calibration

ELIMINATION OF TRANSDUCER DATA

Isolator displacement data were included in the regression analysis in an attempt to improve the calibration results In a few cases, it was possible to obtain more accurate responses in certain axes for certain applied loads by forcing the displacement data into the regression However, the results were not consistent, and in some cases were made much worse The problem seems to arise because the displacement transducers often have low-magnitude responses with very small slopes, but are nevertheless well correlated with the applied loads This results in extremely large regression coefficients and intercepts, sometimes leading to numerical difficulties Although inaccurate for some applied loads, a transducer's output may be consistent enough to be accepted into the regression for the current loading condition The resulting average regression error may be small, but applied-load errors, or possibly errors for different loading conditions, may be very large These problems led to rejection of the displacement transducer data for the forward and lateral isolators

These results were not totally unexpected The self-centering characteristics of the isolators reduces the statistical reliability of their displacement data In particular, the displacement data may not have a proper Gaussian normal error distribution, which is contrary to the mathematical assumptions of the regression analysis Therefore, the inclusion of isolator displacement data could easily give misleading results

The aft isolator is a special case It is normally deactivated and unloaded in flight, and was always deactivated for the calibration It consequently did not try to recenter itself Its displacement data were accordingly free of input caused by attempts of the isolator to correct its own motion This resulted in more reliable displacement data for the aft isolator its displacement transducer showed statistically significant output more often than any other such transducer, and did not cause the problems noted above if it was the only displacement transducer included in the regression All regressions were run both with and without the aft isolator displacement data included (However, no regressions were run with aft isolator displacement data and without corresponding load data, discussed below) No consistently significant differences were noted

Since the aft isolator is normally deactivated, it should produce only very-small-amplitude load data, caused mostly by internal friction Although of low magnitude, this load could be statistically significant, so all regressions were run

both with and without the aft isolator load data Again, no consistently significant differences were noted

The results for aft-isolator displacement and load data were encouraging If including isolator displacement data in the regressions had caused a consistent and significant improvement in calibration accuracy, it would have implied that the isolators were not doing a proper job of keeping themselves centered Furthermore, if including aft isolator load data had led to any important improvements in accuracy, that would mean that the aft isolator was improperly taking up loads All displacement data and the aft isolator load data were deleted from the regression analysis discussed in the main body of this paper

It is possible that these results are partly due to low accuracies of the individual transducers, or to imperfect performance of the load-measurement system as a whole If any improvements are made to the system or its transducers, all transducer data should be collected and analyzed during the first subsequent calibration to ensure that the results noted above continue to hold true

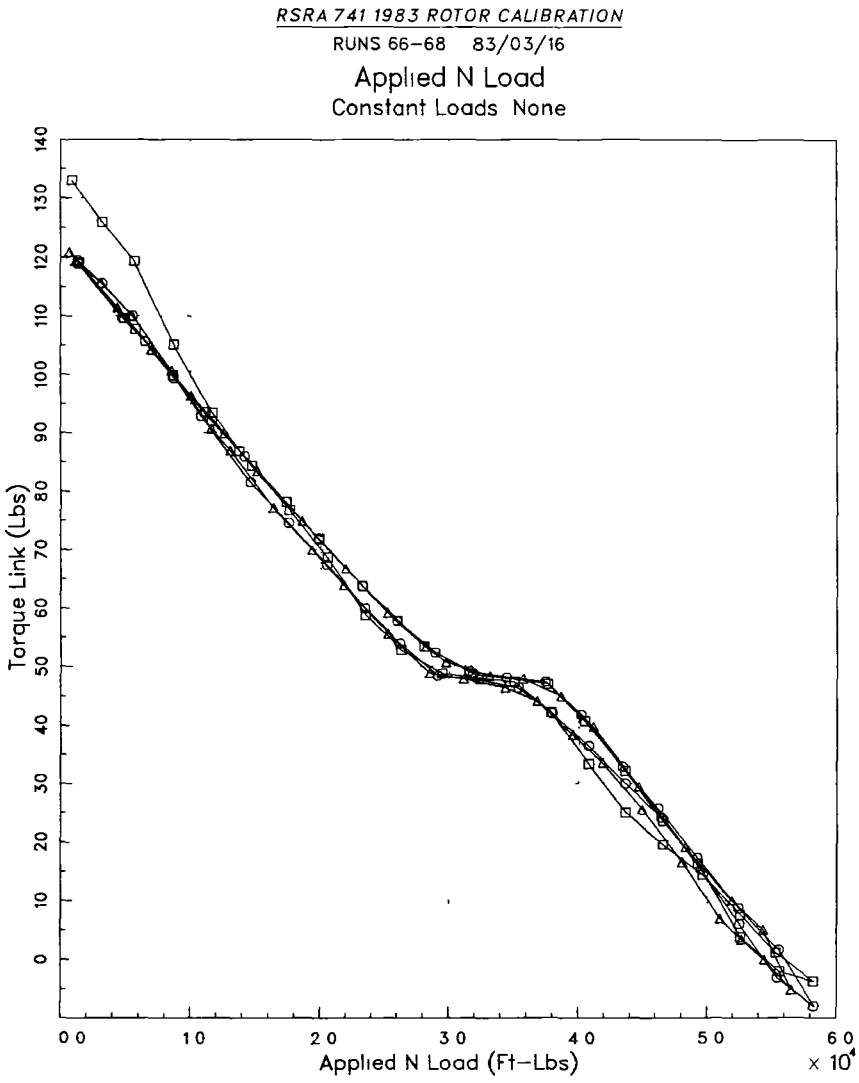

Torque-linkage strain gage response to applied single N load

REFERENCES

1 Burks, J S Rotor Systems Research Aircraft (RSRA) Rotor Force and Moment Measurement System AIAA Paper 81-2516, 1st Flight Testing Conference, Las Vegas, Nevada, November 1981

2 Acree, C W Results of the First Full Static Calibration of the RSRA Rotor Loads Measurement System NASA TP-2327, 1984

3 Acree, C W Preliminary Results of the First Static Calibration of the RSRA Helicopter Active-Isolator Rotor Balance System NASA TM-84395, 1983

4 Walton, W C , Hedgepeth, R K , and Bartlett, F D Report on Rotor Systems Research Aircraft Design for Vibration SAE 1976 Aerospace Engineering and Manufacturing Meeting, San Diego, California, Paper 760895, Nov 30-Dec 21, 1976

5 Kuczynski, W A , and Madden, J The RSRA Active Isolation/Rotor Balance System 4th European Rotorcraft and Powered Lift Aircraft Forum, Stresa, Italy, Paper 18, Sept 13-25, 1978 Proceedings, Vol 1, Costruzion, Aeronautiche Giovanni Agusta S p A , Gallarte, Italy, 1978 Also Journal of the American Helicopter Society, vol 25, no 2, April 1980, pp 17-25

6 Jeffery, P , and Huber, R Design and Development of a Motion Compensator for the RSRA Main Rotor Control Presented at the 13th Aerospace Mechanisms Conference, NASA Johnson Space Center, Houston, Texas, April 26-27, 1979 NASA CP-2081, pp 15-25

7 Acree, C W , et al RSRA Static Calibration Facility Operations Manual NASA TM-84389, 1983

8 Draper, N R , and Smith, H Applied Regression Analysis Wiley, New York, 1966.

1 Report No	2 Government Accession No	3 Recipient's Catalog No
NASA TM-85975		

4 Title and Subtitle	5 Report Date
NUMERICAL ANALYSIS OF THE FIRST STATIC CALIBRATION OF THE RSRA HELICOPTER ACTIVE-ISOLATOR ROTOR BALANCE SYSTEM	February 1985
	6 Performing Organization Code
7 Author(s)	8 Performing Organization Report No
C W Acree, Jr	A-9795
	10 Work Unit No
9 Performing Organization Name and Address	T-3495
Ames Research Center Moffett Field, CA 94035	11 Contract or Grant No
	13 Type of Report and Period Covered
12 Sponsoring Agency Name and Address	Technical Memorandum
National Aeronautics and Space Administration Washington, DC 20546	14 Sponsoring Agency Code 532-03-11

15 Supplementary Notes

Point of Contact C W Acree, Jr , Ames Research Center, Moffett Field, Calif , 94035
(415) 969-6574 or FTS 448-6574

16 Abstract

The helicopter version of the Rotor Systems Research Aircraft (RSRA) is designed to make simultaneous measurements of all rotor forces and moments in flight in a manner analogous to a wind-tunnel balance Loads are measured by a combination of load cells, strain gages, and hydropneumatic active isolators with built-in pressure gages Complete evaluation of system performance requires calibration of the rotor force- and moment-measurement system when installed in the aircraft Derivations of calibration corrections for various combinations of calibration data are discussed

17 Key Words (Suggested by Author(s))	18 Distribution Statement
Rotor load measurement Helicopter static calibration Rotor systems research	Unclassified - Unlimited Subject category 05

19 Security Classif (of this report)	20 Security Classif (of this page)	21 No of Pages	22 Price*
Unclassified	Unclassified	60	A04

*For sale by the National Technical Information Service, Springfield Virginia 22161 NASA Langley, 1985

End of Document